Autologous neutralising antibody specificities in HIV-1 subtype C: Characterising the C3V4 region and defining the mechanisms of escape.

Jinal Nomathemba Bhiman

Dissertation submitted to the Faculty of Health Sciences, University of the Witwatersrand, Johannesburg, in fulfilment of the requirements for the degree of Master of Science in Medicine.

Johannesburg, 2012

Declaration

I, Jinal Nomathemba Bhiman, declare that this dissertation is my own work. It is being submitted for the degree of Master of Science in Medicine in the University of the Witwatersrand, Johannesburg, South Africa. It has not been submitted before for any degree or examination at this or any other university.

Jinal Nomathemba Bhiman

Date

For my parents, Jinny and Alex Bhiman.

Presentations

Jinal N. Bhiman, Nthabeleng Ranchobe, Elin S. Gray, Salim S. Abdool Karim, Lynn Morris, Penny L. Moore and the CAPRISA 002 study team. Autologous neutralising antibody specificities in HIV-1 subtype C: Characterising the C3V4 region and defining the mechanisms of escape. University of the Witwatersrand Faculty of Health Sciences Research Day. 2010. Oral.

Jinal N. Bhiman, Nthabeleng Ranchobe, Elin S. Gray, Salim S. Abdool Karim, Lynn Morris, Penny L. Moore and the CAPRISA 002 study team. Autologous neutralising antibody specificities in HIV-1 subtype C: Characterising the C3V4 region and defining the mechanisms of escape, University of the Witwatersrand Third Cross Faculty Symposium. 2010. Oral.

Jinal N. Bhiman, Nthabeleng Ranchobe, Constantinos Kurt Wibmer, Elin S. Gray, Salim S. Abdool Karim, Carolyn Williamson, Lynn Morris and Penny L. Moore and the CAPRISA 002 study team. Autologous neutralising antibody specificities in HIV-1 subtype C: Characterising the C3V4 region and defining the mechanisms of escape. National Institute for Communicable Diseases Academic Day. 2010. Oral.

Jinal N. Bhiman, Nthabeleng Ranchobe, Constantinos Kurt Wibmer, Elin S. Gray, Salim S. Abdool Karim, Carolyn Williamson, Lynn Morris and Penny L. Moore and the CAPRISA 002 study team. Mechanisms of escape from autologous neutralising antibodies targeting the C3V4 region of the HIV-1 subtype C envelope. Keystone Symposium: X8, Protection from HIV: Targeted Intervention Strategies. 2011. Poster.

Jinal N. Bhiman, Constantinos Kurt Wibmer, Nthabeleng Ranchobe, Elin S. Gray, Salim S. Abdool Karim, Carolyn Williamson, Lynn Morris and Penny L. Moore and the CAPRISA 002 study team. Mechanisms of escape from autologous neutralising antibodies targeting the C3V4 region of the HIV-1 subtype C envelope. 5th SA AIDS Conference. 2011. Poster.

Jinal N. Bhiman, Constantinos Kurt Wibmer, Nthabeleng Ranchobe, Elin S. Gray, Salim S. Abdool Karim, Carolyn Williamson, Lynn Morris and Penny L. Moore and the CAPRISA 002 study team. The C3V4 domain interacts with structurally proximal regions to mediate escape from autologous neutralising antibodies in HIV-1 subtype C infection. AIDS Vaccine Conference. 2011. Poster.

Daniel J. Sheward, Penny L. Moore, Maphuti C. Madiga, Elin S. Gray, Roman Ntale, Zenda L. Woodman, **Jinal N. Bhiman**, Florette Treurnicht, Hayley Harvey, Sengeziwe Sibeko, Koleka Mlisana, Salim S. Abdool Karim, Lynn Morris, and Carolyn Williamson, and the CAPRISA002 study team. Superinfection Results in Potent Neutralising Antibody Responses to the Superinfecting Virus, But Does Not Necessarily Enhance Neutralisation Breadth. AIDS Vaccine Conference. 2011. Poster.

Constantinos Kurt Wibmer, **Jinal N. Bhiman**, Penny L. Moore, Nthabeleng Ranchobe, Salim S. Abdool Karim, Lynn Morris, and Elin S. Gray. Early Autologous Neutralising Epitopes in C3-V4 and β14+V5 are readily adsorbed with monomeric gp120. AIDS Vaccine Conference. 2011. Poster.

Penny L. Moore, Elin S. Gray, Tandile Hermanus, Daniel Sheward, Nancy Tumba, C. Kurt Wibmer, **Jinal N. Bhiman**, Sengeziwe Sibeko, Salim S. Abdool Karim, Carolyn Williamson and Lynn Morris and the CAPRISA 002 study team. Evolution of HIV-1 transmitted/founder viruses results in the formation of epitopes for later broadly cross-neutralising antibodies. AIDS Vaccine Conference. 2011. Oral.

Abstract

Introduction

Most new HIV-1 infections world-wide are caused by subtype C viruses. The C3V4 region, including the alpha2-helix and V4 loop, has been identified as a major target for autologous neutralising antibodies in subtype C infections. Factors associated with the immunogenicity of this region, and the mechanisms of escape from anti-C3V4 responses have not been described, although charge changes in the alpha2-helix have been proposed to mediate neutralisation escape.

Methods

Seventeen HIV-1 subtype C infected individuals were classified as C3V4 responders or non-responders using chimeric viruses in env-pseudotyped neutralisation assays. Longitudinal sequences obtained from C3V4 responders were used to identify putative neutralisation escape mutations. The role of these mutations in mediating escape was investigated using site-directed mutagenesis.

Results

The C3V4 region was confirmed as a major target in HIV-1 subtype C infections. The development of an anti-C3V4 response was associated with shorter V4 loops and fewer potential N-linked glycans (PNGs) in the C3V4 region. Anti-C3V4 responses were associated with higher autologous neutralising titres. Neutralisation escape from an anti-C3V4 response was rarely mediated by charge changes in the alpha2-helix and generally occurred through mutations in other structurally proximal regions of the envelope. This study confirmed the use of glycan shuffling as a predominant escape pathway. In three individuals multiple mechanisms of escape were identified and in two other cases escape mutations within the C3V4 and structurally proximal regions clustered at opposite termini of the alpha2-helix, inconsistent with the surface area of a single epitope.

Conclusion

A more exposed and accessible C3V4 region was more likely to elicit an anti-C3V4 response. The highly immunogenic nature of this region may contribute to the higher overall neutralisation titres in subtype C infections. Distinct clusters of mutations may suggest the existence of two “sub-epitopes” within the C3V4 domain that warrant further investigation. These findings emphasise the adaptability and plasticity of the C3V4 region in the context of viral evasion of host defences.

Acknowledgements

I would like to thank:

- Dr Penny (Lane) Moore, for believing in my ability and providing me with this opportunity to learn under her guidance.
- Prof Lynn Morris for providing me with additional supervision and allowing me to experiment in her laboratory.
- The financial assistance of the National Research Foundation (NRF) towards this research is hereby acknowledged. Opinions expressed and conclusions arrived at, are those of the author and are not necessarily to be attributed to the NRF.
- The Poliomyelitis Research Foundation and Columbia University-Fogarty AITRP for additional student bursaries.
- All the staff and students at the NICD AIDS Unit for encouragement, technical advice and corridor conversations.
- Constantinos Kurt Wibmer (Sista Ketiwe) for being my partner in crime, for challenging me to go beyond my comfort zone, for proof-reading my monster and for buying chocolate and KFC for me during my "trying times".
- My father, Alex Bhiman, for providing me with chocolate, sound advice and a shoulder to lean on and for allowing me to further my education.
- My siblings, Amilcar and Alika Bhiman, for countless laughs, "ooosome-ness" and happiness.
- Bradley Bhiman for starting it all with talk of liposomes.
- The Peters (Ma, Daphne, Chrissy, Judy, Silas, Jayshree, Pauly, Michelle, Cheryl, Neo, Isabella, Biko, Sainesh, Nicole, Damian, Jayden, Cheyenne, Samora, Ethan and Jineve).
- Natasha (Pag) Abraham for relating to me more than anyone else in the past few months and for Nutella. Zaida Halim for "control alt delete."
- Aunty Agnes for being our other mother.
- The Bhimans (Melisha, Tasanya, Aka, Baby, Bentley, Sunny, Cynthia, Joy, Brian, Liaquat, Grace, Pat, Deon, Burton, Duane and everyone else in the extended family).
- The Bickfords (Esther and Franz).
- Jinny, Melanie, Tinka, Steven, Bobby, Gabriel, Bunyan, Moses, Miriam, Joe and Majorie.

Table of Contents

List of Figures

List of Tables

Abbreviations

General Abbreviations

A:	Adenine
ADCC:	Antibody-dependent cellular cytotoxicity
AnAb:	Autologous neutralising antibody
ART:	Antiretroviral therapy
bnAb:	Broadly neutralising antibody
bp:	Base pairs
C:	Cytosine
C1:	Constant region 1
C2:	Constant region 2
C3:	Constant region 3
C4:	Constant region 4
C5:	Constant region 5
CAPRISA:	Centre for the AIDS Programme of Research in South Africa
CCR5:	C-C chemokine receptor type 5
CD4:	Cluster of differentiation 4
cDNA:	Complementary DNA
CXCR4:	C-X-C chemokine receptor type 4
DEAE-dextran:	Diethylaminoethyl dextran
DNA:	Deoxyribonucleic acid
dNTPs:	Deoxynucleoside triphosphates
ddNTPs:	Dideoxynucleoside triphosphates
DMEM:	Dulbecco's Modified Eagle Medium
EDTA:	Ethylenediaminetetraacetic acid
Fab:	Fragment antigen binding region
Fc:	Crystallisable fragment
FBS:	Foetal bovine serum
G:	Guanine
Gag:	Group associated antigen protein
Glc:	Glucose
GlcNAc:	N-acetyl glucosamine
GnTI:	N-acetylglucosamine transferase I
GnTII:	N-acetylglucosamine transferase II
Gp120:	Glycoprotein 120 kDa
Gp41:	Glycoprotein 41 kDa
HEK:	Human epithelial kidney
HEPES:	4-(2-hydroxyethyl)-1-piperazineethanesulfonic acid
HIV-1:	Human Immunodeficiency Virus Type 1
HIV-2:	Human Immunodeficiency Virus Type 2
HR1:	Heptad repeat 1
HR2:	Heptad repeat 2
ID_{50}:	50% inhibitory dilution
Indels:	Insertions and deletions
ITC:	Isothermal titration calorimetry
LB:	Luria Bertani
LTR:	Long terminal repeat
mAb:	monoclonal antibody

Man:	Mannose
MPER:	Membrane proximal external region
nAb:	Neutralising antibody
NHP:	Nonhuman primate
NMR:	Nuclear magnetic resonance
PCR:	Polymerase chain reaction
PDB ID:	Protein data bank identity
p.i:	Post-infection
PNG:	Potential N-linked glycan
PSV:	Pseudovirus
RLU:	Relative light units
rmsd:	Root mean square distance
RNA:	Ribonucleic acid
sCD4:	Soluble cluster of differentiation 4
SDS:	Sodium dodecyl sulphate
SGA:	Single genome amplification
SHIV:	Simian-human immunodeficiency chimeric virus
SIV:	Simian Immunodeficiency Virus
SOC:	Super optimal broth with catabolite repression
T:	Thymine
UNAIDS:	United Nations programme on HIV/AIDS
V1V2:	Variable regions 1 and 2
V3:	Variable region 3
V4:	Variable region 4
V5:	Variable region 5

Symbols and Units

Å:	Angstrom
α:	Alpha
β:	Beta
bp, kb:	Base pairs and kilobases
° C:	Degrees Celsius
Cl:	Chloride
G:	Relative centrifugal force
Mg:	Magnesium
mM, M:	Millimolar and molar
Na:	Sodium
ng, µg, mg:	Nano-, micro- and milligram
nm, µm, cm:	Nano-, micro and centimetre
pmol:	Picomole
rpm:	Revolutions per minute
SO_4:	Sulphate
µl, ml:	Mirco- and millilitre
U:	Enzyme units of activity

Amino Acid Abbreviations

Amino Acid	Three-Letter Abbreviations	One-Letter Symbol
Alanine	Ala	A
Arginine	Arg	R
Asparagine	Asn	N
Aspartic acid	Asp	D
Cysteine	Cys	C
Glutamic acid	Glu	E
Glutamine	Gln	Q
Glycine	Gly	G
Histidine	His	H
Isoleucine	Ile	I
Leucine	Leu	L
Lysine	Lys	K
Methionine	Met	M
Phenylalanine	Phe	F
Proline	Pro	P
Serine	Ser	S
Threonine	Thr	T
Tryptophan	Trp	W
Tyrosine	Tyr	Y
Valine	Val	V

Chapter 1: Introduction

1.1 Background

The global Human Immunodeficiency Virus Type 1 (HIV-1) pandemic is one of the biggest public health issues facing the world today. Of the 33.3 million HIV-infected individuals world-wide, 22.5 million reside in sub-Saharan Africa (UNAIDS 2010, www.unaids.org). A quarter of the 22.5 million Africans infected with HIV-1 are South Africans. Therefore, although this epidemic is of huge global concern, it is most especially a South African burden. HIV-1 subtype C infections dominate in South Africa, and therefore also account for the majority of infections worldwide.

Major advancements have been made in the treatment of HIV-1 and antiretroviral therapy (ART) can successfully suppress viral replication. However the early establishment of a latent viral reservoir suggests that a cure in this manner may not be possible (2008; Cooper et al., 2002; Matthews et al., 2004; May et al., 2006). Currently only a single individual has been cured of HIV-1 infection through a transplant of bone marrow stem cells from a donor with the CCR5Δ32 mutation (Allers et al., 2011; Hutter et al., 2009). However this method is not viable on a large scale and instead a functional cure is the aim for most clinicians. A functional cure results when ART is initiated early enough in infection to allow an individual to remain aviremic when ART is subsequently stopped, however particularly in a South African setting, this is not a feasible public health option for dealing with the epidemic (Hocqueloux et al., 2010; Trono et al., 2010).

Numerous other strategies for coping with the HIV-1 epidemic are being actively pursued. Although male circumcision shows the highest level of protection from HIV-1 infection (Auvert et al., 2005; Gray et al., 2000; Lavreys et al., 1999; Reynolds et al., 2004), other preventative strategies have had successes in recent years. In 2010 a microbicide gel containing 1 % tenofovir (an antiretroviral drug) was shown to be 39 % effective in preventing HIV-1 infection. In women who used the gel with more than 80 % adherence, HIV-1 incidence was 54 % lower (Abdool Karim et al., 2010).

Most recently, the RV144 vaccine trial, which made use of a canarypox prime followed by two HIV-1 protein boosts, was the first vaccine regimen to show efficacy, at 31 %, in low risk Thai men and women between the ages of 18 and 30 years (Rerks-Ngarm et al., 2009). Because this initial trial was carried out in low risk Thai participants, the positive effect of this regimen will be confirmed (in 2014) in two separate trials involving high risk participants from Thailand and South Africa

(Gurunathan, 2011). This study highlights the importance of pursuing vaccine design for the prevention of HIV-1 infection.

1.2 HIV-1

HIV-1 is a lentivirus of the *Retroviridae* family that is closely related to the less pathogenic HIV-2 (Levy, 1993). HIV-1 evolved from the Simian Immunodeficiency Virus (SIV) that infects chimpanzees and gorillas whereas HIV-2 evolved from SIV that infects the sooty mangabey (Lemey et al., 2003; Plantier et al., 2009). HIV-1 is divided into four main phylogenetic groups: M, N, O and P (Plantier et al., 2009; Robertson et al., 2000; Simon et al., 1998). Group M is further categorised into 9 subtypes (A-D, F-H, J and K), 5 sub-subtypes (A1-3 and F1-2) and over 40 circulating recombinant forms (http://www.hiv.lanl.gov), which emphasises the extent of diversity found within this virus.

The HIV-1 virion is icosahedral in shape with a diameter of approximately 120 nm (Gentile et al., 1994; Nermut et al., 1993) (Figure 1).

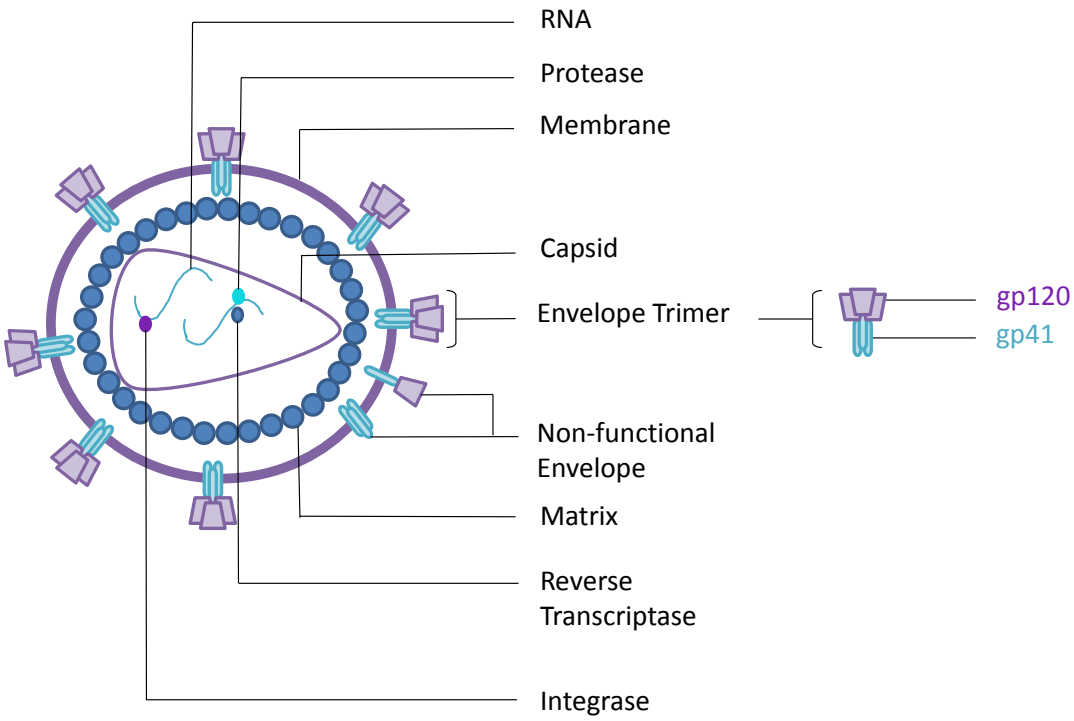

Figure 1. Schematic representation of the HIV-1 virion. Embedded in the lipid membrane that surrounds the HIV-1 virion are the envelope spikes. Each spike is composed of three gp120 and three gp41 proteins, however non-functional versions of the envelope are also found on the viral surface. Within the membrane is a capsid core that encloses two single RNA strands and three enzymes (protease, integrase and reverse transcriptase). Figure adapted from Levy, 1993.

The viral envelope, embedded in the lipid membrane that surrounds the virus, contains functional trimeric spikes composed of three gp120 proteins non-covalently attached to three gp41 proteins (Figure 1) (Lu et al., 1995). In addition to the trimeric form of the envelope, various forms of non-functional envelope proteins exist, including membrane-bound monomeric gp120/gp41 and gp41 stumps as well as freely dissociated gp120 (Burrer et al., 2005; Moore et al., 2006; Parren et al., 1997). The membrane encloses an elongated, conical protein core made of the capsid protein, which surrounds two positive-sense single RNA strands. Closely associated with the RNA strands are the nucleocapsid proteins as well as the reverse transcriptase, protease and integrase enzymes (Levy, 1993).

The HIV-1 genome consists of approximately 9700 nucleotides encoding 9 genes which are translated into 15 proteins (Levy, 1993). Three (*gag*, *pol*, and *env)* are large genes, while six (*vif, vpr, tat, rev, vpu* and *nef*) are smaller accessory genes (Levy, 1993).

1.3 The HIV-1 envelope

The life cycle of HIV-1 begins with attachment of the virus to host cells, followed by fusion of the viral and host membranes. These two processes are mediated by the envelope glycoproteins, gp120 (a cell surface attachment protein) and gp41 (a transmembrane protein) (Wyatt and Sodroski, 1998). The trimeric structure of each functional spike is maintained through interactions between the three gp41 proteins (Helseth et al., 1991; Moore et al., 1994). These envelope spikes are the sole targets of neutralising antibodies (nAbs), which inhibit viral infection by blocking attachment or by preventing conformational changes in the envelope that are required for fusion (Wyatt et al., 1998).

The entry process occurs through conformational changes in the viral spike that harness stored potential energy to overcome fusion barriers (Wyatt and Sodroski, 1998). Conformational changes in gp120, caused by initial binding of the host cell receptor, CD4 (cluster of differentiation 4), trigger a series of subsequent conformational changes within gp41. The conformational changes in gp120 allow for a high affinity interaction with the coreceptor which is usually the β-chemokine receptor CCR5 (C-C chemokine receptor type 5), although a switch to CXCR4 (C-X-C chemokine receptor type 4) usage is often observed in chronic HIV-1 infections (Feng et al., 1996; Sattentau and Moore, 1991). The presentation of the coreceptor binding site and formation of a gp41 prehairpin intermediate occurs simultaneously. These processes in turn promote additional structural

alterations in gp41 that result in the formation of an energetically stable six helix bundle that coincides with fusion of the host and viral membranes (Melikyan et al., 2000; Tan et al., 1997).

Both gp120 and gp41 are encoded by the viral *env* gene and following viral genomic DNA integration, are translated in the rough endoplasmic reticulum as a single polypeptide precursor that varies between 845 and 870 amino acids in size (Allan et al., 1985). Both gp120 and gp41 are heavily glycosylated, although gp120 is more so with half of its mass attributed to glycans (Lasky et al., 1986). Extensive glycosylation begins with the addition of $Glc_3Man_9GlcNAc_2$ moieties (Glc is glucose, Man is mannose and GlcNAc is N-acetyl glucosamine) to the free amide of an asparagine in the sequon NXT/S (where X is any amino acid except proline) (Gagneux and Varki, 1999; Kornfeld and Kornfeld, 1985). In the Golgi apparatus the terminal glucose and mannose moieties are trimmed via mannosidase I trimming (Figure 2) to oligomannose glycans ($Man_5GlcNAc_2$).

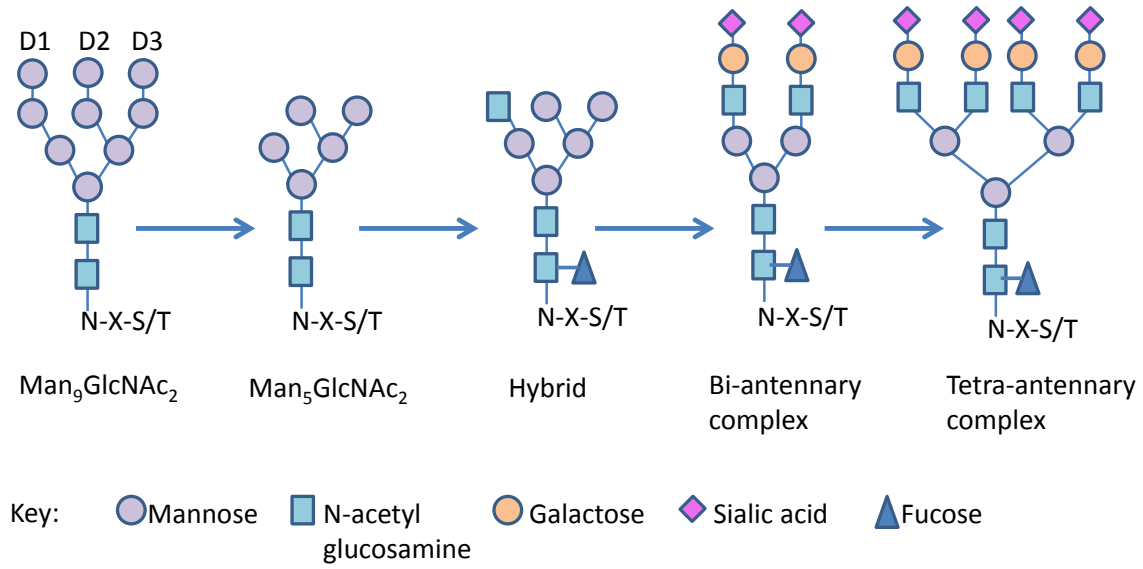

Figure 2. N-linked glycan processing. Five essential steps of glycan processing show the transformation of oligomannose glycans to hybrid and then complex glycans. After initial trimming of terminal mannose residues, conversion from oligomannose to hybrid glycans occurs via addition of N-acetyl glucosamine (GlcNAc) resides to the D1 arm. At this stage fucosylation of the oligomannose stems may occur. Finally complex glycans are created through replacement of the D2 and D3 arm mannose moieties by complex antennae which may contain galactose and sialic acid residues. Adapted from Binley *et al* 2010.

Accessible glycans are then converted to hybrid glycans through the addition of an GlcNAc residue to the D1 arm via N-acetylglucosamine transferase I (GnTI) (Choi et al., 2003). Further processing results in accessible glycans being transformed into complex glycans. The mannose moieties on the D2 and D3 arms of the glycan are replaced by complex antennae (such as sialic acid) via mannosidase II trimming and N-acetylglucosamine transferase II (GnTII) action (Choi et al., 2003; Earl

et al., 1990; Gagneux and Varki, 1999). Finally fucosyl transferase adds an α-1-6-linked fucose moiety to the lower GlcNAc of accessible complex glycan stems (Crispin et al., 2004; Voynow et al., 1991). The mass of an N-linked glycan is approximately 20 times that of the average amino acid side chain (Zhang et al., 2004). Structural modelling of gp120 suggests that mannose-rich and complex glycans occupy distinct regions of the protein (Zhou *et al*, 2002).

Following glycosylation, immature gp160 trimers are formed (Earl et al., 1990). Within the trans-Golgi each gp160 polypeptide is cleaved by furin into functional gp120 and gp41 proteins (Decroly et al., 1997; Hallenberger et al., 1997). The mature spikes are transported to the cell membrane, specifically the lipid rafts, where they are incorporated into the budding virions (Rousso et al., 2000).

1.3.1 Glycoprotein41 (gp41)

The transmembrane protein of the envelope, gp41, is a class I fusion protein (Dimitrov, 2004). It maintains the trimeric structure of the functional envelope oligomer and can be divided into the ectodomain, a highly conserved membrane-spanning domain and a long cytoplasmic tail (Figure 3) (Helseth et al., 1991; Moore et al., 1994).

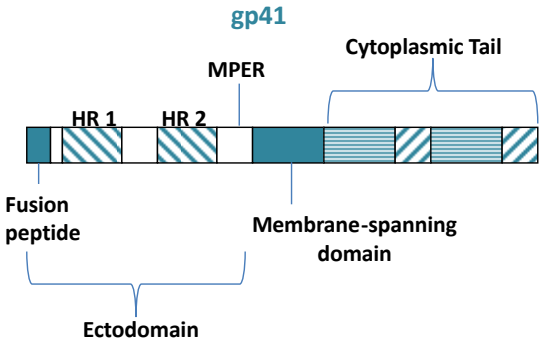

Figure 3. Schematic showing the regions of gp41. Gp41 can be divided into an ectodomain, membrane-spanning domain and cytoplasmic tail. The ectodomain contains the fusion peptide (which inserts into the host cell membrane), heptad repeat 1 (HR 1) and heptad repeat 2 (HR 2) (which are involved in the fusion process) and the membrane proximal external region.

The ectodomain is involved in the fusion process and contains the functionally important heptad repeat 1 (HR 1) or N-helix, heptad repeat 2 (HR 2) or C-helix, the fusion peptide and the membrane proximal external region (MPER). The MPER is a 34 amino acid segment that is highly conserved and forms an important neutralisation epitope (Dimitrov et al., 2003; Munoz-Barroso et al., 1999;

Salzwedel et al., 1999; Zwick et al., 2005). The cytoplasmic tail, which is approximately 150 amino acids in length, has numerous conserved motifs that have been implicated in processes such as envelope incorporation and Gag processing (Freed and Martin, 1996; Piller et al., 2000).

Although the native conformation of gp41 is unknown, the prefusogenic state is believed to be stabilised by a β-sandwich in gp120 (Pancera et al., 2010; Yang et al., 2003). Upon CD4 and CCR5 binding the rearrangement of gp120 induces formation or exposure of three antiparallel coiled coils and destabilises gp41, concomitantly releasing the fusion peptide which inserts into the target membrane (Furuta et al., 1998; LaBranche et al., 2001; Tan et al., 1997). The prehairpin intermediate prior to fusion is short-lived and highly energetically unstable. Collapse of this intermediate is used to bring the viral and cellular membranes together (Melikyan et al., 2000). The free energy released during the subsequent formation of a stable 6-helix bundle allows for the energy barrier that prevents membrane fusion to be overcome (Chan and Kim, 1998; Wyatt and Sodroski, 1998).

1.3.2 Glycoprotein120 (gp120)

HIV-1 binds to the cell via interactions between the cell surface attachment protein, gp120 and cellular receptors, namely the CD4 receptor and the chemokine coreceptors (Klatzmann and Montagnier, 1986). The gp120 is more heavily glycosylated and more variable than gp41, and is divided into five constant regions (C1-C5) interjected with five variable regions (V1-V5) (Figure 4) (Lasky et al., 1986; Leonard et al., 1990).

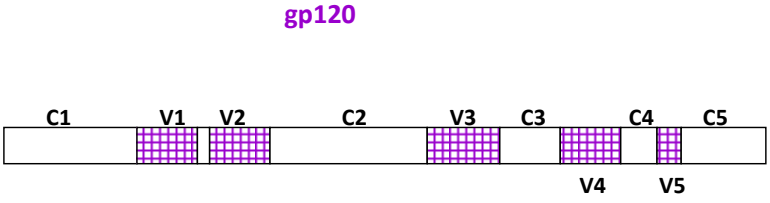

Figure 4. Schematic showing the regions of gp120. The gp120 amino acid sequence is divided into 5 constant (C1 to C5) and 5 variable (V1 to V5) regions.

Each variable region, with the exception of the relatively short V5 loop, is bracketed by cysteines which form disulphide bonds. The C1 and C5 regions form the main contact areas with gp41 (Moore et al., 1994).

The gp120 protein is described as having a neutralising, a non-neutralising and a silent face (Kwong et al., 1998; Wyatt et al., 1998). The silent face is heavily glycosylated with carbohydrate molecules. Although these were originally thought to be recognised as "self" and elicit no immune response, increasing evidence suggests that the evolving glycan shield can also be a target for neutralising antibodies. Recent studies using polyclonal serum samples have implicated glycosylation sites as targets for neutralising antibodies (Gray et al., 2011; Tang et al., 2011; Walker et al., 2010). In addition, these findings have been confirmed through the identification of the epitopes of recently isolated monoclonal antibodies which bind glycans (McLellan et al., 2011; Pejchal et al., 2011; Sanders et al., 2002; Scanlan et al., 2002; Walker et al., 2011).

The non-neutralising face, which is highly conserved, is exposed only on non-functional forms of the envelope (Kwong et al., 1998; Wyatt et al., 1998). The gp160 precursor and freely dissociated monomeric gp120 both have an exposed non-neutralising face and induce a strong immune response (Bachmann and Zinkernagel, 1997; Parren et al., 1997; Poignard et al., 2001). However the non-neutralising face is buried in the context of the functional trimer, and therefore antibodies to this face are binding only and cannot prevent viral entry (Pancera et al., 2010; Sattentau and Moore, 1995; Wyatt et al., 1998).

The focus of this dissertation is the neutralising face, found on the solvent-exposed surface of gp120, which can elicit neutralising antibodies. Many portions of the C2, C3 and C4 regions are themselves targets for neutralising antibodies, but also form several discontinuous neutralising epitopes (Pantophlet and Burton, 2006). The V1V2 loops are highly exposed and are thought to shield neutralisation epitopes such as the highly conserved receptor binding sites (Moore et al., 2007; Rong et al., 2007a). Deletion of the V1V2 loop results in a high level of neutralisation sensitivity supporting this hypothesis (Cao et al., 1997; Pinter et al., 2004; Rusert et al., 2011; Stamatatos and Cheng-Mayer, 1998).

1.3.3 Crystallographic studies of gp120

There has been considerable effort in obtaining the gp120 three-dimensional structure to facilitate immunogen design. Numerous variable loops and glycans make gp120 highly plastic and difficult to crystallise, therefore initial gp120 structures of both HIV-1 (Kwong et al., 1998) and SIV (Chen et al., 2005) were deglycosylated and had truncated N- and C-termini and deleted V1V2 and V3 loops in an attempt to stabilise these proteins. These modified gp120s are referred to as the gp120 core (Kwong et al., 1998).

The original HXBc2 gp120 core structure (Kwong et al., 1998); PDB ID: 1GC1) was further stabilised with a two domain CD4 and the fragment antigen binding (Fab) region of a coreceptor binding monoclonal antibody (17b). According to this and subsequent core structures gp120 can be divided into an inner domain and an outer domain linked by a four-stranded bridging sheet (Figure 5).

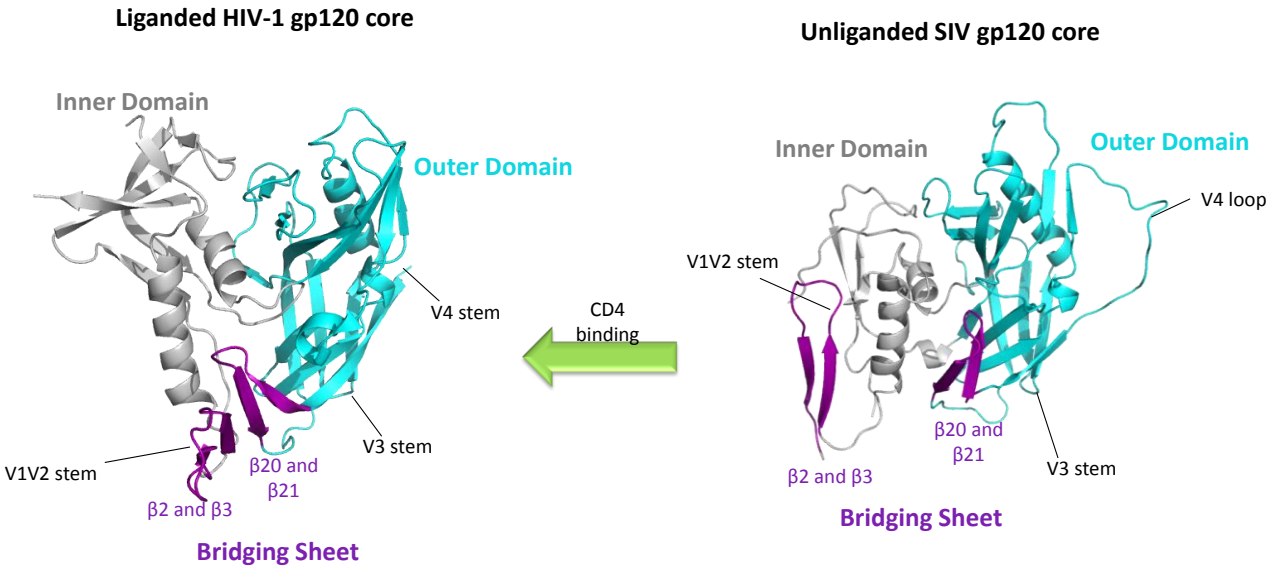

Figure 5. Ribbon diagram of the liganded HIV-1 and unliganded SIV gp120 crystal structures. In both the HIV-1 and SIV gp120 core structures the inner domain (grey), bridging sheet (purple) and outer domain (cyan) are highlighted. The stems of the V1V2, V3 and V4 loops are indicated. In the liganded (1GC1) gp120 the β-strands making up the bridging sheet are proximal to each other, however the unliganded SIV gp120 (2BF1) shows a rearranged bridging sheet with the β2 and β3 sheets displaced 20-25Å from the β20 and β21 sheets. Protein structure images for this and all subsequent protein structure figures (unless otherwise stated) were created using PyMOL (DeLano, W.L. The PyMOL Molecular Graphics System (2002) DeLano Scientific, San Carlos, CA, USA (http://www.pymol.org).

The sparsely glycosylated inner domains of the three gp120 monomers interact with each other and with the three gp41 monomers in the context of the functional trimeric spike. The inner domain consists mainly of the C1 and C5 regions. In contrast, the outer domain is heavily glycosylated so as to cover and thereby protect solvent exposed regions. The bridging sheet is located between the inner and outer domains and is composed of four anti-parallel β-sheets, two of which (β2 and β3) emanate from the V1V2 loop stem and two (β20 and β21) from the C4 region.

Due to the highly dynamic nature of HIV-1 gp120, it has never been crystallised in the absence of ligands bound to its receptor and coreceptor binding sites. However, the SIV and HIV-1 gp120 proteins share sequence similarity, common receptors and coreceptors and perform the same function of viral attachment. The closely related SIV gp120 core protein was crystallised in the unliganded form (Chen et al., 2005; Chen et al., 2009) and provides a useful comparison with the liganded structure. In the unliganded SIV gp120 structure (PDB ID: 2BF1) the outer domain appears to be highly similar to the liganded HIV-1 gp120 in terms of the arrangement of secondary structures, however the inner domain and bridging sheet are greatly altered (Figure 5). Although this unliganded conformation may be a product of the plasticity of gp120 (and thus multiple unliganded forms may exist), the liganded and unliganded structures together with isothermal titration calorimetry (ITC) data (Kwong et al., 2002), suggests that binding of CD4 induces drastic conformational changes in gp120.

Although the complete crystal structure for gp120 has not been solved, numerous additions, such as the V3 loop (Huang et al., 2005) and the N- and C-termini (Pancera et al., 2010), have been made to the core gp120 structure. Most recently the structure of the V1V2 region scaffolded to a bacterial protein has been solved (McLellan et al., 2011). Figure 6 shows a homology model that combines all these features and was generated using the Swiss-PDB Viewer and SWISS-MODEL Server (as were all subsequent homology models) (Arnold et al., 2006; Guex and Peitsch, 1997; Schwede et al., 2003).

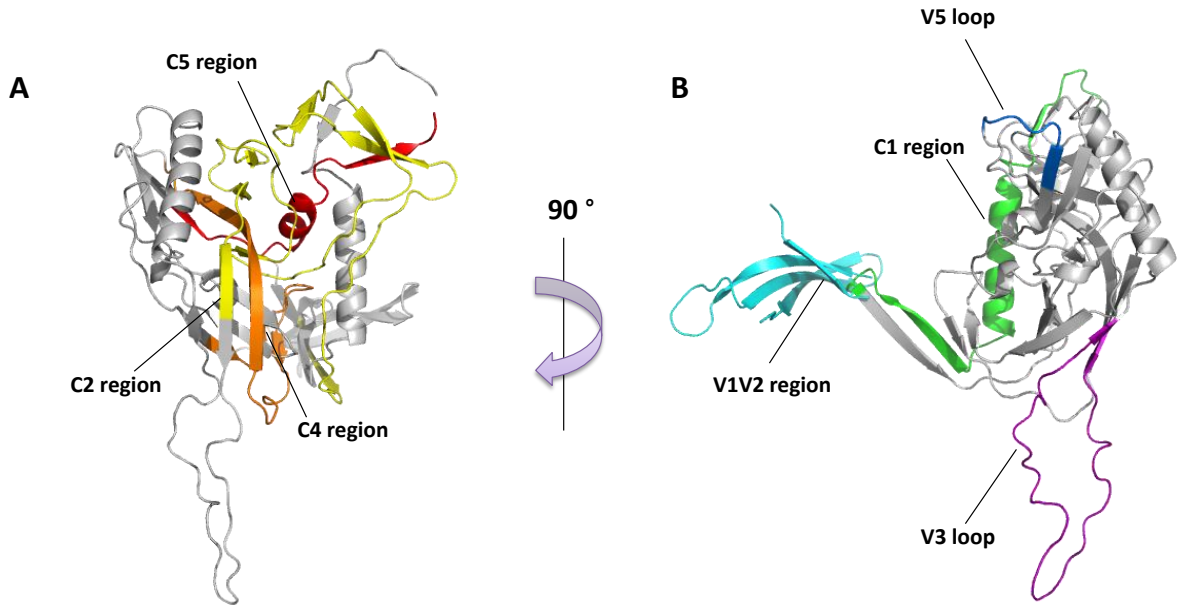

Figure 6. A ribbon representation of a subtype C homology model combining all known structural elements of gp120. Two views with a 90 ° rotation are shown. **(A)** Highlighted in this view of gp120 are the C2 (yellow), C4 (orange) and C5 (red) regions. **(B)** This view of gp120 shows the C1 (green) and V1V2 (cyan) regions as well as the V3 (purple) and V5 (blue) loops. This model was generated by threading a subtype C gp120 sequence into a structural alignment of the JR-FL, HXBc2, CAP210 gp120 and CAP45 V1V2 region crystal structures (PDB ID: 2B4C, 3JWD, 3QAD and 3U4E respectively). This and all subsequent homology models were generated using the SWISS-MODEL Server (Arnold *et al*, 2006; Schwede *et al*, 2003; Guex and Peitsch, 1997; Peitsch, 1995).

The V3 loop of the JR-FL isolate was co-crystallised with two domain CD4 and a monoclonal antibody (X5) targeting the CD4-induced epitope (Huang et al., 2005). The V3 region protrudes as an elongated loop structure from two anti-parallel β-sheets in the outer domain (Figure 6). The base of this structure is stabilised by a disulphide bond located between β12 and β13. The dynamic stem extends away from the gp120 core to form a β-turn at the furthermost tip. When this structure was modelled into that of the trimer, as determined by cryoelectron tomography (Bennett et al., 2007; Briggs et al., 2006; Sougrat et al., 2007; Subramaniam, 2006; Zanetti et al., 2006), the V3 loop tip faced the cell membrane, which is consistent with coreceptor binding. However, an extended V3 loop may only be relevant in the context of a CD4-bound gp120 and it has been proposed that this region may be partially occluded by the V1V2 region in the context of the unliganded trimer (Gram et al., 1994; Krachmarov et al., 2005; Krachmarov et al., 2006; McLellan et al., 2011; Pinter et al., 2004; Schonning et al., 1996).

The unliganded envelope spike possesses a high amount of potential energy that upon receptor binding is harnessed to facilitate the fusion process (Wyatt and Sodroski, 1998). Conformational

changes in gp120, subsequent to CD4 and coreceptor binding results in conformational changes in gp41. The N- and C-termini of g120 were crystallised in the HXBc2 core (stabilised with two domain CD4 and the monoclonal antibody 48d, which targets the CD4-induced epitope) in 2010 by Pancera *et al*. Fifty one and eighteen residues were added to the N- and C-termini of gp120 respectively. These additional residues included the gp41 interactive residues, which were determined via mutagenesis (Finzi et al., 2010). This structure revealed a mechanism whereby gp120 holds gp41 in the stable prefusion state, despite the seemingly weak interaction between the two. The inner domain was therefore further divided into the structurally invariant termini and 7-stranded β-sandwich together with three distinct, flexible and refoldable layers. The invariant structures act as a clamp on gp41 to prevent early transition of the molecule to prefusion intermediates. The three dynamic layers allow gp120 to possess the large conformational diversity it requires for both biological function (receptor binding) and immune evasion (Pancera et al., 2010).

In each of the previous gp120 core structures the truncated V1V2 stem protruded from a similar β-hairpin. In a very recent study, the V1V2 regions of 2 subtype C viruses, CAP45 and Zm109 were incorporated into separate protein scaffolds (derived from streptococcal protein G) with a known β-hairpin structure (McLellan et al., 2011). These scaffolded proteins were complexed with the PG9 monoclonal antibody, which targets a quaternary epitope that is only wholly apparent in the context of the trimeric envelope and is dependent on residues in the V2 region (Walker et al., 2009). The structure revealed a V1V2 region folded into four anti-parallel β-strands with connecting loops (Figure 6 B) and a hydrophobic core. The conserved residues located in four clusters (HXB2 positions 126 to 130, 152 to 164, 166 to 178 and 191 to 196) form the four strands. The intervening variable and highly glycosylated regions make up the two loops that connect the four strands.

A large degree of diversity exists between subtype B and C viruses in various regions of the envelope. Until 2009 only subtype B gp120 crystal structures had been resolved and given that subtype C is the predominant subtype worldwide, there has been a major drive recently to determine the structure of subtype C gp120 proteins. In 2010, Diskin and colleagues solved the gp120 core crystal structure for CAP210, a subtype C virus, stabilised with soluble CD4 (sCD4) and the CD4-induced 21c Fab. The subtype C gp120 core structure was highly similar to those obtained for subtype B viruses, apart from a few differences in the CD4 binding site and the V5 loop (Diskin et al., 2010).

1.3.4 The C3V4 region

Differences in the envelopes of subtype B and C viruses have been observed in numerous regions (Choisy et al., 2004; Gaschen et al., 2002; Gnanakaran et al., 2007; Korber et al., 1994). The C3 region and especially the alpha2-helix have been shown to be particularly variable in subtype C, in comparison to subtype B viruses where the V3 loop is instead very variable (Choisy et al., 2004; Gaschen et al., 2002).

As illustrated in Figure 7, the C3 region, situated slightly upstream of the V3 loop, includes the alpha2-helix and CD4 binding loop (Kwong et al., 1998). The C3 region extends from position 332 to 384 (HXB2 numbering) and contains between three and four potential N-linked glycans (PNGs), including the 332 glycan that has been described as a major neutralisation target (Gray et al., 2011; Kwong et al., 1998; Walker et al., 2011). The alpha2-helix is 18 amino acids in length and is located between positions 335 to 352 according to HXB2 numbering (Kwong et al., 1998).

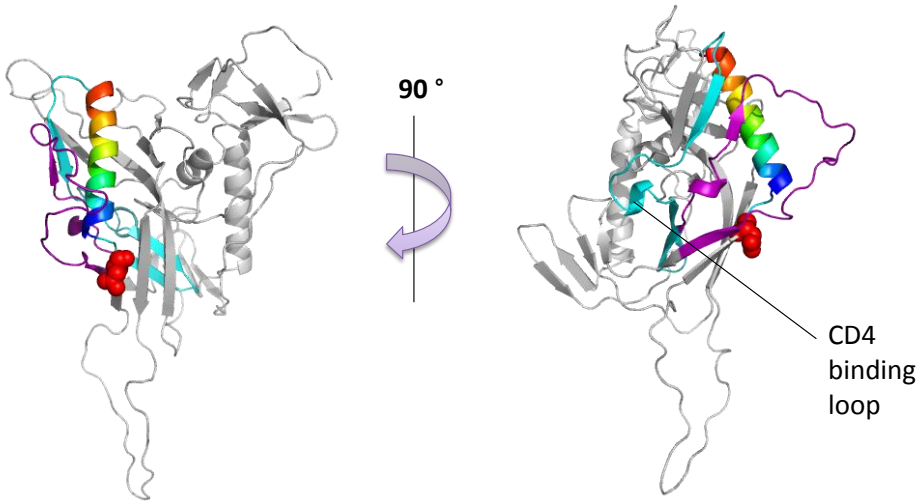

Figure 7. Ribbon representation illustrating the location of the C3V4 region within the monomeric gp120 core structure. Two views of a gp120 homology model, rotated about a 90 ° axis, highlight the position of the C3V4 region. The C3 region (cyan and rainbow colours) is situated in the outer domain of gp120 slightly upstream of the V3 loop. Within the C3 region is the alpha2-helix (rainbow colours) that is found in close proximity to the V4 loop (purple). Residue 332 is shown as red spheres and the CD4 binding loop is indicated. This model was created by threading a subtype C gp120 sequence into the structural alignment of the JR-FL, HXBc2 and CAP210 gp120 structures (PDB ID: 2B4C, 3JWD and 3LQA respectively).

A comparison of subtypes B and C, shows a consistently stronger charge anti-correlation between the alpha2-helix and V4 loop of subtype C, but not subtype B viruses (Gnanakaran et al., 2007). The C-terminus of the V4 loop may therefore interact with the N-terminus of the alpha2-helix. The highly dynamic and variable V4 loop is located between positions 385 and 418 (HXB2 numbering) (Figure 7) and has an average of four PNGs. In addition to sequence differences, the C3V4 region also differs between subtype B and C viruses in terms of electrostatic properties and length (Choisy et al., 2004; Gaschen et al., 1999; Gaschen et al., 2002; Gnanakaran et al., 2007). The C3V4 region has been shown to be a major target for nAbs in subtype C infection (Moore et al., 2008) and this region was therefore the focus of this study.

A comparison of the crystal structures of a subtype C (CAP210) and three subtype B (HXBc2, JR-FL and YU-2) gp120s (Diskin et al., 2010; Huang et al., 2007; Huang et al., 2005; Pancera et al., 2010) provides evidence that the position of the alpha2-helix within gp120 differs between the subtype B and C viruses. In Table 1, the root mean square distance (rmsd), measured in angstroms (Å), gives an indication of the structural similarity or difference between equivalent atoms in each of the gp120 structures being compared, with larger distances indicating a higher degree of variation (Carugo and Pongor, 2001). Comparisons between three different subtype B structures were made separately and then each subtype B structure was compared to the sole subtype C structure. These comparisons were made using all the residues forming the alpha1-helix and the alpha2-helix. The alpha1-helix, an example of a secondary structure that has a conserved position within gp120 irrespective of subtype, has an average rmsd value of 0.465 Å for subtype B to subtype B comparisons and 0.440 Å for subtype B to subtype C comparisons (Table 1). The similarity of the rmsd values for these two groups indicates that their position within gp120 is indeed similar across both clades. In contrast, larger average rmsd values were observed in the comparisons of the alpha2-helix of subtype B and C structures (1.320 Å) than those between different subtype B structures (0.608 Å) (Table 1). As shown in Table 1, the alpha2-helix of subtype C viruses appears to be more solvent-exposed when compared to the alpha2-helix of subtype B viruses. These observations indicate that the alpha2-helix differs in terms of its position in gp120 between the two clades.

Table 1. Comparison of the structural similarity of the alpha1-helix and the alpha2-helix of subtype B and C viruses.

Structures Compared	rmsd (Å) alpha1-helix	rmsd (Å) alpha2-helix	Alpha2-helix superimpositions
Hxbc2 (1GC1) JR-FL (2B4C)	0.497	0.722	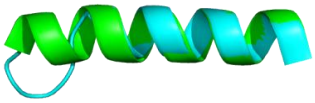
Hxbc2 (1GC1) YU-2 (2QAD)	0.487	0.459	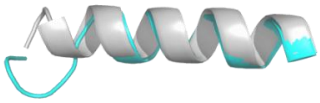
JR-FL (2B4C) YU-2 (2QAD)	0.411	0.644	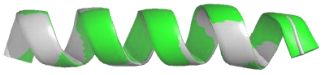
Hxbc2 (1GC1) CAP210 (3LQA)	0.450	1.305	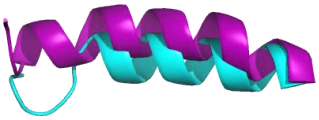
JR-FL (2B4C) CAP210 (3LQA)	0.444	1.376	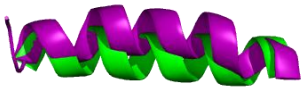
YU-2 (2QAD) CAP210 (3LQA)	0.427	1.278	

rmsd = root mean square distance

All-atom molecular dynamics simulations have shown that the alpha2-helix of subtype C viruses is more amphipathic than subtype B viruses, with distinct polar and non-polar faces that are indicative of a surface helix (Gnanakaran et al., 2007). This observation together with our aforementioned calculations supports the suggestion that the alpha2-helix is more exposed and more immunogenic in subtype C viruses than in subtype B viruses.

Within the alpha2-helix of subtype C viruses, residues were observed to switch charges over time (Gnanakaran et al., 2007). This was in contrast to subtype B viruses where the residues of the alpha2-helix maintained their charges through the course of infection. In addition, unique mutations in the alpha2-helix of subtype C viruses have been associated with resistance to neutralisation (Rong

et al., 2007b). The alpha2-helix may therefore contribute to neutralisation epitopes in subtype C viruses, but may also affect neutralisation epitopes through known interactions with the V4 loop or β-10, β-11, β-14 and β-24 strands (Gnanakaran et al., 2007). The V4 loop, as with the V1V2 and V3 loops, is generally shorter in subtype C viruses than subtype B viruses, which may enhance infectivity at the cost of exposure of neutralisation epitopes (Chohan et al., 2005; Derdeyn et al., 2004; Frost et al., 2005; Gnanakaran et al., 2007; Gray et al., 2007)

These observations are further supported by modelling of N-linked glycans onto the subtype C gp120 homology model described in Section 2.2, where three "unshielded" areas are apparent: the inner domain (Figure 8 A); the alpha2-helix (Figure 8 B) and the CD4, coreceptor and α4β7 binding sites (Arthos et al., 2008; Moebius et al., 1992; Rizzuto et al., 1998) (Figure 8 C).

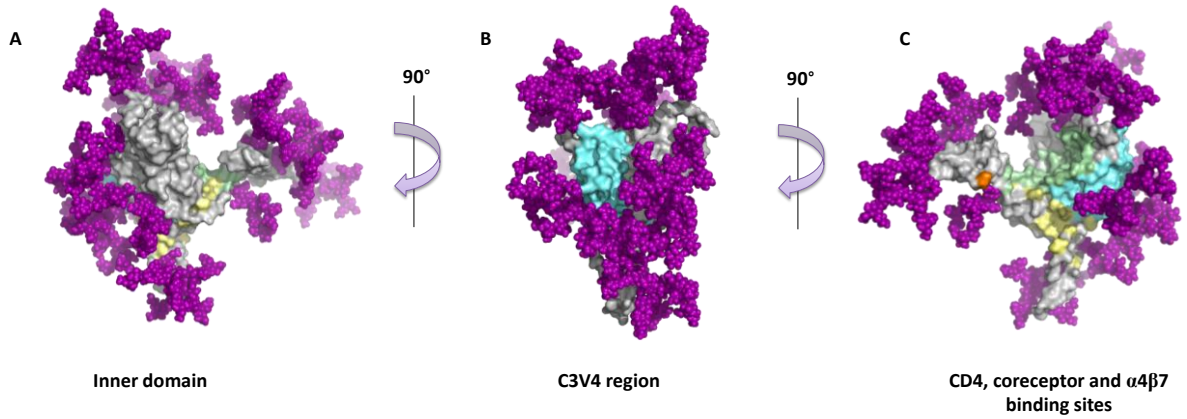

Figure 8. Surface view of a gp120 homology model showing areas that are unshielded by glycans. Three 90° rotations of a subtype C homology model described previously show areas on the gp120 monomer that are less densely glycosylated and thus "unshielded." **(A)** The inner domain (grey) of gp120 is sparsely glycosylated to facilitate ease of trimer association. **(B)** The alpha2-helix found within the C3V4 region (cyan) is clearly visible through the dense mass of N-linked glycans that cloak the outer domain. **(C)** The CD4 (green), coreceptor (yellow) and α4β7 (orange) binding sites are unshielded to facilitate receptor binding. Glycans are depicted as purple spheres. N-linked glycans were modelled using http://www.glycosciences.de/modeling/glyprot/php/main.php

The C3V4 region, specifically the alpha2-helix, is clearly visible through the dense glycan shield that surrounds the outer domain. Whilst the other two "unshielded" regions likely contain fewer glycans to facilitate specific functions of gp120, the C3 region may be a weak spot on gp120 that is specific to subtype C viruses. This supports the theory that the alpha2-helix is more exposed in subtype C viruses and suggests a reason for the highly immunogenic nature of the C3V4 region.

1.4 Neutralising antibodies

Neutralising antibodies (nAbs) recognise epitopes that are present on functional envelope spikes. This is in contrast to non-neutralising antibodies that bind to the highly immunogenic non-functional forms of the envelope, which have been proposed to serve as immunological decoys (Moore et al., 2006). The binding of nAbs to the envelope either blocks attachment or prevents conformational changes needed by both gp120 and gp41 for fusion to occur, thereby preventing HIV-1 infection (Wyatt and Sodroski, 1998). There are between 8 and 14 functional envelope spikes on each HIV-1 virion, all of which must be occupied by at least one nAb for complete neutralisation of the virus (Zhu et al., 2006).

The first detectable B cell responses to HIV-1 are antibody-virion complexes that arise 8 days after transmission (Tomaras et al., 2008). At 13 days post-infection (p.i.) the first free antibody response to HIV-1 develops with the production of binding, non-neutralising anti-gp41 antibodies (Tomaras et al., 2008). These initial anti-gp41 antibodies are polyreactive and highly somatically mutated (Liao et al., 2011). Therefore stimulation of memory B cells that were previously activated by non-HIV antigens occurs during acute HIV-1 infection (Liao et al., 2011). The first gp120-specific antibodies develop at least 27 days after transmission (Tomaras et al., 2008). These initial anti-gp41 and anti-gp120 binding antibodies have no effect on viremia and exert no pressure on the early viruses as determined by sequence analysis (Keele et al., 2008; Tomaras et al., 2008).

However, the autologous neutralising antibody (AnAb) response, which is directed to a person's own virus, is thought to develop much later at 12-20 weeks p.i. giving the virus ample time to establish infection (Delwart et al., 1997; Gray et al., 2007; Li et al., 2006a). The possibility of low levels of neutralising antibodies, undetectable with current assays, but nevertheless able to shape the viral population at early time points, has not yet been excluded (Bar et al., 2012). Despite the delay between transmission and the onset of the AnAb response, the pressure these antibodies exert on the viral population is substantial and therefore the virus continually evolves to escape their effects (Delwart et al., 1997; Frost et al., 2005; Moore et al., 2009; Richman et al., 2003; Rong et al., 2009; Wei et al., 2003). Together, in a continual evolutionary "arms race", both virus and antibody adapt in response to each other (Figure 9). This rapid viral escape, a direct consequence of the error-prone viral reverse transcriptase, occurs in the form of shifts in the glycan shield, single amino acid substitutions as well as insertions and deletions (indels) especially in the variable regions (Moore et

al., 2009; Nakowitsch et al., 2005; Rong et al., 2009; Sagar et al., 2006; Tang et al., 2007; Wei et al., 2003).

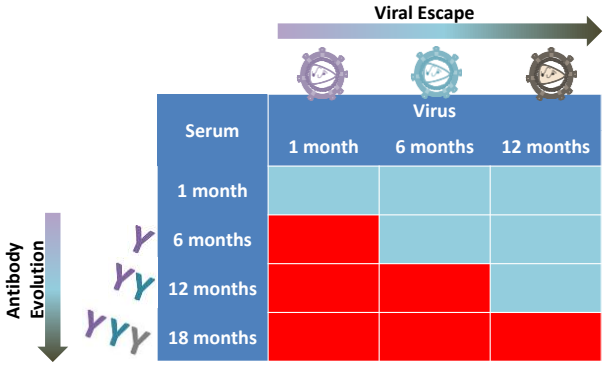

Figure 9. Schematic depicting the "evolutionary arms race" between HIV-1 and the host immune response over time. The 1 month p.i. serum sample from an infected individual is unable to neutralise viruses isolated from any time point as the antibody response only develops between 12 and 20 weeks p.i. After the development of the initial AnAb response, continual viral escape is followed by antibody evolution. Therefore a given serum sample cannot neutralise the virus present at the same time point. Red squares indicate sensitivity and blue squares indicate resistance of the virus to that serum sample.

Individuals infected with subtype C viruses tend to develop a highly type-specific, yet more potent AnAb response than those infected with subtype B viruses (Li et al., 2006a; Li et al., 2006b). These early responses have a limited number of specificities (Lynch et al., 2011; Moore et al., 2009; Rong et al., 2009) and although the V4 and V5 loops do play a minor role as neutralisation epitopes for AnAbs, the larger majority of the response appears to be directed to the V1V2 loop or the C3V4 region of gp120 in subtype C infections (Moore et al., 2008; Moore et al., 2009). Although the early AnAb response in subtype C infections has been shown to differ somewhat within the first year of infection compared to subtype B infections (Gray et al., 2007; Li et al., 2006a; Moore et al., 2008; Moore et al., 2009), a recent study has shown that early AnAbs in subtype B infections target an epitope at the base of the V3 loop that involves PNGs in both the C3 and V4 regions (Tang et al., 2011), suggesting the presence of a common epitope in both subtype types.

Unlike AnAbs which develop in all HIV-1 infected individuals, only approximately 10 to 20% of HIV-1 infected individuals develop antibodies that are capable of neutralising heterologous viruses, including viruses from different subtypes (Euler et al., 2010; Gray et al., 2011; Piantadosi et al., 2009; Sather et al., 2009; Walker et al., 2009; Walker et al., 2010). These broadly neutralising antibodies (bnAbs) often only develop after at least 2 years of infection (Gray et al., 2011) and target three broad categories of epitopes on the envelope: the CD4 binding site (such as b12 and VRC01) (Burton

et al., 1994; Wu et al., 2010), the MPER (such as 2F5 and 4E10) (Burton et al., 1994; Muster et al., 1993; Stiegler et al., 2001; Zwick et al., 2001) and the glycan shield (such as 2G12, PGT128 and PG9) (Trkola et al., 1996; Walker et al., 2011; Walker et al., 2009). The relationship between early AnAbs and later bnAbs is not known and current research aims to determine the ontogeny of bnAbs through the isolation of AnAbs over the course of HIV-1 infection.

1.5 Prevention of HIV-1 through vaccine-induced immunity

Passive or active antibody-based immunity is important for protection against numerous human pathogens, such as rabies virus, hepatitis B virus, mumps virus, respiratory syncytial virus, measles virus, rubella virus, human herpesvirus 3, human enterovirus C and cytomegalovirus (Bahmanyar et al., 1976; Beasley et al., 1983; Gellis et al., 1945; Groothuis et al., 1993; Hammon et al., 1953; Janeway, 1945; Korns, 1952; Ross, 1962; Snydman et al., 1987). Therefore the role of antibodies in protection from HIV-1 infection has been a focus of many studies.

Following the development of a simian-human immunodeficiency chimeric virus (SHIV), which expresses an HIV-1 envelope in a SIV backbone, the potential role of anti-HIV-1 nAbs in mediating protection from SHIV infection in non-human primate (NHP) models was investigated (Li et al., 1992; Luciw et al., 1995; Sakuragi et al., 1992; Shibata et al., 1991). A cocktail of two or more anti-HIV-1 nAbs, administered intravenously, was shown to offer sterilising protection after both intravenous and mucosal SHIV challenge (Mascola et al., 1999; Mascola et al., 2000) and topically administered nAbs could protect against vaginal SHIV challenge (Veazey et al., 2003). In addition protection from oral SHIV challenge in neonatal rhesus macaques after prenatal nAb administration, and prior to postnatal nAb administration, has been observed (Baba et al., 2000; Hofmann-Lehmann et al., 2001). These studies showed that high concentrations of nAbs were required to prevent SHIV infection in both the adult and neonatal rhesus macaques. However two subsequent studies showed that intravenous administration of low concentrations of the anti-HIV-1 monoclonal antibody 2G12 in NHPs could confer protection, although the underlying mechanisms were not determined (Hessell et al., 2009; Parren et al., 2001).

Both nAbs and binding antibodies can also exert anti-viral effects *in vivo* by other mechanisms (Parren and Burton, 2001). Proteins of the complement system as well as the crystallisable fragment

(Fc) receptors can bind to the Fc part of an antibody to cause activation of the complement system or antibody-dependent cellular cytotoxicity (ADCC) respectively (Burton, 2002). A study in 2007 showed that binding of the Fc receptor, but not complement, enhanced antibody-mediated protection from SHIV infection, although this was not an absolute requirement (Hessell et al., 2007).

In 2005 Trkola and colleagues showed a delay in viral rebound upon ART cessation when nAbs were administered to HIV-1 infected individuals (Trkola et al., 2005). The effect of these nAbs was more pronounced in acutely, rather than chronically HIV-1 infected individuals, but nonetheless highlighted the fact that nAb responses have the capacity to supress HIV-1 replication *in vivo*.

Despite the fact that these studies support a role for nAbs in HIV-1 control, eliciting bnAbs has proven difficult. Although more than 30 candidate HIV-1 vaccines, such as viral vectors with HIV-1 gene inserts, HIV-1 virus-like particles, soluble HIV-1 DNA plasmids or HIV-1 proteins, have been used to immunise NHPs, only 4 have progressed to Phase IIb and Phase III human clinical trials (D'Argenio and Wilson, 2010; Mascola and Montefiori, 2010; McElrath and Haynes, 2010; Plotkin and Plotkin, 2011; Ross et al., 2010). The RV144 trial, which made use of a recombinant canarypox vector with a gp120 protein boost regimen, was the only one of these four trials that showed efficacy, albeit modest at 31% (Gilbert et al., 2011; Rerks-Ngarm et al., 2009). A case control analysis compared the immune response in uninfected vaccinees, infected vaccinees and infected individuals who received the placebo (Haynes, 2011). This analysis showed that development of an anti-V2 response was inversely proportional to infection, suggesting an important role for antibodies in the prevention of HIV-1 infection.

The aforementioned facts illustrate the potential of antibody-mediated immune responses in HIV-1 disease prevention. However due to the limited successes of past HIV-1 vaccine development strategies, further investigation into the interaction between the host immune responses and the pathogenesis of the virus is needed. This study therefore investigated the interplay between antibody-mediated immune responses and HIV-1 with specific reference to the C3V4 region of gp120 of the viral envelope.

1.6 Study objectives

The C3V4 region is strongly immunogenic and is a major target for early AnAbs in HIV-1 subtype C infections (Moore et al., 2008). The alpha2-helix, found within the C3 region, has been implicated in contributing to the immunogenicity of the region in subtype C viruses (Gnanakaran et al., 2007). The study of autologous responses may inform HIV-1 vaccine design. This study therefore proposed to characterise the early AnAb response directed to the C3V4 region in subtype C infected individuals. Firstly, understanding the development and specificities of early AnAb responses may inform the ontogeny of epitopes that elicit bnAbs. Second, an understanding of neutralisation escape pathways from early, easily-escaped, type-specific responses may inform the design of immunogens that have a reduced potential for escape. We hypothesised that a more exposed C3V4 region may lead to an early autologous anti-C3V4 response and that mutations in the alpha2-helix mediate neutralisation escape from these anti-C3V4 responses.

1.6.1 Main objectives

The main objectives of this study were to characterise anti-C3V4 neutralising responses in 17 subtype C infected individuals and to investigate mechanisms of escape employed by the virus.

1.6.2 Specific objectives

- To determine the frequency of anti-C3V4 responses in 17 subtype C infected individuals.
- To determine virological factors that contribute to the elicitation of anti-C3V4 responses.
- To characterise the effect of anti-C3V4 responses on overall neutralisation titres.
- To investigate the role of the alpha2-helix in mediating neutralisation escape.
- To determine whether neutralisation escape can occur through regions that are structurally proximal to the alpha2-helix.

Chapter 2: Materials and Methods

2.1 The CAPRISA 002 Acute Infection cohort

The CAPRISA 002 Acute Infection cohort was established in Durban, South Africa in 2004 by enlisting a group of 245 high risk HIV negative women. Sixty participants subsequently became infected and have volunteered blood samples consistently at various times points before and after seroconversion (Gray et al., 2007; van Loggerenberg et al., 2008). Enrolment samples for this project were obtained at the earliest available time point following HIV-1 infection. Individuals from the CAPRISA 002 cohort were selected for this study based on the availability of a cloned pre-seroconversion or enrolment (acute) envelope, previous and on-going characterisation of neutralisation breadth and longitudinal follow-up exceeding 2 years p.i.

Five individuals (CAP45, CAP63, CAP84, CAP88 and CAP239) were previously assessed for a neutralising antibody response targeting the C3V4 region of the envelope (Moore et al., 2008). In this project a further seventeen individuals were classified as either C3V4 responders or non-responders. Five individuals (CAP136, CAP206, CAP228, CAP244 and CAP255) who developed a C3V4 response were characterised in greater depth.

2.2 Cell lines

The JC53BL-13 (TZM-bl) cell line, engineered by J. Kappes and X. Wu, was obtained from the NIH AIDS Reagent and Reference Program. The human epithelial kidney (HEK) derived 293T/17 cell line was obtained from Dr George Shaw (University of Alabama, Birmingham, AL). Both cell lines were cultured in Dulbecco's Modified Eagle Medium (DMEM) (Gibco BRL Life technologies) containing 10 % heat-inactivated foetal bovine serum (FBS) (Gibco BRL Life technologies) and 50 µg/ml gentamicin (Sigma-Aldrich). Cell monolayers were disrupted at confluency by treatment with 0.25 % trypsin in 1 mM ethylenediaminetetraacetic acid (EDTA) (Sigma-Aldrich).

2.3 Production of env-pseudotyped viruses (pseudoviruses)

Envelope-containing plasmids were co-transfected into 293T/17 cells with the pSG3$^{\Delta Env}$ plasmid (which encodes the entire HIV-1 genome but contains stop codons in the *env* gene). The pSG3$^{\Delta Env}$ plasmid, engineered by J. Kappes and X. Wu, was obtained from the NIH AIDS Reagent and Reference Program. Pseudoviruses (PSVs) generated by this method have functional envelopes from the *env*-expressing plasmid and therefore can infect susceptible reporter cells, however they are

unable to produce infectious progeny virions thereafter due to the incorporation of an incomplete HIV-1 genome.

293T/17 cells (2 x 10^6 cells) were seeded into 10 cm^2 sterile cell culture dishes in DMEM containing 10 % heat-inactivated FBS, 25 mM 4-(2-hydroxyethyl)-1-piperazineethanesulfonic acid (HEPES) (Gibco BRL Life technologies) and 50 µg/ml gentamicin (complete DMEM). Dishes were incubated at 37°C, 5% CO_2 for 24 hours.

Transfection reactions were prepared by incubating 500 µl of serum free DMEM with 24 µl of FuGENE®6 Transfection Reagent (Roche) before adding 4 µg each of the pSG3$^{\Delta Env}$ plasmid and an envelope-containing plasmid. This transfection mixture was mixed gently and incubated for 45 minutes before being added drop by drop to the 293T/17 cells. The transfected cells were incubated at 37 °C, 5 % CO_2 for 48 hours, after which supernatants containing the PSVs were harvested. The supernatants were filtered through a 0.45 µm filter (Satorius) and additional FBS was added to bring the final percentage of FBS to 20 % (as a cryopreservant). These stocks were divided into 1 ml aliquots and frozen at -70 °C until use.

2.4 Neutralisation assay

The neutralisation assay used in this study measures the ability of antibodies to prevent HIV infection in JC53BL-13 (TZM-bl) cells. These are HeLa cells engineered to constitutively express the CD4, CCR5 and CXCR4 receptors (Platt et al., 1998). The JC53BL-13 cells also contain the firefly luciferase gene, under the control of the HIV-1 long-terminal repeat (LTR) (Montefiori, 2004; Wei et al., 2002; Wei et al., 2003). Infection of these cells with PSVs results in induction of the reporter luciferase gene *in trans* by the viral tat protein. This luminescence is directly proportional to the number of infectious viral particles or PSVs infecting the cells and inversely proportional to the ability of nAbs to block infection (Montefiori, 2009; Wei et al., 2002).

Plasma samples were heat-inactivated at 56 °C for 45 minutes to inactivate complement (Montefiori et al., 1994). The first two columns of a sterile, low evaporation 96-well plate (Corning) were used as a cell control and virus control respectively (Figure 10). Five plasma samples were serially diluted

(from a starting dilution of 1:40) in duplicate in the remaining ten columns. The serially diluted plasma was incubated with a dilution of PSV that yielded relative light units (RLU) of 40 000 in a total volume of 50 µl complete DMEM for 1 hour at 37 °C, 5 % CO_2. Twenty microlitres JC53BL-13 cells at a concentration of 5 x 10^5 cells/ml containing 70 µg/µl diethlyaminoethyl (DEAE)-dextran (Sigma-Aldrich) was added per well. DEAE-dextran is polycationic and is known to enhance viral infectivity (Kaplan, *et al* 1967; Fiala, *et al* 1969; Park *et al* 1998). Twenty-four hours later 130 µl of complete DMEM was added per well.

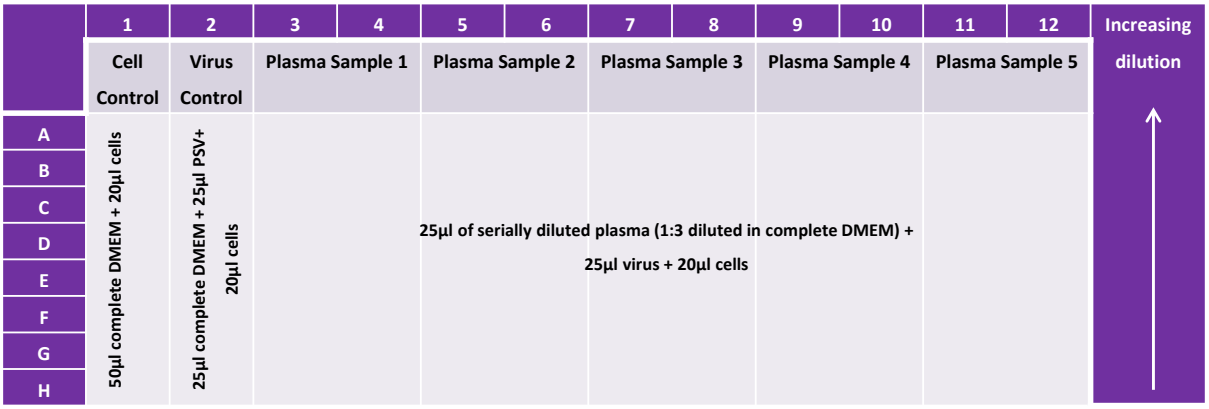

Figure 10. Schematic layout of a typical neutralisation assay. Column 1 represents the cell control, containing only complete DMEM and cells. Column 2 represents the virus control containing complete DMEM, virus and cells. Columns 3 to 12 represent wells containing serial plasma dilutions incubated with PSV and cells.

Twenty-four hours thereafter, luminescence was measured using the Bright-Glo™ Luciferase Assay System (Promega). These reagents include a detergent for lysing the cells and luciferin (the substrate upon which luciferase acts). In infected cells translation of the gene encoding firefly luciferase results in oxidation of luciferin in a light-producing reaction. A hundred microlitres of the supernatant was removed from each well before addition of 100 µl Bright-Glo™ Luciferase Assay reagent. The reagent was incubated for 2 minutes at room temperature to allow for cell lysis. The supernatant and cell layer were mixed by pipette action and 150 µl was transferred to a LumiNunc™ 96 Microwell™ black plate. Luminescence was measured in RLUs using the Victor^3 1420 Multilabel Counter (Perkin-Elmer). The antibody titre was reported as the dilution of plasma needed to inhibit half the viruses from infecting the reporter cell (ID_{50}). Neutralisation assays were repeated a minimum of three times.

2.5 Generation of C3V4 chimeras by overlapping polymerase chain reaction

An overlapping polymerase chain reaction (PCR) strategy was used to generate C3V4 envelope chimeras (Figure 11). The C3V4 region from a previously cloned envelope of interest, and flanking regions from a resistant envelope backbone were amplified in separate reactions. Thereafter the fragments were linked using overlapping PCR. Primers were designed using the OligoCalc website to calculate the melting temperatures and prevent potential internal secondary structures (Kibbe, 2007).

The high fidelity PfuUltra™ II enzyme and 10X PfuUltra™ II reaction buffer (Stratagene) were used as per the manufacturer's recommendations with 0.4 pmol/µl primers (see Appendix 1), 0.2 mM deoxynucleoside triphosphates (dNTPs) (Roche), and between 5 ng and 50 ng of plasmid DNA. Each reaction was made up to 50 µl with sterile water (Sigma). The thermocycling conditions were as follows: initial denaturation at 98 °C for 3 minutes; 35 cycles of 98 °C for 30 seconds, 55 °C for 30 seconds, 72 °C for 30 seconds per 750 bp depending on the length; and a final extension of 72 °C for 7 minutes. PCR products were screened on 1 % molecular grade agarose (Bioline) gels.

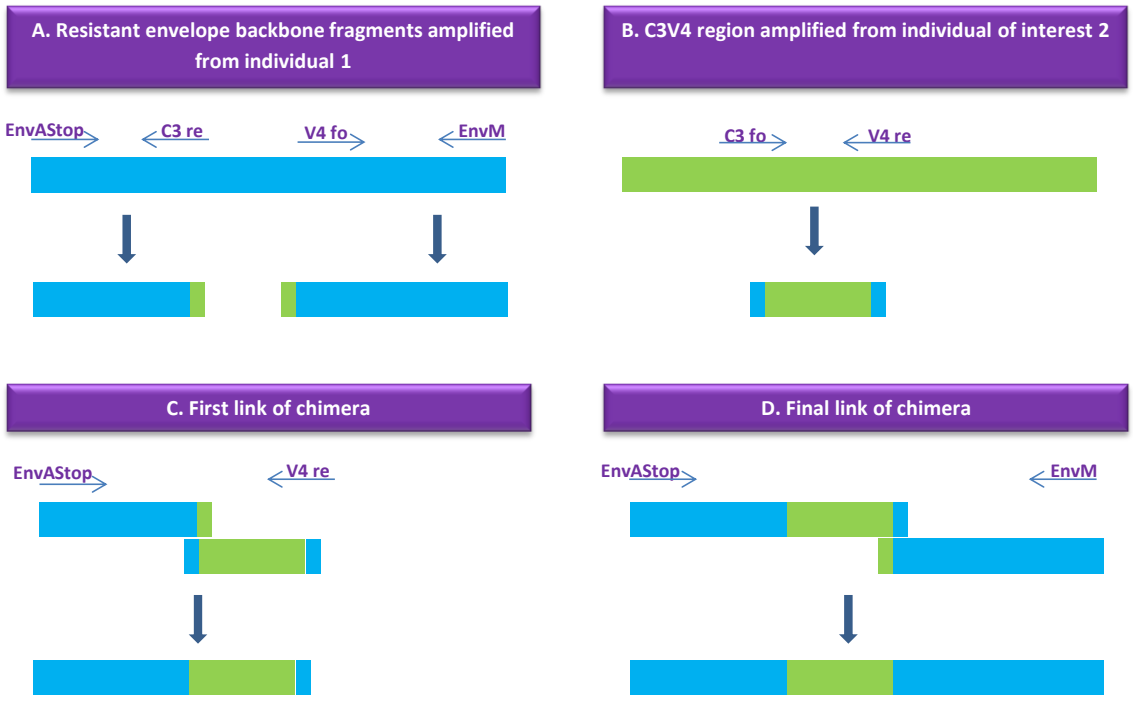

Figure 11. C3V4 chimera generation. **(A)** Amplification of the two regions flanking the C3V4 region from a neutralisation resistant envelope backbone. **(B)** Amplification of the C3V4 region from the participant of interest. **(C and D)** Overlapping PCR reactions that produce the C3V4 envelope chimera. Primers are represented by small labelled arrows. Sequences of primers are shown in Appendix 1.

2.6 Gel extraction of DNA

PCR amplified DNA fragments of the desired size were gel purified using the QIAquick Gel Extraction Kit (QIAGEN) which utilises a specialised silica membrane to adsorb DNA in the presence of high salt concentrations. Excised agarose gel slices containing the desired bands were weighed, and three volumes of buffer QG were added to 1 volume of gel to solubilise the agarose and optimise the pH and salt concentration. This was incubated at 50 °C for 10 minutes (to melt the gel) and mixed thoroughly. This mixture was transferred to a QIAquick spin column and centrifuged at 14 000 rpm for 1 minute on a table-top microcentrifuge. All subsequent centrifugation steps were carried out using a table-top microcentrifuge, unless units are given in G. Five hundred microlitres of QG buffer followed by 750 µl PE buffer were run through the column at 14 000 rpm for 1 minute each. The column was dried by centrifugation at 14 000 rpm for 1 minute before eluting the DNA in 30 µl of the low salt containing EB buffer (centrifuged at 14 000 rpm for 1 minute). DNA was quantified using the NanoDrop® ND-1000 Spectrophotometer (Thermo Scientific).

2.7 Ligation into expression vector

Gel extracted 3 kb full length chimeric envelopes were ligated into the pcDNA™ 3.1D/V5-His-TOPO® vector using the pcDNA™ 3.1 Directional TOPO® Expression Kit (Invitrogen). This vector makes use of oligonucleotides charged with topoisomerase I enzyme from the Vaccinia virus to directionally clone blunt-ended PCR products. A 5' GTGG TOPO®-charged overhang in the vector attacks the CACC four-base sequence in the PCR product, anneals to it and stabilises it in the appropriate direction. The CACC sequence and a Kozak translation initiation site were included at the 5' end of the EnvAStop primer. The vector encodes the β-lactamase gene which inactivates the antimicrobial activity of ampicillin. Briefly, 1 µl of salt solution (1.2 M NaCl, 0.06 M $MgCl_2$) was added to 10 ng insert followed by 1 µl of pcDNA™ 3.1D/V5-His-TOPO® and reactions were made up to 6 µl with sterile water supplied in the ligation kit. This ligation mixture was then incubated at room temperature for 10 minutes before being transformed into bacterial cells (as described in Section 2.8).

2.8 Transformation of XL-10 Gold cells

XL-10 Gold Ultracompetent cells (Stratagene) were thawed on ice. For every 150 µl of thawed cells, 4 µl of β-mercaptoethanol (Stratagene) was added to increase transformation efficiency. Each 6 µl ligation reaction was added to 50 µl cells. The transformation reaction was incubated on ice for 30 minutes, followed by a heat shock for 35 seconds at 42 °C. The heat shock method facilitates cellular

uptake of DNA by creating pores in the cell membranes. Super optimal broth with catabolite repression (SOC) media (Invitrogen), which enhances transformation efficiency and recovery of cells (Hanahan, 1983), was added to the transformation reaction and incubated, while shaking at 225 rpm at 37 °C, for 1 hour. The transformed cells (100 µl) were plated on LB (Luria-Bertani) Agar with 100 µg/ml ampicillin (Sigma-Aldrich) and incubated overnight at 37 °C.

2.9 Colony polymerase chain reaction

Colony PCR was used to screen for bacterial clones containing plasmids with inserts of the correct size and orientation using the T7 primer (which binds the vector at the 5' end of the insert) and the EnvM primer (which binds the 3' end of the envelope insert). Individual colonies were inoculated into a single well of a 96-well plate containing 100 µl of LB broth (Invitrogen) containing 100 ng/ml ampicillin. The 96-well plate was incubated at 225 rpm at 37 °C for 90 minutes. During this incubation, the colony PCR mixture was prepared.

The PCR master mix contained SuperTherm *Taq* polymerase and SuperTherm Taq polymerase buffer (Hoffman-La-Roche) as per the manufacturer's instructions, 0.5 mM $MgCl_2$ (Hoffman-La-Roche), 0.2 mM dNTPs (Roche), 0.4 pmol/µl primer T7 and 0.4 pmol/µl primer EnvM. Each reaction was made up to 10 µl with sterile water (Sigma). The master mix was dispensed into a 96-well PCR plate. One microlitre of bacterial culture broth from each colony was added to the colony PCR plate as the template. The PCR cycling conditions were as follows: 94 °C for 5 minutes, 35 cycles of 94 °C for 30 seconds, 55 °C for 30 seconds, 68 °C for 4 minutes and a final extension time of 68 °C for 10 minutes. The products of the colony PCR were screened for 3 kb inserts on a 1 % molecular grade agarose gel.

2.10 Plasmid extraction

Colonies containing plasmids with an insert of the correct size and in the correct orientation were cultured in 5 ml LB broth containing 100 µg/ml ampicillin overnight at 37 °C while shaking at 225 rpm. Plasmids were extracted using the QIAprep Spin Miniprep kit (QIAGEN) which utilises a silica membrane spin column to adsorb and elute DNA at high and low salt concentrations respectively. Cultures were centrifuged at 5 000 rpm for 10 minutes at 4 °C and pellets were resuspended in 250 µl Buffer P1 (containing RNase A). Cells were lysed with concurrent denaturation of chromosomal and plasmid DNA by addition of 250 µl Buffer P2 (containing sodium dodecyl sulphate (SDS) and

sodium hydroxide). Addition of 350 µl Buffer N3 caused precipitation of proteins, chromosomal DNA, cellular debris and SDS. The reactions were centrifuged at 13 000 rpm for 10 minutes at room temperature. Supernatants were transferred to a QIAprep spin column and centrifuged at 13 000 rpm for 1 minute. To remove endonucleases, 500 µl Buffer PB was passed through the column at 13 000 rpm for 1 minute. Salts were removed by addition of 750 µl Buffer PE, passed through the column at 13 000 rpm for a further 1 minute. Excess Buffer PE was removed by a 1 minute centrifugation at 13 000 rpm. Fifty microlitres Buffer EB was passed through the column at 13 000 rpm for 1 minute to elute the plasmid DNA, which was quantified using the NanoDrop® ND-1000 Spectrophotometer (Thermo Scientific).

2.11 Sequence validation of chimeras

Cloned chimeric envelopes were sequenced to confirm chimerism. The Sanger chain termination method was used, with each sequencing reaction containing 300 ng of plasmid DNA, 0.2 pmol/µl sequencing primer, 5.4 µl half dye buffer (Bioline), 2.6 µl ABI Prism BigDye® Terminator V3.1 Cycle Sequencing Ready Reaction reagent (Applied Biosystems), made up to 20 µl with sterile distilled water (Sigma-Aldrich). The BigDye® Terminator V3.1 Cycle Sequencing Ready Reaction reagent includes the four dideoxynucleoside triphosphates (ddNTPs) each labelled with a different fluorescent dye. This reaction was thermocycled as follows: 25 cycles of 96 °C for 10 seconds, 50 °C for 5 seconds and 60 °C for 4 minutes. The primer sequences are shown in Appendix 1.

The products were purified by alcohol precipitation. For a full 96-well plate of sequencing reactions, a mixture containing 8 ml absolute ethanol (Platinum Line from Associated Chemical Enterprises) and 320 µl 3 M sodium acetate (Invitrogen) pH 5.2 was made. Fifty microlitres of this mixture were added to each well and plates were centrifuged at 2 000 x g for 30 minutes. Plates were inverted and supernatants were removed by centrifuging at 150 x g for 1 minute. After addition of 100 µl ice-cold 70% ethanol the plates were centrifuged for a further 5 minutes at 2000 x g followed by removal of the ethanol as described previously. The products were dried for 5 minutes at 60 °C before being resuspended in 10 µl of Hi-Di™ Formamide (Applied Biosystems). Capillary electrophoresis was used to separate the extension products on the ABI Prism® 3100 Genetic Analyzer. Chromatograms were edited and assembled into complete gp160 sequences using Sequencher 4.5 (Gene Codes Corporation) and alignments were created using BioEdit 7.0.9 (Ibis Biosciences). Chimera sequences were compared with existing sequences of both parental envelopes.

2.12 Single genome amplification

A pivotal pre-requisite for the success of this project was the amplification of envelopes from individual HIV genomes as opposed to quasispecies (a group of closely related, but non-identical viruses). This allows for phenotypic characteristics to be attributed to exact genotypes. Previous methods of deriving viral sequences from HIV-infected samples, such as bulk and near-endpoint limiting dilution of samples, were limited in that they caused the generation of PCR recombinants *in vitro* that did not exist *in vivo*, introduction of *Taq* polymerase-mediated errors as well as a non-proportional representation of sequences due to template resampling (Salazar-Gonzalez et al., 2008). The use of single genome amplification (SGA) prevents intragenic recombination and reduces *in vitro* artefacts, with PCR errors introduced at a rate of less than 8 x 10^{-5} nucleotides per 3 kb envelope for the entire procedure due to the use of high fidelity enzymes (Salazar-Gonzalez et al., 2008). HIV-1 envelope genes were amplified from cDNA that was diluted based on the viral load of the original plasma sample. If less than 30% of reactions contained a first round PCR product, then according to Poisson distribution each PCR product would have been generated from a single template in 80 % of cases (Salazar-Gonzalez et al., 2008).

2.12.1 Viral RNA extraction

HIV-1 RNA was extracted from plasma samples at 6 or 12 months p.i. using the QIAmp Viral RNA Mini Kit (QIAGEN). This kit utilises silica gel-based columns that selectively bind nucleic acids. The plasma sample was thawed on ice. In the interim 560 µl of Buffer AVL was added to 5.6 µl of carrier RNA and vortexed briefly, before addition of 140 µl of the plasma sample. This mixture was incubated at room temperature for 10 minutes to allow the chaotropic elements in Buffer AVL to inactivate any RNases as well as to lyse the viral particles. The carrier RNA enhances RNA binding to the column and reduces RNase activity. After addition of 560 µl absolute ethanol the sample was briefly centrifuged at 8 000 rpm. The sample-Buffer AVL-ethanol mixture was added to a spin column provided in the kit and centrifuged at 8 000 rpm for 1 minute. Contaminants were washed away through the addition of 500 µl Buffer AW1 followed by centrifugation at 8 000 rpm for 1 minute. An additional step to eliminate contaminants was performed through the addition of 500 µl Buffer AW2 followed by centrifugation at 13 200 rpm for 3 minutes. The flow through was discarded and the column centrifuged at 13 200 rpm for 1 minute to remove residual buffer. The column was incubated for 1 minute with 50 µl Buffer AVE (RNase free water with 0.04 % sodium azide) before being centrifuged at 8 000 rpm for 1 minute to elute the RNA, which was used immediately for cDNA synthesis.

2.12.2 cDNA synthesis

The Invitrogen SuperScript® III Reverse Transcriptase, genetically modified to reduce RNase H activity and maintain cDNA synthesis at the high temperatures required to melt secondary structure, was used to synthesise viral complementary DNA (cDNA) from extracted RNA as follow: an initial mixture of 8.5 µl sterile water (Sigma-Aldrich), 0.4 pmol/µl OFM19 primer, 0.8 nmol/µl dNTPs (Roche) and 50 µl RNA was incubated in a thermocycler for 5 minutes at 65 °C. A second mixture consisting of 20 µl 5X First Strand Buffer (Invitrogen), 5 nmol/µl DTT (Invitrogen), 200 U Protector RNase Inhibitor (Roche) and 1 000 U SuperScript® III Reverse Transcriptase was added to the first mixture. The resulting 100 µl reaction was incubated as follows: 50 °C for 1 hour, 55 °C for 1 hour (to melt secondary structure and allow cDNA synthesis) and 70 °C for 15 minutes (to heat inactivate the SuperScript® III Reverse Transcriptase). Once cDNA synthesis was complete, 2 U RNase H (Invitrogen) was added to the reaction and incubated at 32 °C for 20 minutes to digest the DNA/RNA hybrid.

2.12.3 First and second round of polymerase chain reaction amplification

Platinum®*Taq* DNA Polymerase High Fidelity enzyme (Invitrogen) (a mixture of a high fidelity and a 3' to 5' proofreading polymerase) was used for first and second round SGAs. This enzyme includes a Platinum *Taq* Antibody that forms complexes with, and inhibits the polymerase activity until the initial PCR denaturation at 94 °C, which results in increased specificity, sensitivity and yield.

For each first round reaction the following reagents were used: 10X High Fidelity PCR Buffer (Invitrogen) as per the manufacturer's direction, 2 mM $MgSO_4$ (Invitrogen), 0.2 mM dNTPs (Roche), 0.5 U Platinum®*Taq* DNA Polymerase High Fidelity enzyme, 0.2 pmol/µl OFM19 and VIF1 with the reaction made up to 19 µl with sterile water (Sigma-Aldrich). cDNA was diluted based on the viral load of the sample. For example, a viral load of 20 000 copies/ml would yield approximately 2000 cDNA copies in a 100 µl cDNA reaction, which would then be diluted to result in a 1 copy/µl concentration. Diluted cDNA made up 1 µl of the reaction volume. The cycling conditions included an initial denaturation at 94 °C for 2 minutes, 35 cycles of 94 °C for 15 seconds, 55 °C for 30 seconds, 68 °C for 4 minutes, and a final extension of 68 °C for 20 minutes. First round SGA products were used as templates for second round reactions before being stored at -70 °C.

Second round amplification was performed using the same reagents except the EnvAStop and EnvM primers (Appendix 1) were used and the template consisted of 1 µl of the first round reactions. The thermocycling conditions were 94 °C for 5 minutes, 45 cycles of 94 °C for 15 seconds, 55 °C for 30 seconds and 68 °C for 4 minutes, with a final extension of 68 °C for 20 minutes. The products were visualised on a 1 % agarose gel. If less than 30 % of the total number of reactions were positive these were considered to be derived from single templates and selected for further use. Independent PCRs were performed at least twice for each cDNA.

The first and second round SGA reactions were performed using small volumes as most were required to be negative. Therefore positive single genome amplicons were re-amplified from their first round products in larger reaction volumes (50 µl each) for sequencing and cloning. Reactions were performed with Platinum®*Taq* DNA Polymerase High Fidelity enzyme and products were purified with the QIAquick PCR Purification Kit (QIAGEN). Five volumes of Buffer PBI were added to the PCR reactions and mixed before being loaded onto a QIAquick column and centrifuged for 1 minute at 14 000 rpm. Seven hundred and fifty microlitres of Buffer PE was added and centrifuged for 1 minute at 14 000 rpm and after removal of the flow-through the column was centrifuged again. The DNA was eluted from the column after incubating for 1 minute with 50 µl Buffer EB by centrifugation at 14 000 rpm for 1 minute.

Sequencing (as described in section 2.11) initially only of the V1V2 region was performed on purified amplicons. The V1V2 region is highly variable and therefore facilitates detection of double peaks, indicative of amplicons derived from more than one envelope gene. If double peaks were detected, these amplicons were discarded. If no double peaks were detected, the entire gp160 envelope gene was sequenced. If double peaks were present in the fully sequenced envelope, these amplicons were also discarded.

2.13 Sequence alignments, phylogenies and cloning

Sequence alignments, which included the acute sequences derived from previous studies (Abrahams et al., 2009; Gray et al., 2007)were constructed using BioEdit 7.0.9 (Ibis Biosciences). The neighbour-joining (distance), maximum likelihood and Bayesian interference (character) methods were used to generate phylogenetic trees in Mega5. Multiple methods (minimum evolution, maximum likelihood,

maximum parsimony and neighbour-joining) were employed to establish upper and lower limits of confidence, compensate for long branch attraction and confirm the reliability of phylogenies. Phylogenetic tree reliability was further confirmed using the bootstrapping method.

A subset of amplicons, chosen based on the diversity of the phylogenies, was selected for further investigation. These amplicons were re-amplified with the high fidelity PfuUltra™ II enzyme to generate a sufficient amount of error-free PCR product in the same reaction described in section 2.5. The reaction products were run on a 1 % agarose gel and the 3 kb bands were gel extracted, ligated and cloned into pcDNA™ 3.1D/V5-His-TOPO® and transformed into XL-10 Gold cells (as described in section 2.8). PSVs for these 6 month and 12 month envelope clones were produced (as described in section 2.3).

2.14 Site-directed mutagenesis

The QuikChange® Lightning Site-Directed Mutagenesis Kit (Stratagene) allowed for site-specific mutations to be introduced into double-stranded plasmid DNA in a PCR. The plasmid of interest was used as the template in the amplification reaction which made use of a derivative of the PfuUltra® high-fidelity DNA polymerase. *Pfu* Ultra extended the forward and reverse primers designed to incorporate mutations and generated complementary strands of the vector containing the mutation. The amplification product was treated with *Dpn* I, an endonuclease which acts on methylated and hemimethylated DNA only. The digestion with *Dpn* I ensured that the parental plasmid, which did not contain the mutation, was destroyed. Plasmids containing the mutation were transformed and grown in *E. coli*.

The following were included in a 50 µl reaction (made up with sterile water): 5 µl 10X QuikChange® Lightning Buffer, 1.5 µl QuikSolution™ reagent, 1 µl QuikChange® Lightning Enzyme and 1 µl dNTP mix as per the manufacturer's instruction, 100 ng double stranded DNA and 2.5 ng each of the specifically designed forward and reverse primers containing the mutation. This reaction was initially denatured at 95 °C for 2 minutes, followed by 18 cycles of 95 °C for 20 seconds, 60 °C for 10 seconds and 68 °C for 4 minutes, with a final extension of 68 °C for 5 minutes. The reaction was then treated with *Dpn* I restriction enzyme (Stratagene) at 37 °C for 1 hour. XL-10 Gold Ultracompetent cells (Stratagene) were transformed (as described in section 2.8) using 3 µl of the *Dpn* I treated

mutagenesis reactions. The introduction of mutations was confirmed by sequence analysis (described in Section 2.11), and mutants were used to make PSVs for neutralisation assays described in Section 2.2 to 2.4).

When more than 4 mutations were located in close proximity to each other, the design of primers for site-directed mutagenesis was difficult, therefore autologous chimeras were used. An autologous C3V4 chimera for example would contain the C3V4 region of the acute clone in the backbone of the 6 month clone. These chimeras were created using overlapping PCR, confirmed by sequence analysis and were used to make PSVs for neutralisation assays as previously described in sections 2.2 to 2.11.

2.15 Shannon entropy plot generation

Entropy plots were generated using the Entropy-One tool from the Los Alamos National Laboratory HIV Sequence Database (http://www.hiv.lanl.gov/content/sequence/ENTROPY/entropy_one.html) to determine which regions of gp120 were highly variable among longitudinal clones. Shannon entropy is a quantitative measure of uncertainty in a data set. This tool uses a Monte Carol randomisation strategy to identify variability between aligned sequences. Each position in the sequence alignment undergoes multiple test or comparisons after which a Bonferroni correction is applied to set the threshold.

2.16 Homology modelling using the SWISS-MODEL server

Homology models were created using the SWISS-MODEL server (project mode) (Schwede *et al*, 2003; Bordoli *et al*, 2006) to identify amino acid positions in the context of the three dimensional gp120 structure. Target sequences (for which the crystal or nuclear magnetic resonance (NMR) structure was unknown) were edited by deleting the signal peptide, V1V2 loops (in the majority of cases) and gp41 region in BioEdit 7.0.9 (Ibis Biosciences). The gp120 core crystal structures with PDB IDs 2B4C, 3JWD and 3LQA were used as templates. The 2B4C structure possesses a V3 loop and an ordered V4 loop. The 3JWD structure contains the gp41 interactive terminal regions. Finally the 3LQA structure represents a subtype C virus (CAP210.2.00.E8). Each edited target sequence was threaded through a structural alignment of the templates using Swiss PDB Viewer (Guex and Peitsch, 1997). Following manual refinement of the target and template sequence alignment, the model was constructed using the SWISS-MODEL server homology modelling pipeline. This pipeline employs

domain assignment (InterPro DomainScan), secondary structure (PSIPRED), disorder (DISOPRED) and putative transmembrane domain (MEMSAT) predictions. Estimates of local qualities at the amino acid level (ANOLEA and GROMOS), stereochemistry or geometric accuracy of the model (PROCHECK and WhatCheck) and global model energies (QMEAN and DFIRE) were used to assess the quality of the models. The entire process was repeated several times to ensure efficient model refinement.

2.17 Statistical analysis

The non-parametric Mann-Whitney Test and the Fischer's Exact Test were used to compare the properties of C3V4-responders and non-responders.

Results

Chapter 3: Definition of a C3V4 Responder

The initial aim of this project was to determine which factors make the C3V4 region immunogenic in many individuals infected with subtype C viruses. This chapter firstly describes the detection of AnAb responses targeting the C3V4 region, through the use of C3V4 chimeras. This allowed for the distinction between individuals who mounted an anti-C3V4 response and those who did not. Secondly the two groups were compared to define features of the envelope that were associated with a C3V4 response. Finally this chapter assessed the consequence of having an anti-C3V4 response on the overall neutralising responses to HIV-1 subtype C.

3.1 Construction of C3V4 chimeras

The ability to mount an AnAb response to the C3V4 region was assessed in 17 individuals in this study (and 5 individuals in a previous study) using chimeric envelopes containing the C3V4 region of interest in a neutralisation resistant backbone. To identify a resistant envelope backbone, five envelope genes, cloned from acutely infected subjects, were tested for resistance to neutralisation by plasmas (from 3 years p.i.) from each of the 22 individuals (Figure 12). The 3 year time point was selected to ensure longitudinal assessments of the neutralising response could be performed.

Participant ID	Acute Envelope Clones			
	CAP88.B5	CAP84.32	CAP63.A9	CAP45.G3
CAP45	45	**45**	45	6968
CAP63	**45**	ND	1633	ND
CAP69	ND	**45**	ND	ND
CAP84	45	3622	45	**45**
CAP88	2640	45	**45**	45
CAP136	ND	**45**	ND	ND
CAP174	**45**	ND	ND	ND
CAP200	**45**	45	45	45
CAP206	223	**45**	173	4720
CAP225	**45**	45	45	45
CAP228	45	**45**	45	45
CAP244	45	**45**	45	45
CAP255	45	**45**	45	45
CAP314	**45**	45	ND	ND
CAP8	45	**45**	45	45
CAP210	45	**45**	ND	ND
CAP221	**45**	45	45	45
CAP224	**45**	ND	ND	ND
CAP239	45	**45**	45	45
CAP248	**45**	229	45	601
CAP256	45	**45**	1495	10 227
CAP269	**45**	45	45	45

Figure 12. Neutralisation of five heterologous envelope clones by 22 plasma samples from 3 years p.i. Autologous titres are shown in green and heterologous titres are in red. Blue represents neutralisation resistance, while bold dark blue indicates the resistant backbone that was used in each C3V4 chimera. ND = not done.

Figure 12 shows the neutralisation checkerboard obtained. Green shading highlights autologous neutralisation, which is the ability of a plasma sample to neutralise the virus cloned from that individual. For example, the CAP45 plasma neutralised the CAP45.G3 virus. Red shading indicates heterologous neutralisation, and was confined to CAP206, CAP248 and CAP256, all of whom have been shown to develop broadly cross-neutralising antibodies (Gray et al., 2011). Blue depicts neutralisation resistance with bold, dark blue representing the neutralisation resistant backbone that was selected for use in making each C3V4 chimera. In this manner, a neutralisation resistant backbone was identified for each of the 22 individuals.

Following identification of resistant backbones for each individual, overlapping PCR was employed to create C3V4 chimeras. The C3V4 region from each of the 22 acute viruses (parent 1) cloned from 1-2 months p.i. was amplified (Figure 13 fragment Y). The two regions flanking the C3V4 region (from the signal peptide to the beginning of the C3 region and from the end of the V4 loop to the end of gp41) of the resistant backbone (parent 2) were amplified in separate reactions (Figure 13 fragments W and X). The C3V4 region of interest was grafted onto the resistant backbone via overlapping PCR to create C3V4 chimeras.

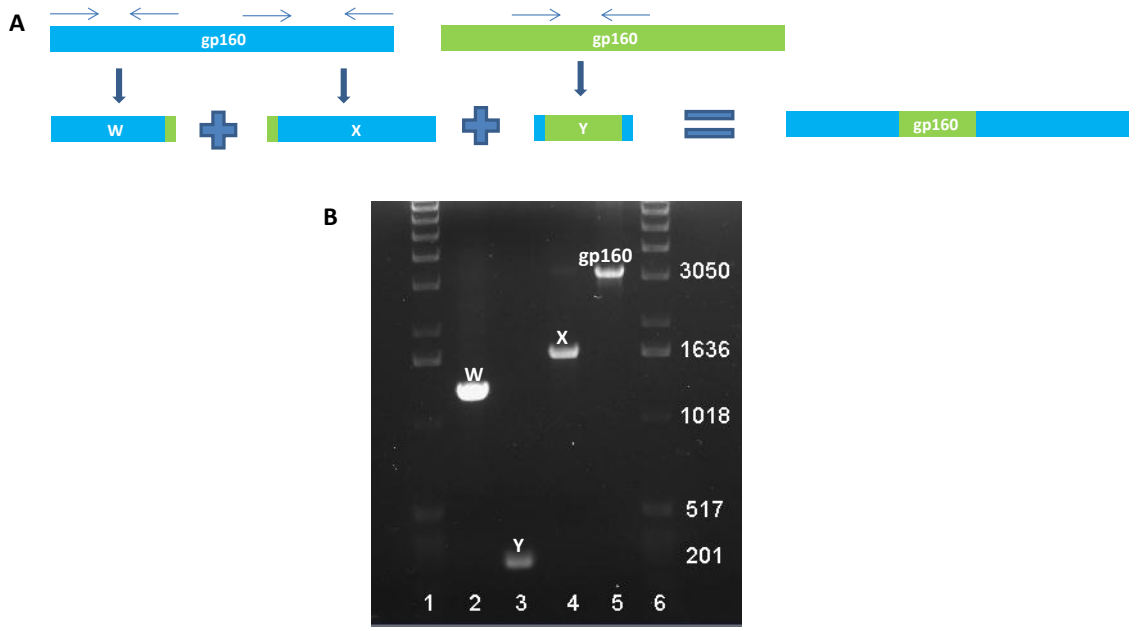

Figure 13. C3V4 chimera PCR products. (A) Diagram showing amplification of fragments W, X, Y and the full C3V4 chimera gp160 envelope. **(B)** DNA electrophoresis gel image. Lanes 1 and 6: Molecular weight marker (band sizes on the right of lane 6). Lane 2: Fragment spanning from the signal peptide to the beginning of the C3 region of the resistant backbone envelope (labelled W). Lane 3: C3V4 region amplified from the individual of interest (labelled Y). Lane 4: Fragment spanning from the end of the V4 loop to the end of gp41 derived from the resistant backbone envelope (labelled X). These pieces were then linked in overlapping PCR reactions to generate the full length envelope amplicon (labelled gp160).

Chimeras were verified by gp160 sequence analysis using 8 to 10 different sequencing primers (shown in Appendix 1), and transfected into 239T/17 cells for the generation of PSVs that were used in neutralisation assays.

3.2 Verification of the conformational integrity of C3V4 chimeras

The C3V4 region is approximately 86 amino acids in length. Therefore during the generation of C3V4 chimeras, a number of structural constraints and characteristics of the envelope may be perturbed, resulting in unusual exposure of neutralisation determinants. Exposure of the normally inaccessible V3 loop and CD4 binding site is a measure of these changes in conformation. During chronic infection both anti-V3 and anti-CD4 binding site antibodies are produced in almost all subjects (Binley et al., 2004; Conley et al., 1994; Corti et al., 2010; Davis et al., 2009; Gorny et al., 2006; Hioe et al., 2010). The functional integrity of the C3V4 chimeras was therefore confirmed by testing chimeras against heterologous plasma from CAPRISA participants at 1 year p.i. (Figure 14) as in similar previous studies (Moore et al., 2008). With the exception of autologous titres against CAP45, no other neutralisation was observed. These results indicate that the conformational integrity of all 22 C3V4 chimeras was maintained, with no evidence of exposure of normally occluded epitopes.

C3V4 chimera	Plasma samples						
	CAP45	CAP221	CAP255	CAP244	CAP228	CAP237	CAP278
CAP45	744	45	45	45	45	45	45
CAP63	45	45	45	45	45	45	45
CAP69	45	45	45	45	45	45	45
CAP84	45	45	45	45	45	45	45
CAP88	45	45	ND	45	45	45	45
CAP136	45	45	45	ND	ND	45	45
CAP174	45	45	45	45	45	45	45
CAP200	45	45	ND	45	45	45	45
CAP206	45	45	45	ND	ND	45	45
CAP225	45	45	45	45	45	45	45
CAP228	45	45	45	ND	ND	45	45
CAP244	45	45	45	ND	ND	45	45
CAP255	45	45	ND	45	45	45	45
CAP314	45	45	45	45	45	45	45
CAP8	45	45	ND	45	45	45	45
CAP210	45	45	ND	45	45	45	45
CAP221	45	45	ND	45	45	45	45
CAP224	45	45	45	45	45	45	45
CAP239	45	45	ND	45	45	45	45
CAP248	45	45	ND	45	45	45	45
CAP256	45	45	ND	45	45	45	45
CAP269	45	45	45	45	45	45	45

Figure 14. Neutralisation of 22 C3V4 chimeras by heterologous plasma samples from 1 year p.i. Each C3V4 chimera was tested against at least 5 heterologous plasma samples to confirm conformational integrity. ID_{50} titres are coloured with blue for neutralisation resistance and green for autologous neutralisation. ND = not done.

3.3 Classification of C3V4 responders and non-responders

To identify individuals who developed an anti-C3V4 response, multiple time points from enrolment to 1 year p.i., from all 22 individuals were used to test the neutralisation sensitivity of each respective C3V4 chimera. In three individuals (CAP206, CAP244 and CAP314) neutralisation assays were performed using plasma from enrolment to 2 years p.i. as the C3V4 chimeras were only sensitive to neutralisation after 10 months p.i. Neutralisation profiles of the chimeras were compared to those of both parental envelopes. Five individuals (CAP45, CAP63, CAP84, CAP88, and CAP239) were classified in a previous study (Moore et al., 2008), whilst the remaining 17 individuals were classified here. Figure 15 shows the results of the screening for C3V4 responses. Where the chimera was resistant to neutralisation, like that of the resistant parental backbone, it was determined that the C3V4 region was not a target of AnAbs during early infection and the individual was classified as a C3V4 non-responder. In contrast, if transfer of the C3V4 region into the neutralisation resistant backbone resulted in some transfer of neutralisation sensitivity, the individual was classified as a C3V4 responder. We used this approach to identify 14 C3V4 responders (Figure 15 A) and 8 C3V4 non-responders (Figure 15 B).

The titres and timing of the neutralisation curves suggested that the anti-C3V4 response ranged from being the dominant AnAb response to a more minor component of the overall neutralising response. For example, in CAP63 and CAP88 the neutralisation sensitivity of the C3V4 chimeras (Figure 15 A) matched that of the autologous parent from which the C3V4 region was isolated, suggesting that in these two individuals the anti-C3V4 response early in infection was the predominant AnAb response. In contrast the majority of C3V4 responder chimeras were less sensitive than the autologous parents. In some individuals (such as CAP45, CAP136, CAP200 and CAP314) titres for the chimera were substantially lower (up to 30-fold) than the autologous parent suggesting that the AnAb response may not only be directed to the C3V4 region. In 9 individuals (CAP136, CAP174, CAP200, CAP206, CAP225, CAP228, CAP244, CAP255 and CAP314) the chimera only became neutralisation sensitive at a later time point than the autologous parent, in some cases as late as 56 weeks p.i., suggesting that the anti-C3V4 response may not be the first specificity to develop. In CAP136, CAP228, CAP244 and CAP255, an initial peak, a dip and then a second peak was observed in the neutralisation titres of the chimera, suggesting the presence of two anti-C3V4 responses over time. In all the individuals classified as non-responders, the C3V4 chimera was completely neutralisation resistant.

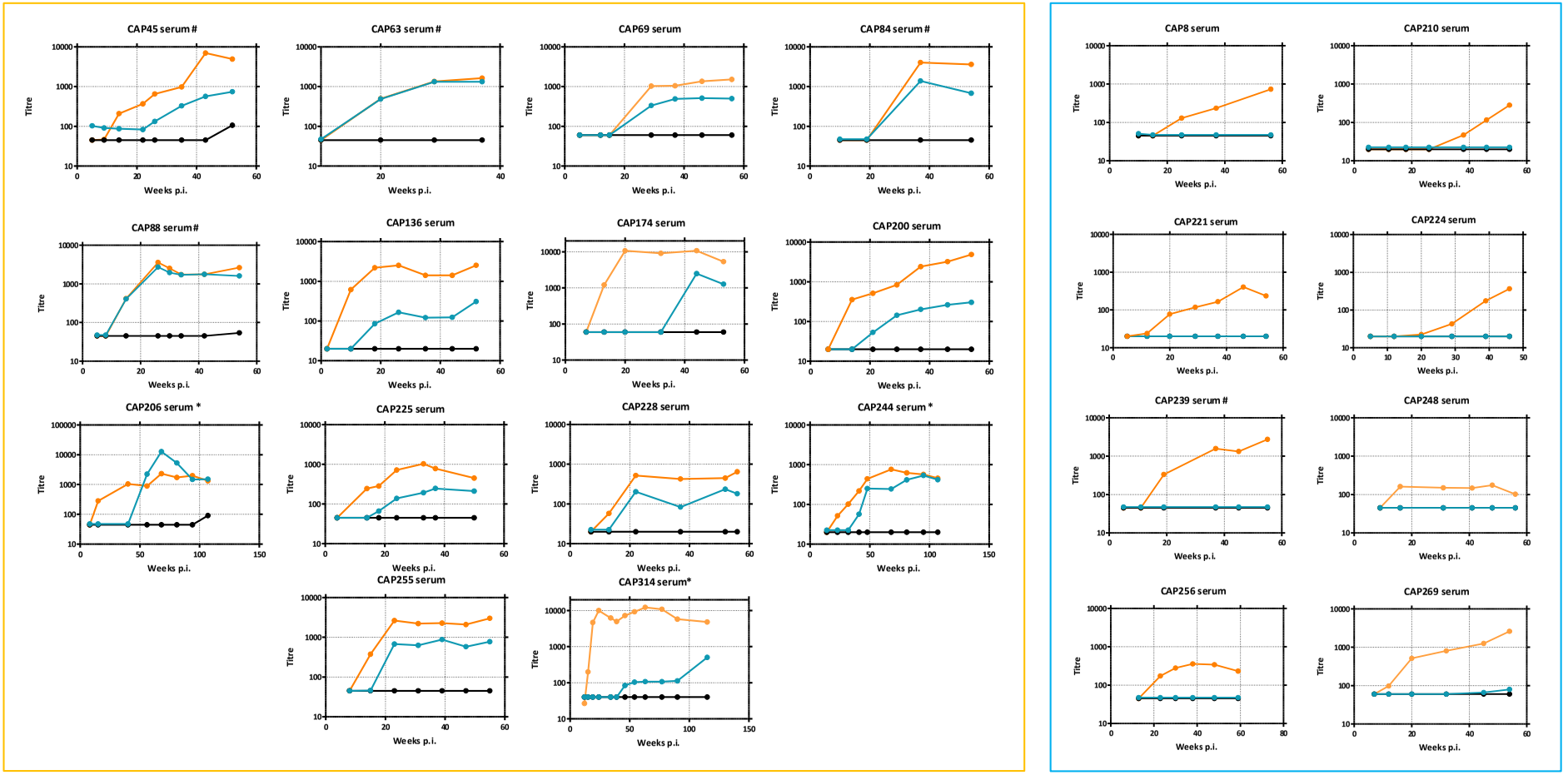

Figure 15. Neutralisation of parental and C3V4 chimera envelopes to determine C3V4 responders and non-responders. (A) Fourteen C3V4 responders and **(B)** eight C3V4 non-responders were identified. Chimeric envelopes (turquoise), resistant backbone envelopes (black) and acute envelopes (orange) were tested for neutralisation sensitivity to longitudinal autologous plasma. Previously identified responders and non-responders are indicated with a # (Moore et al, 2008). Individuals who developed an anti-C3V4 response after 10 months p.i. are highlighted with a *. y axis: ID_{50} titres. x axis: weeks post-infection (p.i.)

3.4 Characteristics of the envelope associated with the development of an anti-C3V4 response

Acute envelope sequences were available for all 14 C3V4 responders and 8 non-responders from previous studies (Abrahams et al., 2009; Gray et al., 2007). These sequences were analysed to identify features of the envelope, specifically in the C3V4 region, that could be correlated with the development of an anti-C3V4 response.

The sequences of the C3V4 region for each of the envelopes used in the generation of the chimeras are shown in Figure 16 and were aligned to ConC (a sequence generated from the consensus amino acid of at each position in of the envelope gene in an alignment of subtype C sequences on the Los Alamos HIV Sequence Database in 2001) (Gao et al., 2003). The alignment highlights the highly variable nature of both the alpha2-helix and V4 loop within the C3V4 region, which is in line with previous bioinformatics studies (Gnanakaran et al., 2007).

Gnanakaran and colleagues (2007) have shown that the alpha2-helix and V4 loop of subtype C viruses often exhibit a stronger charge anti-correlation than subtype B viruses. In addition, all-atom molecular dynamics simulations have shown that the N-terminus of the alpha2-helix and the C-terminus of the V4 loop interact (Gnanakaran et al., 2007). These observations suggest that through a charge anti-correlation the alpha2-helix and V4 loop may interact more strongly in subtype C viruses, potentially making this region less dynamic. A potential increased charge anti-correlation between the alpha2-helix and V4 loop in C3V4 responders compared to non-responders was considered as a factor contributing to the immunogenicity of the region. We therefore determined the charges of the alpha2-helices and V4 loops of the 14 C3V4 responders and 8 non-responders.

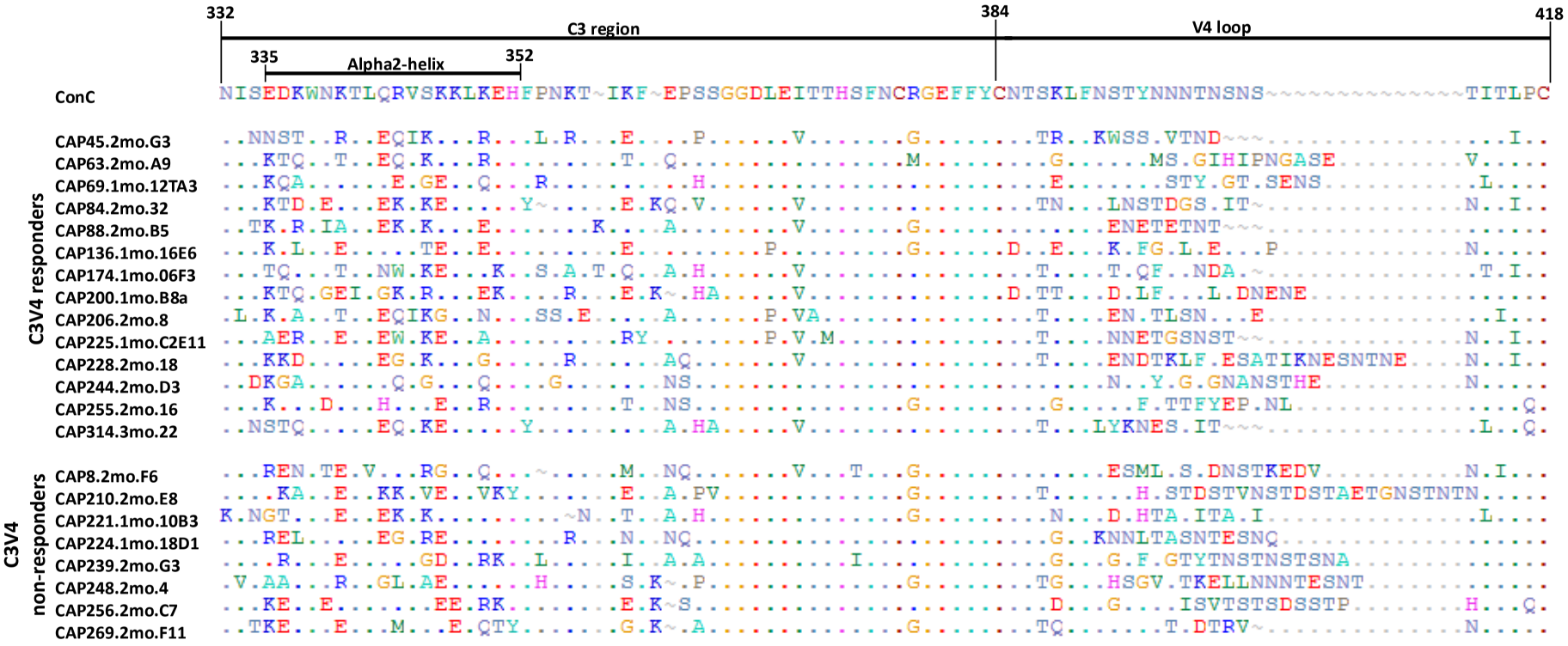

Figure 16. Protein sequence alignment of the C3V4 regions of responder and non-responder acute envelopes. Sequences were aligned to ConC, a sequence generated from the consensus amino acid at each position of the envelope gene in an alignment of subtype C sequences on the Los Alamos HIV Sequence Database in 2001. Numbers above the alignment refer to HXB2 numbering as is the convention in HIV-1 alignments. Amino acids are represented by single letter codes and gaps are shown as tildes.

The charges of the alpha2-helix and V4 loop alone were not significantly different between the two groups, with p-values of 0.5571 and 0.9723 respectively (Figure 17 A). In addition the number of individuals with an oppositely charged alpha2-helix and V4 loop (data not shown) did not significantly differ between the groups (p = 0.1932). These results suggest that the overall electrostatic properties of the C3V4 regions of C3V4 responders and non-responders are similar, and do not influence the elicitation of an anti-C3V4 response.

Shorter variable loops in subtype C viruses have been correlated with higher autologous neutralising titres in comparison to subtype B viruses (Li et al., 2006b). Similarly fewer PNGs in the envelope were correlated with higher autologous neutralisation titres in subtype C viruses (Gray et al., 2007). N-linked glycans protrude 15 -20 Å from the gp120 surface and then extend to form an "umbrella" consisting of at least 4 mannose residues (Wei et al., 2003). These observations suggest that a generally more neutralisation-sensitive phenotype may be associated with exposure of epitopes due to shorter variable loop lengths and fewer PNGs in the envelope (Gray et al., 2007; Li et al., 2006b; Pugach et al., 2004; Saunders et al., 2005; Stamatatos et al., 1998). Variable loop lengths and number of PNGs were therefore proposed to contribute the accessibility and exposure of the C3V4 region.

The V4 loop, as with most HIV-1 variable regions, can contain many indels and is therefore very flexible in length. This loop may therefore be an important determinant for the exposure of neutralisation epitopes within the C3 region. Sequences were therefore used to compare the length of the V4 loop and the number of PNGs in the C3V4 region between responders and non-responders. The length of the V4 loop was found to be significantly shorter (p = 0.046) in the C3V4 responders (Figure 17 B), suggesting increased exposure of the C3V4 region in C3V4 responders.

Although the number of PNGs found in the alpha2-helix (p = 0.6608), C3 region (p = 0.0555) and V4 loop (p = 0.2349) alone was not significantly different between the groups (Figure 17 C) a trend toward fewer PNGs in the C3 region of C3V4 responders was observed. The number of PNGs within the entire C3V4 region of the C3V4 responders were significantly lower (p = 0.0483) than in the C3V4 non-responders, which suggests that a less densely glycosylated C3V4 region may be more accessible to AnAbs. However when the number of PNGs were calculated as a percentage of the total amino acid residues in the C3V4 region, this difference was no longer significant (p = 0.1422).

This suggests that the number of PNGs in the C3V4 region of responders is a consequence of the shorter V4 loop length. These results indicate that a shorter V4 loop and fewer PNGs in the C3V4 region are characteristics of a virus able to elicit an AnAb response directed to the C3V4 region.

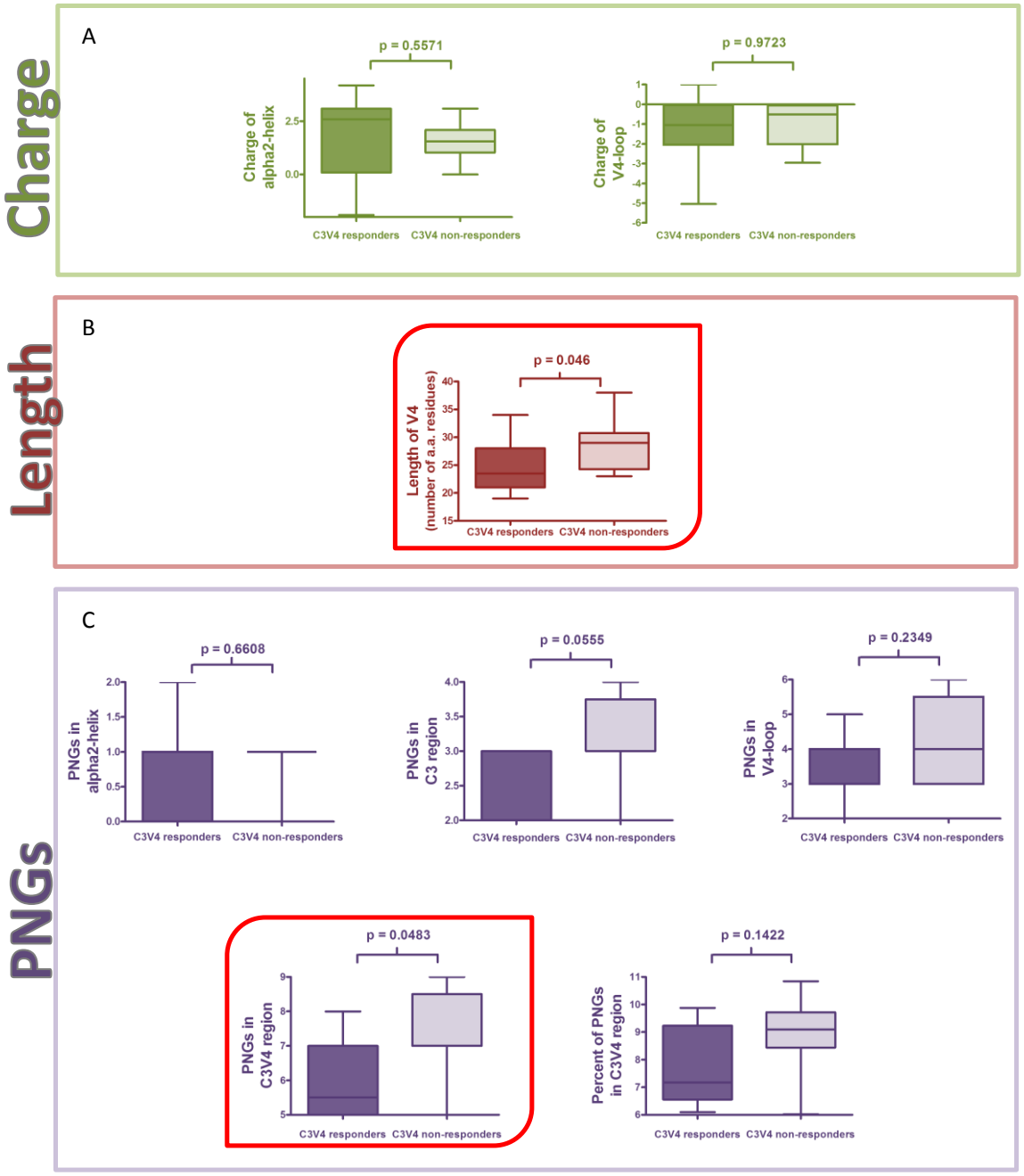

Figure 17. Comparison of envelope characteristics between C3V4 responders and non-responders. Comparison of **(A)** charge in the alpha2-helix and V4 loop, **(B)** V4 loop length and **(C)** number of potential N-linked glycosylation sites (PNGs) between C3V4 responders and non-responders. Plots where differences between the C3V4 responders and non-responders were statistically significant are outlined in red.

3.5 Impact of an anti-C3V4 response on overall AnAb titres

This work has confirmed results from a previous study which showed that the C3V4 region is a highly immunogenic region in HIV-1 subtype C infections (Moore *et al,* 2008). To further characterise the immunogenicity of the region we tested whether a response to the C3V4 region of the envelope affected the overall AnAb titres during early infection. We therefore compared autologous neutralising titres in responders and non-responders. Both the autologous titres at 1 year p.i. (p = 0.0125) and the peak autologous titres within 2 years p.i. (p = 0.0374) were significantly higher in the C3V4 responders compared to the non-responders (Figure 18). The observation that the overall AnAb response in C3V4 responders is more potent may be a direct consequence of the strongly immunogenic nature of the C3V4 region.

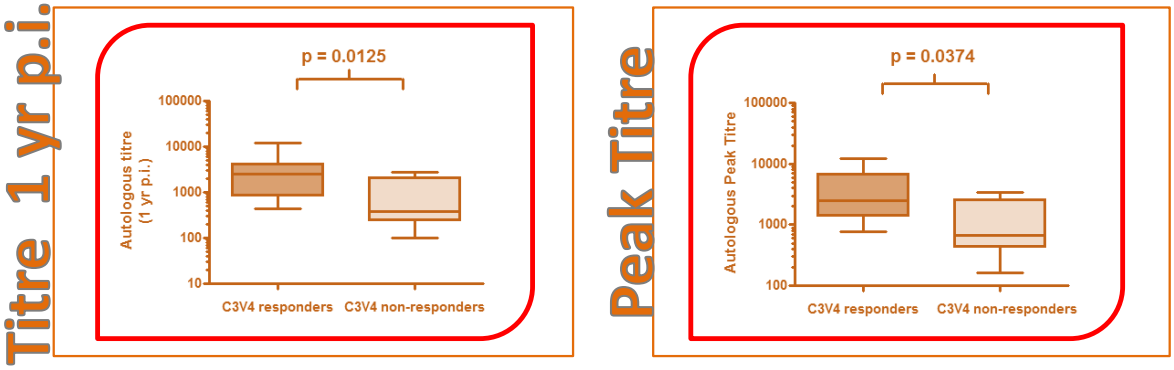

Figure 18. Comparison of the overall autologous titres of C3V4 responders and non-responders. C3V4 responders had significantly higher titres at 1 year p.i. and peak autologous titres compared to non-responders.

3.6 Summary

This chapter described the identification of 14 C3V4 responders and 8 non-responders. A comparison of the features of the C3V4 region between the two groups showed that a shorter V4 loop and fewer PNGs in the C3V4 region were correlated with an anti-C3V4 response. The overall AnAb titres in C3V4 responders were shown to be higher than in non-responders, emphasising the importance of this region with respect to nAb responses in subtype C infection.

Chapter 4: Multiple Mechanisms of Escape from an Anti-C3V4 Response

The highly amphipathic nature of the alpha2-helix in the C3 region of subtype C viruses as opposed to subtype B viruses suggests that this region may be a pivotal part of a subtype C specific neutralising epitope (Gnanakaran et al., 2007). Variable amino acids in the alpha2-helix of subtype C viruses have been shown to alternate between positively and negatively charged side chains during the course of infection (Gnanakaran et al., 2007), a finding that suggested that such charge changes may mediate neutralisation escape. In addition, the alpha2-helix may affect neutralisation epitopes through interactions with other regions (Gnanakaran et al., 2007). Therefore in order to investigate whether changes in the alpha2-helix as well as mutations in regions structurally proximal to the alpha2-helix can mediate escape from AnAbs targeting the C3V4 region, we extensively characterised the mechanisms of viral escape in 5 C3V4 responders. To characterise neutralisation escape, single genome amplification (SGA) and sequence analysis was used to identify potential escape mutations. Likely escape mutations were experimentally confirmed using mutagenesis and neutralisation assays.

4.1 CAP228: Escape via the C2 region and/or alpha2-helix

The development of the anti-C3V4 response in CAP228, as indicated by the sensitivity of the C3V4 chimera to CAP228 plasma, was observed by 5 months p.i. with titres approximately half that of the autologous parent. The generation of envelope SGAs (described in section 2.11) was therefore performed using CAP228 plasma from 6 months p.i., resulting in 6 envelope amplicons. The full length envelope sequences for these amplicons were used to construct phylogenetic trees using 4 methods. A representative phylogeny, created using the minimum evolution method is shown in Figure 19. Three amplicons (CAP228.6mo.1, CAP228.6mo.3 and CAP228.6mo.4) were selected for cloning as they encompassed much of the diversity within all phylogenies.

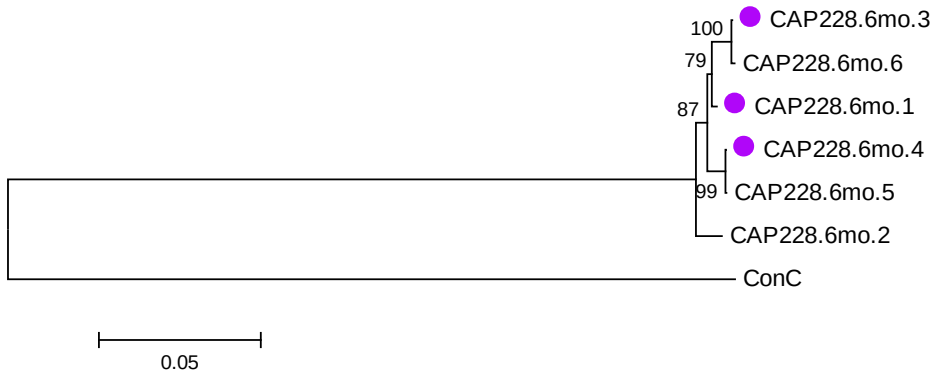

Figure 19. Minimum evolution phylogenetic tree for the CAP228 6 month SGAs. Amplicons that were selected for cloning are indicated by a purple dot. Bootstrap values are shown for each grouping. ConC was used as the reference sequence for rooting the phylogeny. The scale represents evolutionary distance measured by number of amino acid substitutions per site.

Six month clones were tested for neutralisation sensitivity against longitudinal autologous plasma and compared to the acute CAP228 clone. The three CAP228 6 month clones all showed neutralisation escape when compared to the acute 2 month clone (Figure 20). This was evident from the fact that the 2 month clone was neutralised from 7 weeks p.i. but the 6 month clones were resistant to all plasma samples prior to 9 months p.i. The sensitivity of the 6 month clones to later time points suggested the subsequent development of new AnAb responses.

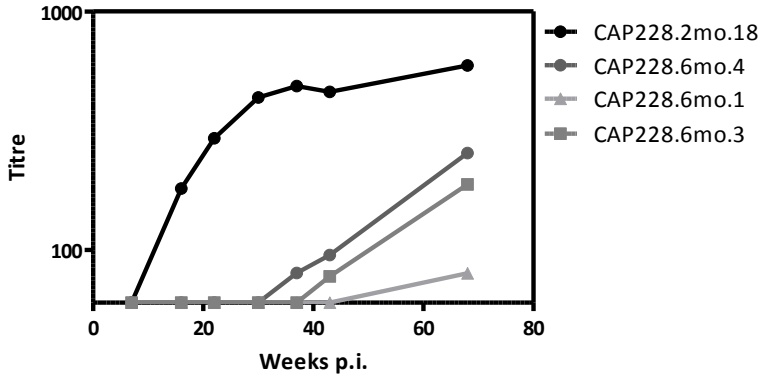

Figure 20. Neutralisation escape of CAP228 6 month clones. The acute clone (CAP228.2mo.18) and three 6 month clones (CAP228.6mo.4, CAP228.6mo.1 and CAP228.6mo.3) were tested against longitudinal autologous plasma. y axis: ID_{50} titre. x axis: weeks p.i.

To identify areas likely to contain escape mutations, an entropy plot comparing the acute and 6 month clones (Figure 21 A) was used to identify highly variable regions in gp120 within the first 6 months of infection. Regions with the highest entropy were potentially under the most immune pressure. Although mutations in the C3V4 region were identified, multiple other regions were also highly variable (Figure 21 A). All these potential escape mutations were plotted onto a homology model constructed for CAP228.6mo.3 (Figure 21 B). Mutations in the C3 region formed a tight cluster at the N-terminus of the alpha2-helix (Figure 21 B). Only one other high entropy cluster, in the C2 region, was structurally proximal to the potential escape mutations located in the alpha2-helix of the C3 region (Figure 21 B) by 6 months p.i. We therefore focussed on investigating the role of potential escape mutations in the C2 region and alpha2-helix.

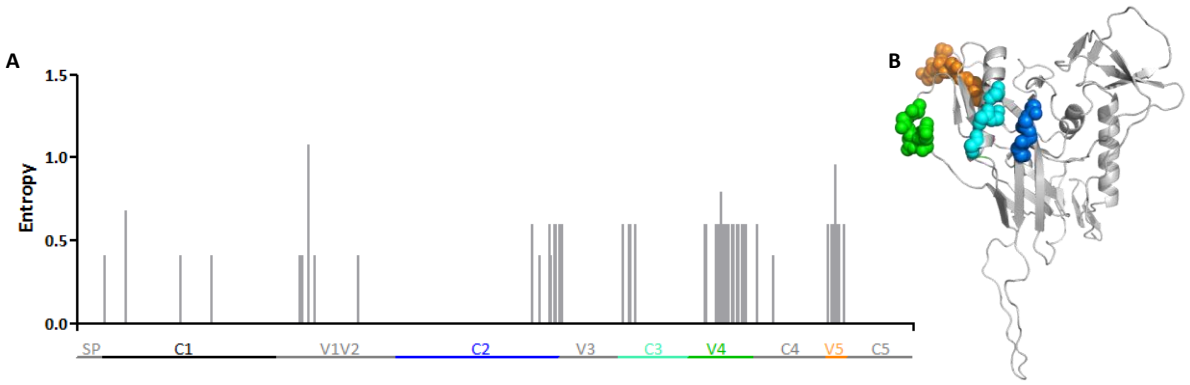

Figure 21. Identification of potential escape mutations in CAP228. (A) Entropy plot of gp120 residues from acute and 6 month clones. y axis: entropy. x axis: regions in gp120. **(B)** The C2 region (blue), alpha2-helix (cyan), V4 loop (green) and V5 loop (orange) residues with the highest entropy, are shown on the homology model of CAP228.6mo.3 gp120.

The potential escape mutations in the alpha2-helix of the 6 month clones were located between HXB2 positions 336 and 344 (Figure 22 A), while those located in the C2 region occurred between positions 289 and 295 (Figure 22 B). Mutations located between positions 278 and 283 in the C2 region were not structurally proximal to the alpha-2helix and were therefore not tested.

Figure 22. CAP228 protein sequence alignment of acute and 6 month SGA sequences. (A) The C3 region. **(B)** A portion of the C2 region. Sequence identity to the acute 2 month clone is depicted as a dot. HXB2 numbering is indicated above the alignment. Amino acids are represented by their 1-letter symbols. Cloned amplicons are indicated by purple circles.

In CAP228.6mo.4 two mutations (K340E and G344R) were present in the alpha2-helix, but none had arisen in the C2 region. In CAP228.6mo.1 one mutation was found in the alpha2-helix (K336Q) and another in the C2 region (E290K). The third clone, CAP228.6mo.3, had a single mutation in the

alpha2-helix (T341A) and four mutations (N289K, I292V, E293K and V295E) in the C2 region that were structurally proximal to the alpha2-helix.

The role of the mutations described above in mediating escape from AnAbs was examined through the generation of back-mutants, where mutations in the 6 month clones were reverted to match the sequence of the acute clone (Figure 23). An alpha2-helix back-mutant would therefore contain the alpha2-helix of the acute clone in the backbone of the 6 month clone. The back-mutants were then tested for neutralisation sensitivity against longitudinal plasma and compared to the acute and 6 month clones.

In CAP228.6mo.4 the alpha2-helix was back-mutated to match the sequence of the acute clone through the introduction of the E340K and R344G mutations. The neutralisation sensitivity of CAP228.6mo.4 E340K R344G was compared to that of the acute and 6 month clones. The neutralisation curve of the alpha2-helix back-mutant (CAP228.6mo.4 E340K R344G) shifted to the left to match that of the acute clone, indicating that escape in this 6 month clone was mediated by two charge changes in the alpha2-helix alone (Figure 23 A).

CAP228.6mo.1 contained a single mutation in the alpha2-helix of the C3 region at position 336. However when the Q336K back-mutation was introduced in the alpha2-helix (to create CAP228.6mo.1 Q336K), there was no significant increase in neutralisation sensitivity (Figure 23 B). This suggested that unlike CAP228.6mo.4, neutralisation escape was not mediated by changes in the alpha2-helix alone. A single mutation, at position 290 in the C2 region was found to be structurally proximal to the 336 mutation in the alpha2 helix. Therefore the K290E back-mutation was introduced into the 6 month clone either alone (CAP228.6mo.1 K290E) or in conjunction with the Q336A mutation in the alpha2-helix (CAP228.6mo.1 K290E Q336K). The CAP228.6mo.1 K290E back-mutant only showed partial neutralisation sensitivity, indicating that this mutation alone contributed somewhat to the neutralisation escape, but could not mediate complete escape. However simultaneous introduction of back-mutations in the alpha2-helix and the C2 region (CAP228.6mo.1 K290E Q336K) restored complete neutralisation sensitivity (Figure 23 B). This suggested that neutralisation escape in CAP228.6mo.1 was mediated by two mutations, one in the C2 region and the other in the alpha2-helix.

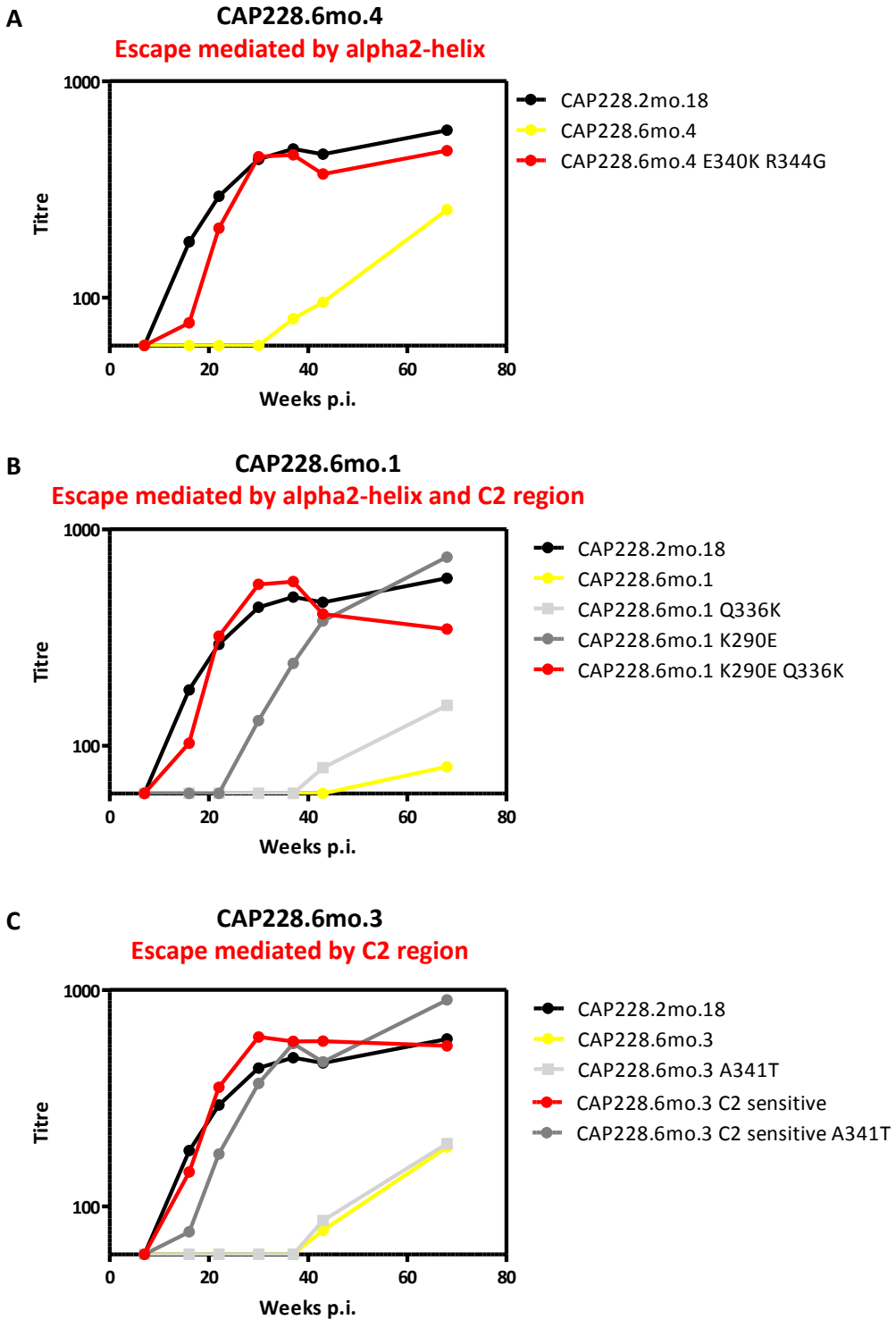

Figure 23. Pathways of neutralisation escape in CAP228. The 2 month (acute) and the respective 6 month clones are shown in black and yellow respectively. **(A)** In CAP228.6mo.4 escape was mediated by the E340K and R344G mutations in the alpha2-helix alone (red). **(B)** In CAP228.6mo.1 the K290E mutation in the C2 region and the Q336K mutation in the alpha2-helix in conjunction (red) mediated escape. The K290E mutation alone (grey circles) had only a partial effect on neutralisation. The Q336K mutation in the alpha2-helix alone (grey squares) had no effect on neutralisation sensitivity. **(C)** In CAP228.6mo.3 although the CAP228.6mo.3 C2 sensitive A341T construct (grey circles) was as sensitive as the acute clone, escape was mediated entirely through mutations found only in the C2 region (K289N, V292I, K293E and E295V) as shown by the red curve. The A341T back-mutation in the alpha2-helix (grey squares) alone did not have any effect on neutralisation sensitivity. y axis: ID_{50} titres. x axis: weeks p.i.

In CAP228.6mo.3 multiple changes (N289K, I292V, E293K and V295E) in the C2 region (Figure 22 A) clustered with a single alpha2-helix mutation (T341A) on the gp120 structure. Reversion of all the mutations in the alpha2-helix and C2 region (to create CAP228.6mo.3 C2 sensitive A341T) of this 6 month clone restored complete neutralisation sensitivity. However in order to dissect the roles of the mutations in each region, separate alpha2-helix (CAP228.6mo.3 A341T) and C2 region (CAP228.6mo.3 C2 sensitive) back-mutants were made and tested for neutralisation. The alpha2-helix back-mutant (CAP228.6mo.3 A341T) showed no difference in neutralisation when compared to the 6 month clone. In contrast, the C2 region back-mutant (CAP228.6mo.3 C2 sensitive) was as sensitive as the 2 month clone (Figure 23 C). Therefore four mutations in the C2 region of CAP228.6mo.3 were sufficient to mediate complete escape, and changes in the alpha2-helix of the C3 region did not contribute to neutralisation escape in this clone.

In all three 6 month clones of CAP228 a limited number of mutations mediated escape and often caused a change or removal of a charged amino acid, however potential N-linked glycosylation sequons were affected in one clone. Neutralisation escape in each clone was mediated via a distinct pathway. One clone escaped via mutations in the alpha2-helix alone, a second via mutations in both the alpha2-helix and the C2 region and the third via mutations in the C2 region alone.

4.2 CAP255: Escape via the V3 loop and C3V4 region

The development of the anti-C3V4 response in CAP255, indicated by the sensitivity of the C3V4 chimera to CAP255 plasma, was observed from 4 months p.i. with titres 3-fold lower than those observed for the acute clone. Thereafter the SGA of the envelope gene for CAP255 was performed using plasma from 6 months p.i. Three amplicons (CAP255.6mo.4, CAP255.6mo.5 and CAP255.6mo.10) were selected as representatives of the diversity found within the ten amplicons generated at this time point, as shown in the minimum evolution phylogenetic tree (Figure 24).

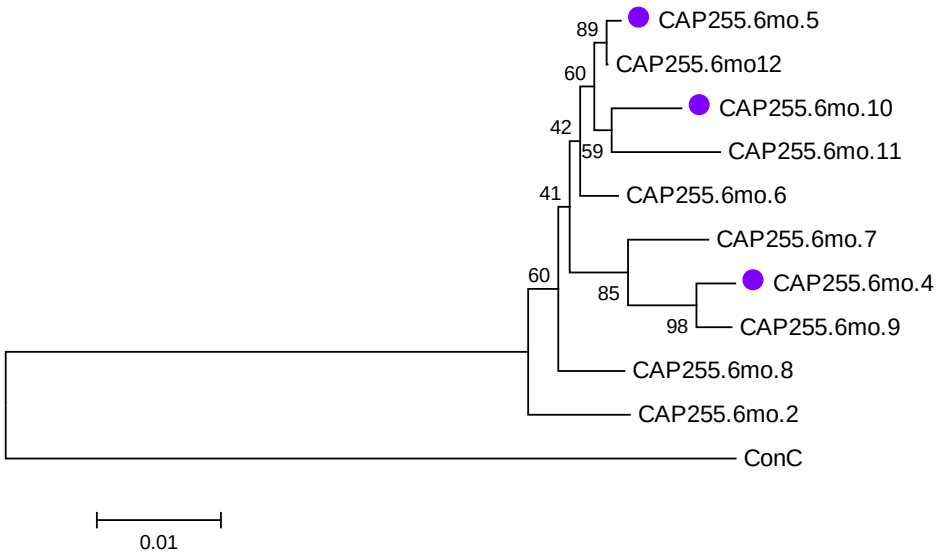

Figure 24. Minimum evolution phylogenetic tree for the CAP255 6 month p.i. SGAs. Amplicons that were selected for cloning are indicated by a purple dot. Bootstrap values are shown for each grouping. ConC was used as the reference sequence for rooting the phylogeny. The scale represents evolutionary distance measured by number of amino acid substitutions per site.

Potential escape mutations in the C3V4 region arose by 6 months p.i. in the CAP255 clones. An entropy plot highlighted additional regions within gp120 that were highly variable by 6 months p.i. A single mutation located in the V3 loop was structurally proximal to mutations in the C3V4 region (Figure 25). Thus the role of potential escape mutations in the C3V4 region and V3 loop were determined.

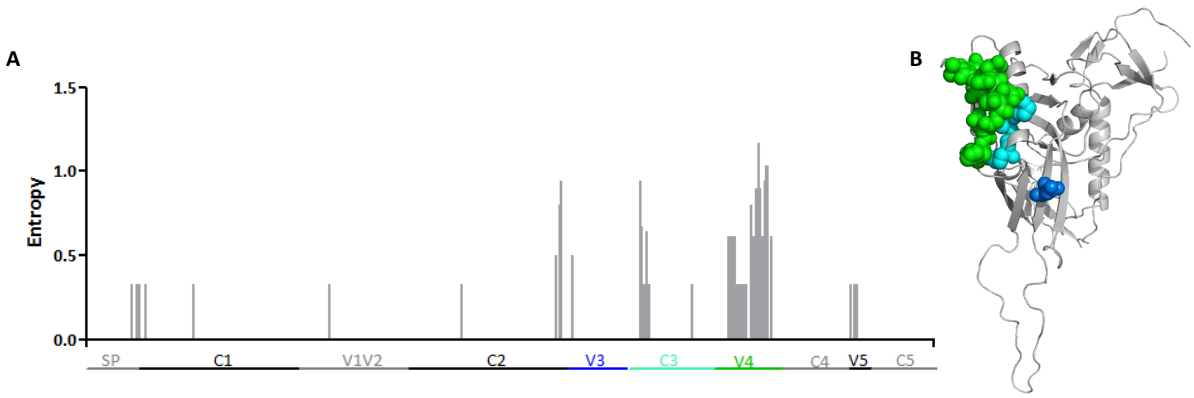

Figure 25. Identification of potential escape mutations in CAP255. (A) Entropy plot of gp120 residues created using acute and 6 month clones. y axis: entropy. x axis: regions in gp120. **(B)** The V3 loop (blue), C3 region (cyan) and V4 loop (green) mutations with the highest entropy, are shown on the homology model of CAP255.6mo.4 gp120.

In all three 6 month clones of CAP255, mutations occurred between positions 335 and 340 of the alpha2-helix (Figure 26 A), whilst both insertions and single amino acid mutations were found between positions 393 and 412 in the V4 loop (Figure 26 B).

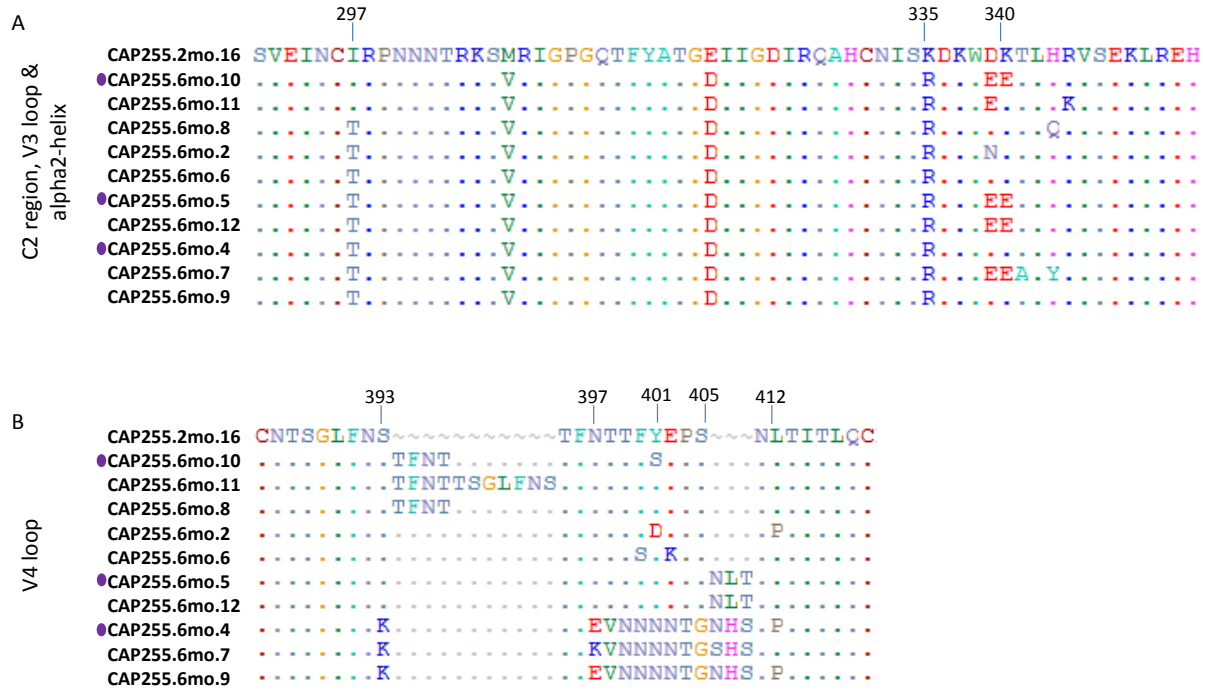

Figure 26. CAP255 protein sequence alignment of the acute clone and 6 month SGA sequences. (A) A portion of the C2 region (that was proximal to the alpha2-helix), V3 loop and the alpha2-helix. **(B)** The V4 loop. Sequence identity to the 2 month clone is depicted as a dot and gaps appear as tildes. HXB2 numbering is shown above the alignment. Amino acids are represented by their 1-letter symbols. Cloned amplicons are indicated by purple circles.

CAP255.6mo.10 had three mutations in the alpha2-helix (K335R, D339E and K340E) as well as a 4 amino acid insertion at position 393 (Thr-Phe-Asn-Thr) and another single amino acid substitution (Y401S) in the V4 loop. The same mutations in the alpha2-helix were present in CAP255.6mo.5, but in the V4 loop a three amino acid insertion at position 405 (Asn-Leu-Thr) occurred. CAP255.6mo.4 possessed a single mutation (K335R) in the alpha2-helix. The V4 loop of CAP255.6mo.4 contained 8 single amino acid substitutions (Glu-Val-Asn-Asn-Asn-Asn-Thr-Gly) between positions 397 and 405, a three amino acid insertion (Asn-His-Ser) at position 405 and a L412P mutation. In both CAP255.6mo.4 and CAP255.6mo.5, an I297T mutation (Figure 26 A) which added a potential N-linked glycosylation sequon at the cusp of the V3 loop, also arose. The mutations and insertions in the V4 loop in all three clones caused addition and removal, and therefore possible shuffling of at least one potential N-linked glycosylation sequon.

The effect of the mutations in the C2 and C3V4 regions in mediating neutralisation escape were investigated by creating back-mutants for each of the three 6 month clones as shown in Figure 27. In CAP255.6mo.10 three back-mutations in the alpha2-helix (R335K, E339D and E340K), a 4 amino acid deletion (Thr-Phe-Asn-Thr) and S401Y back-mutation in the V4 loop were introduced into the 6 month clone to match the sequence of the entire C3V4 region of the acute clone. The deletion at position 393 in the V4 loop caused an alteration in a potential N-linked glycosylation sequon. The neutralisation of this construct (CAP255.6mo.10 C3V4 sensitive) by autologous CAP255 plasma was equal in titre and kinetics to that of the acute clone, indicating that neutralisation escape was mediated by the changes in the C3V4 region alone (Figure 27 A).

Because the mutations in the V4 loop of CAP255.6mo.5 altered a potential N-linked glycosylation sequon, a V4 loop back-mutant was created (CAP255.6mo.5 V4 sensitive), but this construct was only partially sensitive to neutralisation when compared to the acute clone (Figure 27 B). Therefore an autologous C3V4 chimera was created that contained an alpha2-helix with the R335K, E339D and E340K back-mutations as well as a V4 loop with an Asn-Leu-Thr deletion at position 405. The neutralisation sensitivity of the C3V4 back-mutant (CAP255.6mo.5 C3V4 sensitive) was lower than that for the V4 loop back-mutant (CAP255.6mo.5 V4 sensitive). This surprising result may suggest that the residues in the C3 region of the acute clone affected binding of the antibody (ies) that the V4 loop mutations escaped. The partial neutralisation sensitivity of both the V4 loop and C3V4 region back-mutants suggested a role for other regions in mediating escape, unlike in CAP255.6mo.10.

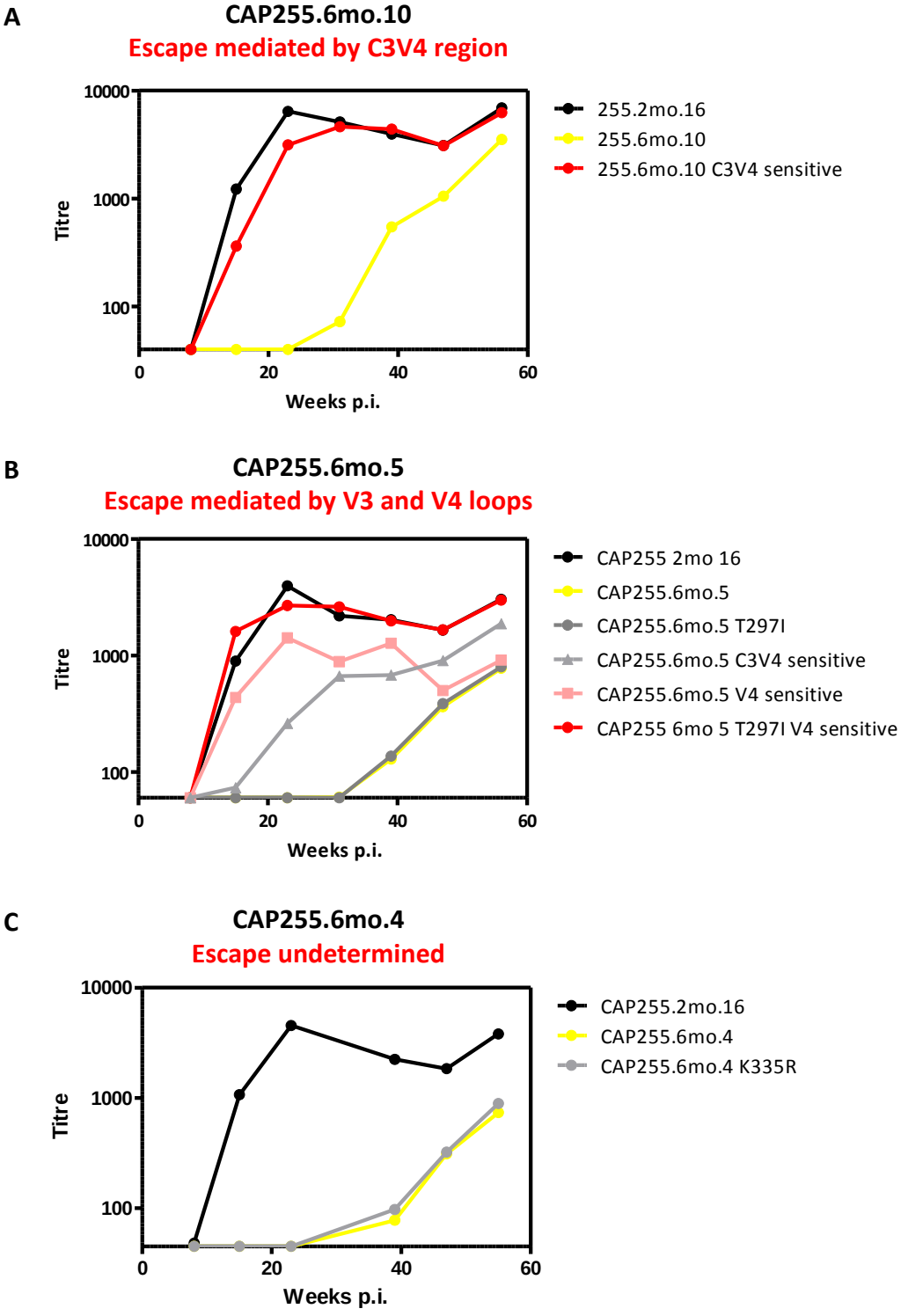

Figure 27. Mechanisms of neutralisation escape in CAP255. The 2 month (acute) and each of the 6 month clones are shown in black and yellow respectively. **(A)** In CAP255.6mo.10 escape was mediated by three mutations in the alpha2-helix (K335R D339E and K340E) in conjunction with a four amino acid insertion (Thr-Phe-Asn-Thr) between at position 393 and a Y410S mutation in the V4 loop (red curve). **(B)** Escape in CAP255.6mo.5 was mediated by the I297T mutation in the V3 loop along with a three amino acid insertion (Asn-Leu-Thr) at position 405 in the V4 loop (red curve). Unexpectedly the V4 loop back-mutant (pink squares) was more sensitive than the C3V4 region back-mutant (grey triangles). Reversion of position 297 alone had no effect on neutralisation sensitivity. **(C)** In CAP255.6mo.4 a single mutation (K335R) in the alpha2-helix did not alter neutralisation sensitivity (grey). y axis: ID_{50} titres. x axis: weeks p.i.

A mutation at position 297 in the V3 loop showed a high level of entropy and therefore this residue in CAP255.6mo.5 was mutated from a Thr to an Iso. Back-mutation of the 297 residue alone (to generate the CAP255.6mo.5 T297I construct) did not result in a change in neutralisation sensitivity. However when position 297 and the V4 loop were simultaneously back-mutated (creating CAP255.6mo.5 T297I V4 loop sensitive), complete neutralisation sensitivity was restored, suggesting that mutations in both these regions were required to mediate neutralisation escape. The mutation at position 297 and the Asn-Leu-Thr insertion in the V4 loop both caused alterations in potential N-linked glycan sequons, which may have contributed to escape.

In the third clone, CAP255.6mo.4, escape could not be attributed to the single mutation that occurred in the alpha2-helix by 6 months p.i., with this back-mutant (CAP255.6mo.4 R335K) remaining neutralisation resistant (Figure 27 C). There were 13 differences, including insertions and single amino acid substitutions, within the V4 loop of CAP255.6mo.4 when compared to the acute clone. However, simultaneous back-mutation of the alpha2-helix and V4 loop in the 6 month clone resulted in a construct (CAP255.6mo.4 C3V4 sensitive) that was no longer infectious and could not be assessed for neutralisation sensitivity. Deletion of the V4 loop disrupts gp160 folding (Olshevsky et al., 1990; Pollard et al., 1992), therefore the large difference in the V4 loop sequence between the acute and 6 month clones may have had structural and functional implications for the envelope trimer. Therefore the mechanism of escape in CAP255.6mo.4 could not be determined.

Escape mutations in the C3V4 region of two CAP255 6 month clones were numerous and affected both charge changes and potential N-linked glycosylation sequons. In addition, in one of these clones the insertion of a PNG in the V3 loop was also needed to mediate neutralisation escape. Overall, in CAP255 escape was mediated via alterations in the C3V4 region in one 6 month clone, while in a second clone alterations in the V3 and V4 loops were required. Escape in a third clone was undetermined.

4.3 CAP136: Escape via the C3V4 and/or the C4 regions

The development of the anti-C3V4 response in CAP136, as indicated by the sensitivity of the C3V4 chimera to CAP136 plasma, was observed by 4 months p.i. and although the titre at each time point was at least 10-fold lower than those of the autologous parent, the biphasic shapes of the two curves were similar. SGA of the envelope region was performed using plasma from 6 months p.i. and

7 amplicons were generated. A minimum evolution phylogeny indicating the major groupings of the amplicons is shown in Figure 28. CAP136.6mo.3, CAP136.6mo.6 and CAP136.6mo.7 were selected for cloning and characterisation of neutralisation escape.

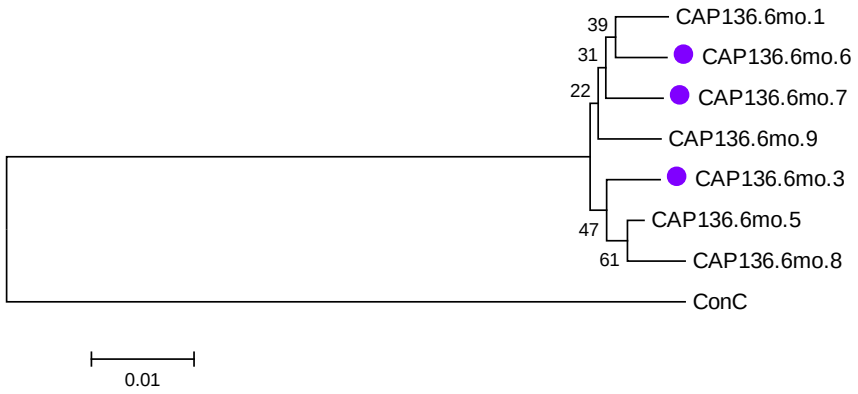

Figure 28. Minimum evolution phylogenetic tree for the CAP136 6 month SGAs. Amplicons that were selected for cloning are indicated by a purple dot. Bootstrap values are shown for each grouping. ConC was used as the reference sequence for rooting the phylogeny. The scale represents evolutionary distance measured by number of amino acid substitutions per site.

In all three 6 month clones, mutations in the C3V4 region were present. An entropy plot comparing the acute and 6 month clones (Figure 29 A) was used to identify other regions of gp120 with high variability. Multiple regions were highly variable, but only one high entropy cluster, in the C4 region (blue in Figure 29 B), was structurally proximal to the mutations found in the C3V4 region (cyan and green in Figure 29 B) of the 6 month clones. Therefore the role of potential escape mutations in the C3V4 and C4 regions was examined.

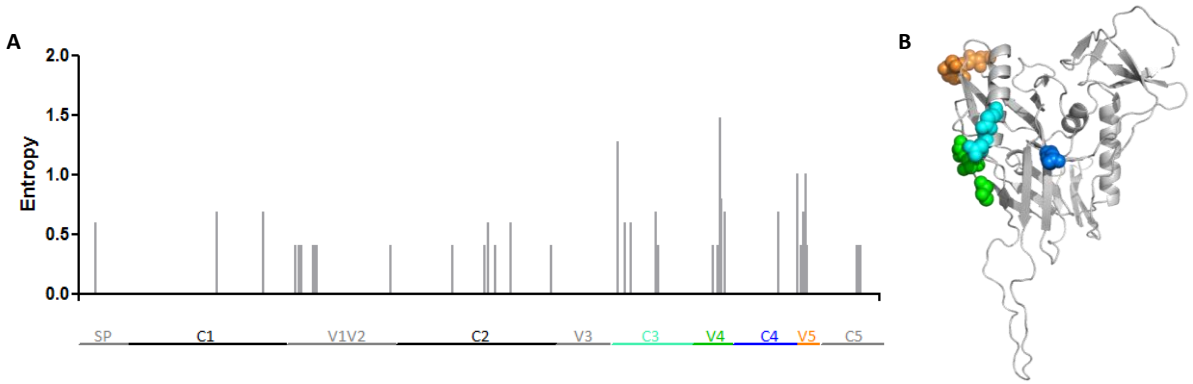

Figure 29. Identification of potential escape mutations in CAP136. (A) Entropy plot of gp120 residues created using acute and 6 month clones. y axis: entropy. x axis: regions in gp120. **(B)** The C4 region (blue), C3 region (cyan), V4 loop (green) and V5 loop (orange) residues with the highest entropy, are shown on the homology model of CAP136.6mo.3 gp120.

Although 7 SGAs were amplified from CAP136 at 6 months p.i., one amplicon (CAP136.6mo.8) that contained a deleted C3V4 region was predicted to be non-functional and was subsequently excluded from the sequence alignment (Figure 30).

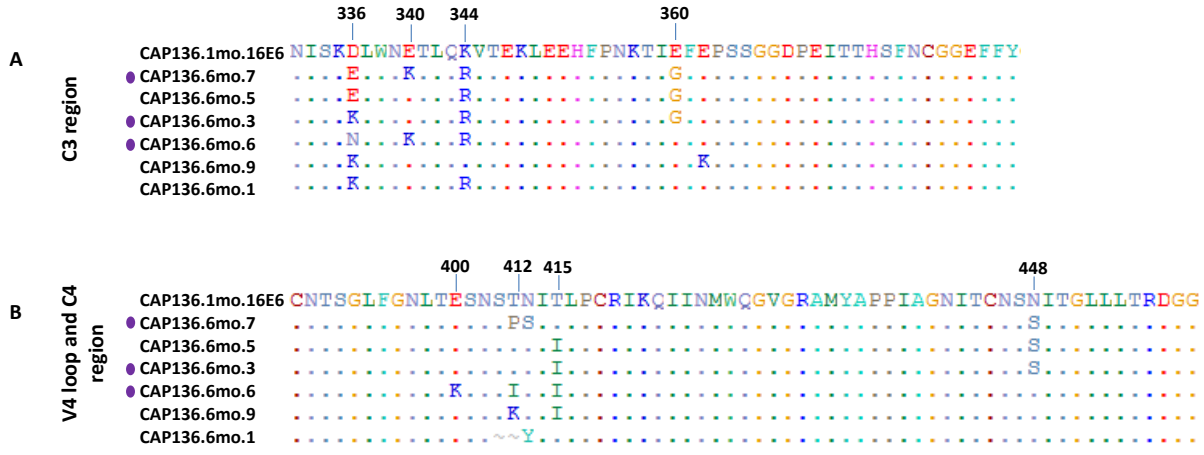

Figure 30. CAP136 protein sequence alignment of acute and 6 month sequences. (A) The C3 region. **(B)** The V4 loop and C4 region. Sequence identity to the 1 month amplicon is depicted as a dot and gaps appear as tildes. HXB2 numbering is shown above the alignment. Amino acids are represented by their 1-letter symbols. Cloned amplicons are indicated by purple circles.

CAP136.6mo.7 had 4 mutations in the C3 region (D336E, E340K, K344R and E360G) and 2 in the V4 loop (T412P and N413S) (Figure 30). A second clone, CAP136.6mo.3, had three mutations in the C3 region (D336K, K344R and E360G) and a T415I change in the V4 loop (Figure 30). Apart from the mutations in the C3V4 region, both CAP136.6mo.3 and CAP136.6mo.7 contained an additional mutation in the C4 region (N448S) that was in close proximity to the mutations in the C3V4 region and also altered a potential N-linked glycosylation sequon. The third clone, CAP136.6mo.6 had 3 mutations in the alpha2-helix (D336N, E340K and K344R) and three mutations in the V4 loop (E400K, T412I and T415I) when compared to the acute clone (Figure 30). While the majority of mutations in the C3 region of all three clones were charge changes, mutations in the V4 loop affected potential N-linked glycosylation sequons.

The role of the potential escape mutations in the C3V4 and C4 regions of the three CAP136 6 month clones was therefore investigated using back-mutants (Figure 31). In CAP136.6mo.6 (Figure 31 A) the alpha2-helix back-mutant (CAP136.6mo N336D K349E R344K) did not have a significant effect on neutralisation titres. However when an additional three mutations in the V4 loop were simultaneously introduced (creating the CAP136.6mo.6 C3V4 sensitive construct), the neutralisation

sensitivity matched that of the acute clone. Therefore escape in this clone was mediated by changes in the C3V4 region.

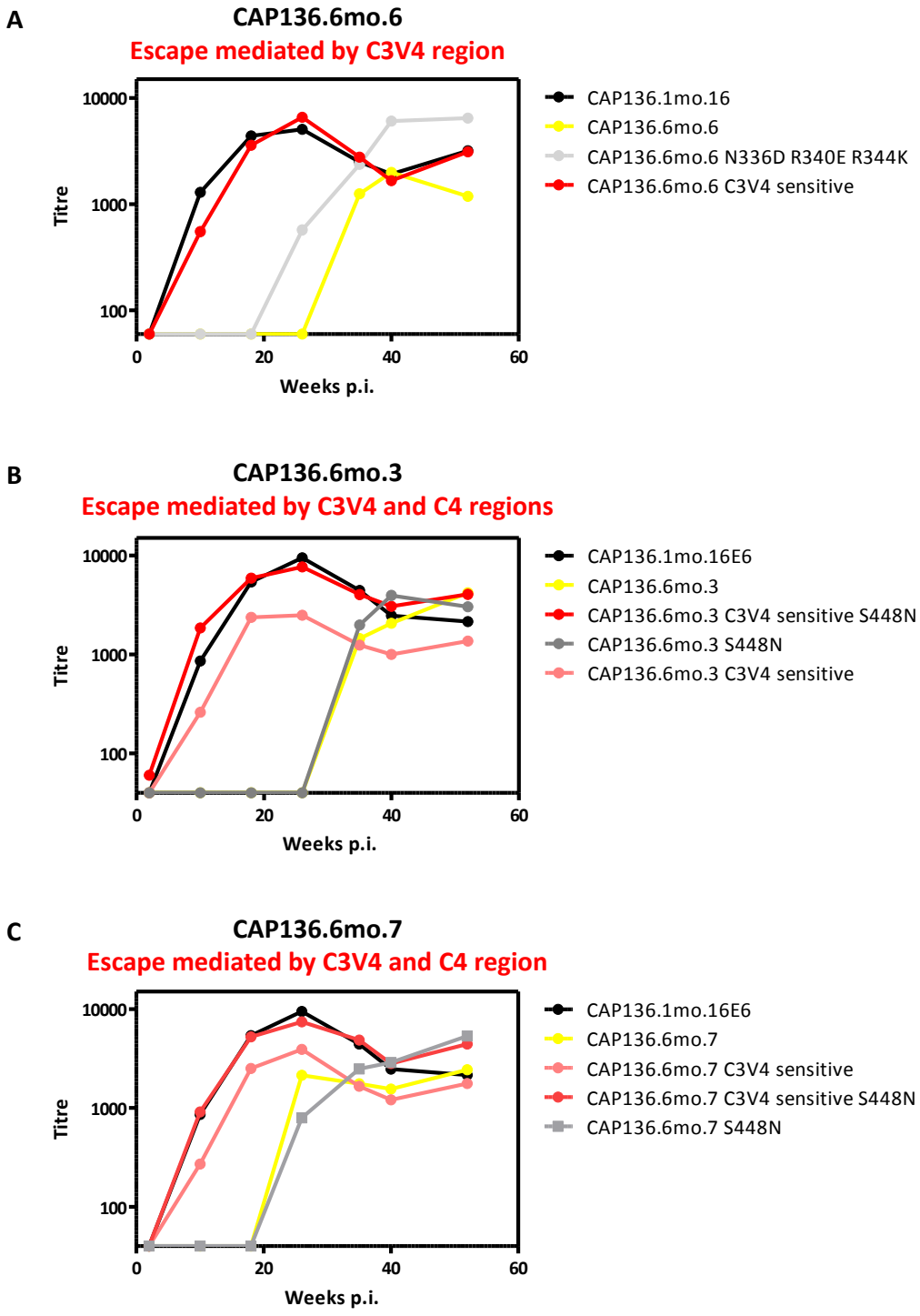

Figure 31. Pathways of neutralisation escape in CAP136. The 1 and 6 month clones are shown in black and yellow curves respectively. **(A)** In CAP136.6mo.6 escape was mediated by three mutations in the alpha2-helix and three in the V4 loop (red). Reversion of mutations in the alpha2-helix alone did not affect sensitivity of this 6 month clone (grey). **(B and C)** In CAP136.6mo.3 and CAP136.6mo.7 escape was mediated through mutations in the C3V4 and C4 regions (red). The C3V4 region back-mutants were only partially sensitive (pink) and in both 6 month clones the S448N mutation alone had no effect on neutralisation sensitivity (grey). y axis: ID_{50} titres. x axis: weeks p.i.

In contrast, in both CAP136.6mo.3 and CAP136.6mo.7 the C3V4 back-mutants (CAP136.6mo.3 C3V4 sensitive and CAP136.6mo.7 C3V4 sensitive) showed only partial sensitivity when compared to the acute clone (Figure 31 B and C). In both clones a mutation at position 448 in the C4 region was structurally proximal to the C3V4 mutations. When position 448 was reverted together with the changes in the C3V4 region (to create CAP136.6mo.3 C3V4 sensitive S448N and CAP136.6mo.7 C3V4 sensitive S448N) the neutralisation sensitivities matched that of the acute clone. The S448N back-mutation alone (CAP136.6mo.3 S448N and CAP136.6mo.7 S448N) however had no effect on escape in either clone. Therefore in CAP136.6mo.3 and CAP136.6mo.7 escape was mediated by changes in both the C3V4 and C4 regions.

Although loss of potential N-linked glycosylation sequons were observed in the V4 loop and C4 region, the majority of escape mutations in the C3 region affected charged residues in the three 6 month clones isolated from CAP136. These data show that in CAP136 by 6 months p.i. two pathways of escape were employed. One clone escaped the AnAb response via the changes in the C3V4 region only, while in two other clones escape was mediated by mutations in the C3V4 region together with a mutation at position 448 in the C4 region.

4.4 CAP244: Escape via the C3V4 and V5 regions

The C3V4 chimera for CAP244 showed sensitivity to the autologous plasma from 10 months p.i. suggesting that an anti-C3V4 response did not develop before this time. After 10 months p.i., the chimera showed less than 2-fold lower titres compared to the acute clone. As the anti-C3V4 response developed relatively late, SGAs were generated at 12 months p.i. to characterise escape from the anti-C3V4 response. A representative phylogenetic tree, created using the minimum evolution method, shows the diversity within the 12 month SGAs (Figure 32). CAP244.12mo.3 and CAP244.12mo.4 were selected for cloning.

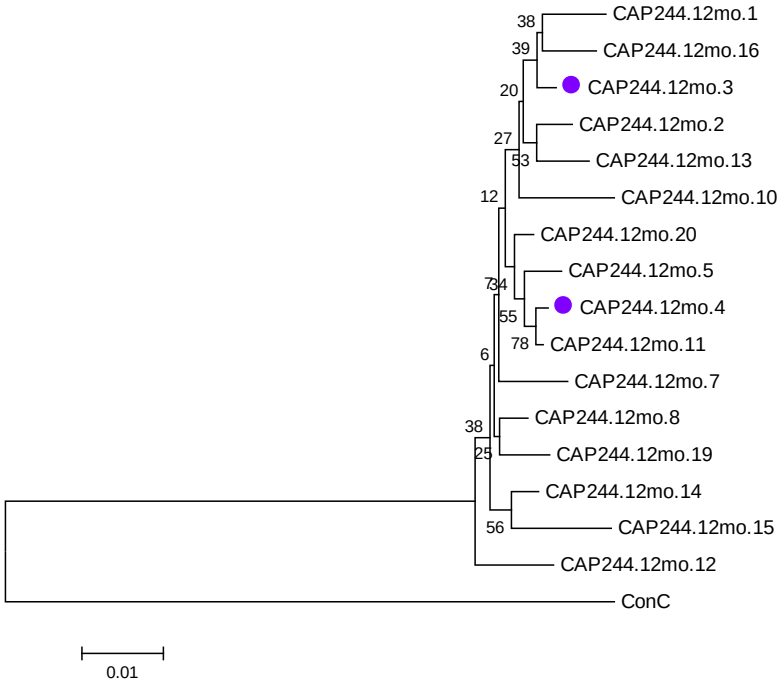

Figure 32. Minimum evolution phylogenetic tree for the CAP244 12 month p.i. SGAs. Amplicons that were selected for cloning are indicated by a purple dot. Bootstrap values are shown for each grouping. ConC was used as the reference sequence for rooting the phylogeny. The scale represents evolutionary distance measured by number of amino acid substitutions per site.

Numerous potential escape mutations were present in the C3V4 region of the CAP244 12 month amplicons. An entropy plot comparing the 2 month clone to the 12 month clones also highlighted many other regions with high entropy, consistent with the longer duration of infection (Figure 33 A). However the V5 loop was the only region, other than the C3V4 region, that had residues with especially high entropy values. The mutations in the alpha2-helix (cyan in Figure 33) formed two distinct clusters, with those at the N-terminus grouping with the mutations in the V4 loop (green Figure 33) and those at the C-terminus grouping with the V5 loop (orange in Figure 33).

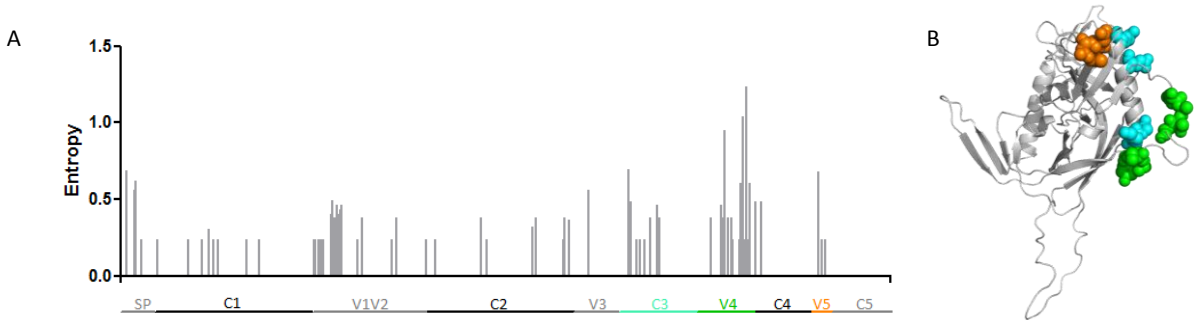

Figure 33. Identification of potential escape mutations in CAP244. (A) Entropy plot of gp120 from acute and 12 month clones. y axis: entropy. x axis: regions in gp120. **(B)** The residues with the highest entropy in the C3 region (cyan), V4 loop (green) and V5 loop (orange) are shown on the homology model of CAP244.12mo.4 gp120.

In CAP244.12mo.3 four mutations (D334S, A337D, K347E and E351K) were found in the C3 region (Figure 34 A). Two non-contiguous insertions occurred in the V4 loop, at position 400b (Ala-Thr-Gly-Asn) and at position 411 (Thr-Tyr-Ile) (Figure 34 B). In the C3 region and V4 loop of CAP244.12mo.4, a similar set of mutations (D334S, G336R, K347E and E351K) and insertions (at 400b: Gly-Thr-Gly-Asn and 411: Thr-His-Ile) were observed (Figure 34 A and B). Additionally in both clones two mutations (G462aD and I465T) in the V5 loop (Figure 34 C) were structurally proximal to the N-terminus of the alpha2-helix. The majority of the mutations in the C3 region were at positions occupied by charged residues. The D334S mutation in the C3 region, insertions in the V4 loop and I465T mutation in the V5 loop caused changes in potential N-linked glycosylation sequons (Figure 34).

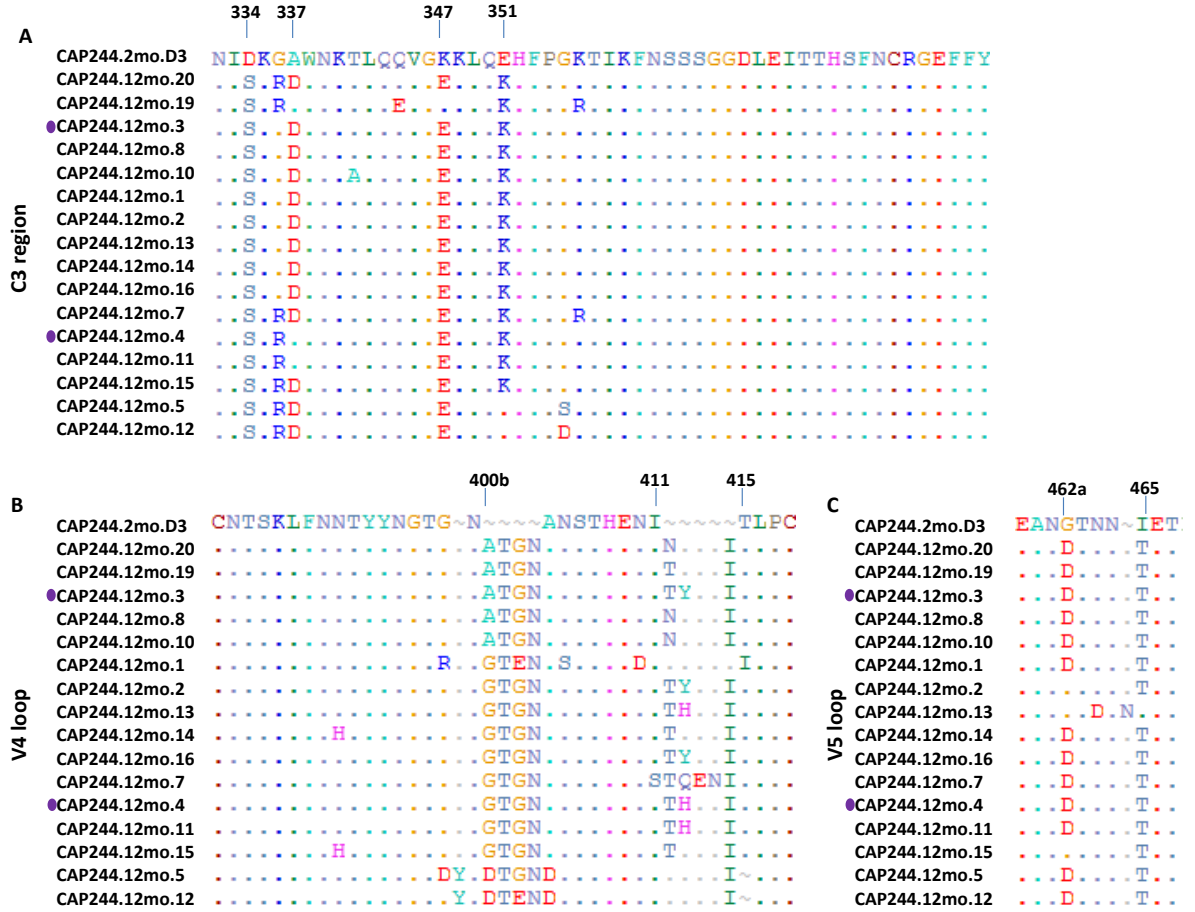

Figure 34. CAP244 protein sequence alignment of the acute and 12 month sequences. (A) The C3 region. **(B)** The V4 loop. **(C)** The V5 loop. Sequence identity to the acute amplicon is depicted as a dot and gaps appear as tildes. HXB2 numbering is shown above the alignment. Amino acids are represented by their 1-letter symbols. Cloned amplicons are indicated by purple circles.

Back-mutating all 11 changes in the C3V4 region of both 12 month clones, creating CAP244.12mo.3 C3V4 sensitive and CAP244.12mo.4 C3V4 sensitive, resulted in significantly increased sensitivity to autologous neutralisation, but neutralisation profiles did not match the acute clone (Figure 35). CAP244.12mo.3 C3V4 sensitive (Figure 35 A) was more sensitive to autologous neutralisation than

CAP244.12mo.4 C3V4 sensitive (Figure 35 B), suggesting that the former was more dependent on mutations in the C3V4 region for mediating neutralisation escape.

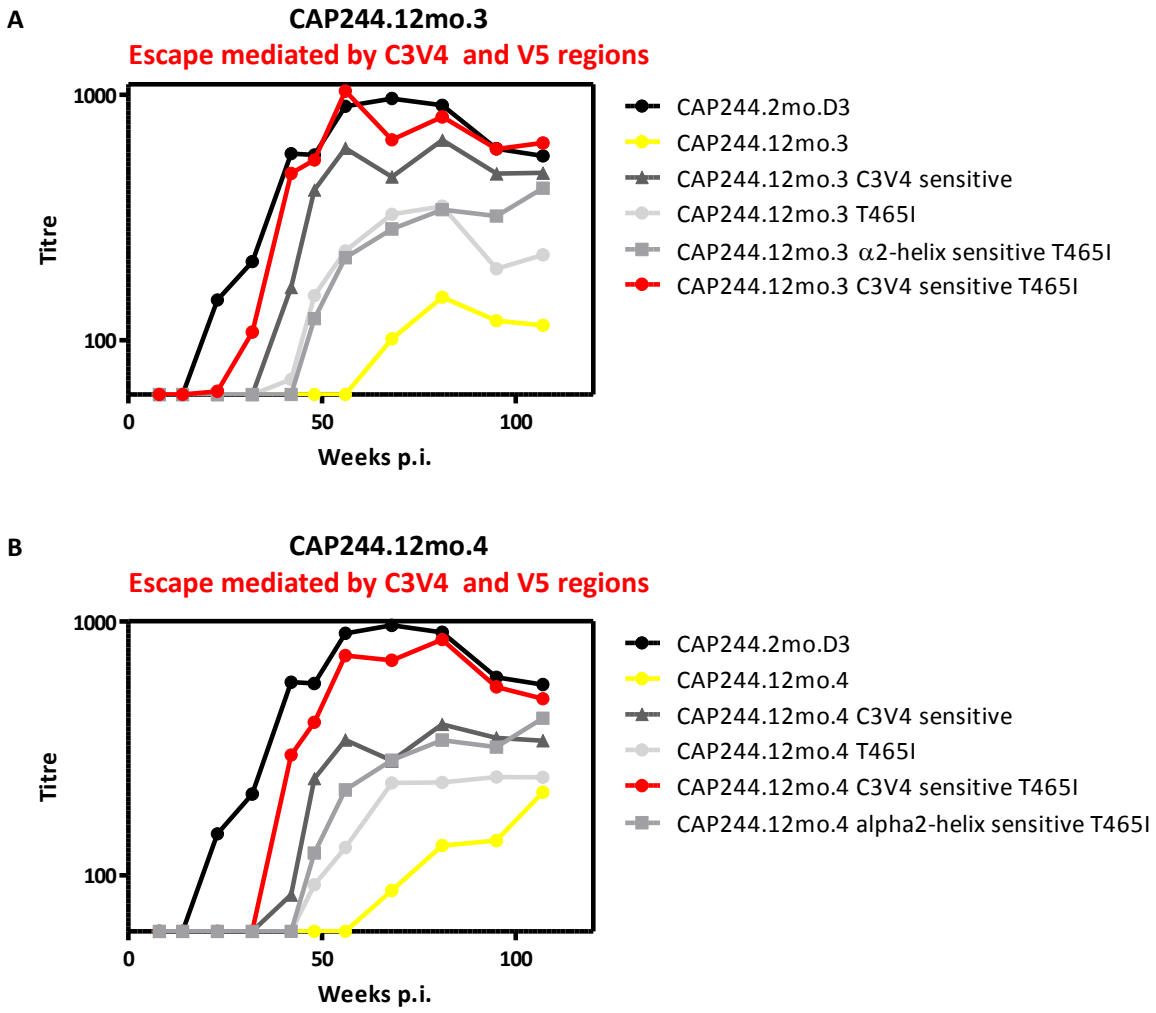

Figure 35. Mechanisms of neutralisation escape at 12 months p.i. in CAP244. The acute and 12 month clones are shown in black and yellow respectively. **(A and B)** In both CAP244.12mo.3 and CAP244.12mo.4 escape was mediated by mutations and insertions in the C3V4 region together with a mutation at position 465 in the V5 loop (red). The C3V4 back-mutant (grey triangles) had higher titres than the T465I back-mutant (grey circles) in CAP244.12mo.3, however both these constructs showed a similar level of sensitivity in CAP244.12mo.4. In both clones the C3V4 region back-mutants (grey triangles) were only partially sensitive to autologous plasma. Concurrent reversion of the alpha2-helix and position 465 (grey squares), did not alter the neutralisation sensitivity when compared to that of the T465I back-mutant (grey circles) in both clones. y axis: ID_{50} titres. x axis: weeks p.i.

The I465T mutation, which affected a PNG in the V5 loop, was structurally proximal to mutations at the C-terminus of the alpha2-helix and was present in all but one of the 12 month SGAs, therefore the role of this mutation was investigated. Position 465 was back-mutated alone and in conjunction with those mutations in the C3V4 region. The CAP244.12mo.3 T465I and the CAP244.12mo.4 T465I back-mutants showed some increase in sensitivity, but as with changes in the C3V4 region alone, did

not confer complete neutralisation sensitivity (Figure 35). Both the CAP244.12mo.3 C3V4 sensitive T465I and CAP244.12mo.4 C3V4 sensitive T465I constructs were as sensitive as the acute clone after 8 months p.i. (Figure 35). Taken together with the fact that the CAP244 C3V4 chimera was not sensitive to neutralisation by the autologous plasma until 10 months p.i., these results provide evidence to strongly suggest that the first AnAb response in CAP244 did not target the C3V4 region. Therefore changes in the C3V4 region and V5 loop mediated escape from the anti-C3V4 response which only developed after 8 months p.i. The first specificity, which does not target the C3V4 region, has not been investigated here.

In order to dissect the roles of specific mutations, the alpha2-helix (rather than the complete C3V4 region) was back-mutated simultaneously with position 465. The CAP244.12mo.3 alpha2-helix sensitive T465I and CAP244.12mo.4 alpha2-helix sensitive T465I back-mutants showed the same level of sensitivity as the T465I mutant alone, suggesting that mutations within the alpha2-helix did not contribute significantly to neutralisation escape (Figure 35).

Overall, the neutralisation profile of the C3V4 chimera suggests that the anti-C3V4 response in CAP244 did not develop until after 8 months p.i. This was supported by the neutralisation escape pathways in two 12 month clones. Although potential N-linked glycan sequons in the C3, V4 and V5 regions were affected, multiple charge changes in the C3 region were also present by 12 months p.i. In both 12 month clones of CAP244, escape was mediated via mutations in the C3V4 region and V5 loop, despite minor differences in the mutations in both clones.

4.3 CAP206: Escape via the C2 region and alpha2-helix

The SGAs and cloning for this individual had been completed previously (Gray *et al* in preparation). Similarly to CAP244, the CAP206 anti-C3V4 response only developed after 10 months p.i, as indicated by the sensitivity of the C3V4 chimera. Neutralisation titres of the C3V4 chimera were up to 6-fold higher than for the acute autologous clone after 10 months p.i., however the shape of the neutralisation curve for the chimera was similar to that for the acute clone, therefore neutralisation escape was investigated in a 12 month clone (CAP206.12mo.13.).

Numerous mutations were located in the C3 region (cyan in Figure 36) of CAP206.12mo.13, however positions with high entropy in the V4 loop (green in Figure 36) were not mutated in this clone. At 12 months p.i many other sites within gp120 had high entropy (Figure 36 A), consistent with to the longer period of infection. Regions with high entropy that were structurally proximal to the C3 region were the C2 region (blue in Figure 36), C4 region (purple in Figure 36) and V5 loop (orange in Figure 36). Mutations in the C4 region and V5 loop were located close to those at the C-terminus of the alpha2-helix, while mutations in the C2 region clustered with those at the N-terminus of the alpha2-helix. The high entropy residues in the C4 region, as with the V4 loop, were not mutated in CAP206.12mo.13. The V1V2 region has not been crystallised in the context of the complete gp120, therefore the influence of mutations in the V1V2 region in mediating escape from an anti-C3V4 response may not be apparent from a structural prediction of gp120. However a large degree of variability in the V1V2 region was present by 12 months p.i. Mutations in the V1V2, C2, C3 and V5 regions were therefore investigated for their role in mediating neutralisation escape.

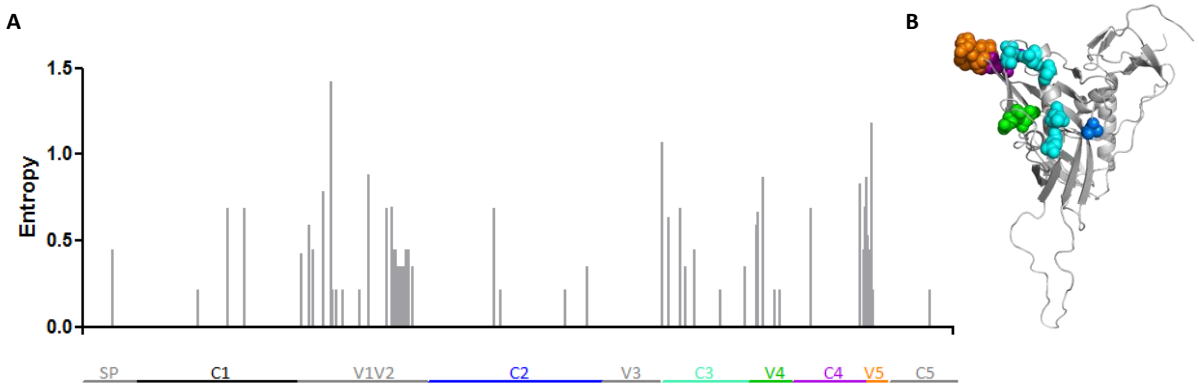

Figure 36. Regions with high entropy in gp120 of the CAP206 12 month p.i. clones. (A) Entropy plot of gp120 using acute and 12 month clones. $\boldsymbol{y}$ axis: entropy. $\boldsymbol{x}$ axis: regions in gp120. **(B)** Residues with the highest entropy in the C2 region (blue), C3 region (cyan) and C4 region (green) V5 loop (orange, are shown on the homology model of CAP206.12mo.13 gp120.

Within the V1V2 loop four single amino acid mutations were present (S137N, N147Y, Q171H and S188Y) as well as an 8 amino acid insertion (Lys-Ala-Asn-Ser-Ser-Glu-His-Ser) at position 186a (Figure 37). However, only the S188Y and Δ186a to 186h mutations in the V1V2 loop and D336N, S355G and Δ461 in the C3V4 region had arisen after to 6 months p.i., suggesting that the earlier mutations, which preceded the anti-C3V4 response, probably did not contribute to neutralisation escape. Twelve mutations had accumulated in CAP206.12mo.13. These were located in the C2 region (A290S), C3 region (D336N, G347R, N350K and S355G) and V5 loop (deletions between 460 to 462, S463N and S464N) (Figure 37).

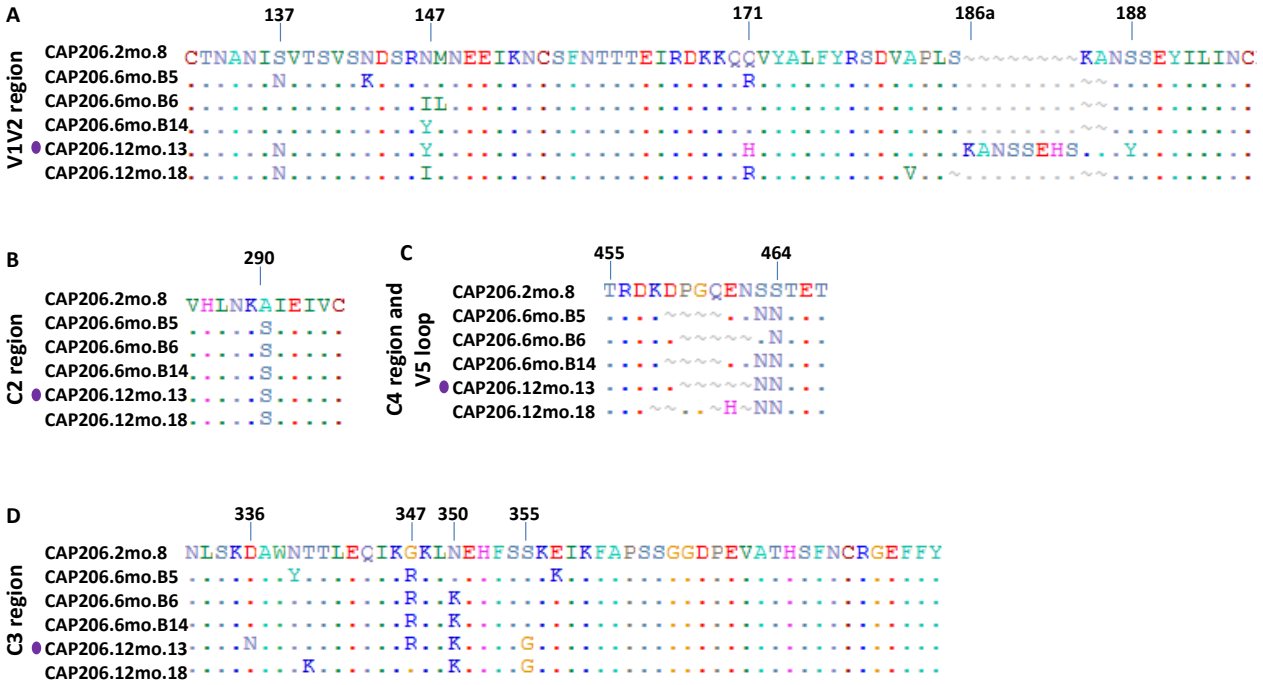

Figure 37. CAP206 protein sequence alignment of clones from 8 weeks to 12 months p.i. (A) The V1V2 region. **(B)** A portion of the C2 region. **(C)** A portion of the C4 region and the entire V5 loop. (D) The C3 region. Sequence identity to the acute clone is depicted as a dot and gaps appear as tildes. HXB2 numbering is shown above the alignment. Amino acids are represented by their 1-letter symbols.

The role of the mutations in the V1V2, C2 and C3 regions as well as the V5 loop were investigated in CAP206.12mo.13 by comparing the neutralisation profiles of back-mutants to those of the acute and 12 month clones (Figure 38).

The mutations in the V1V2 loop and C3 region were back-mutated individually (to create CAP206.12mo.13 V1V2 sensitive and CAP206.12mo.13 C3 sensitive), however both these constructs showed no significant increase in neutralisation sensitivity as shown by Figure 38 A. Similarly, when the changes in these two regions were back-mutated in conjunction with each other in the CAP206.12mo.13 V1V2 + C3 sensitive construct, neutralisation sensitivity was not altered. This suggested the involvement of other regions in mediating escape.

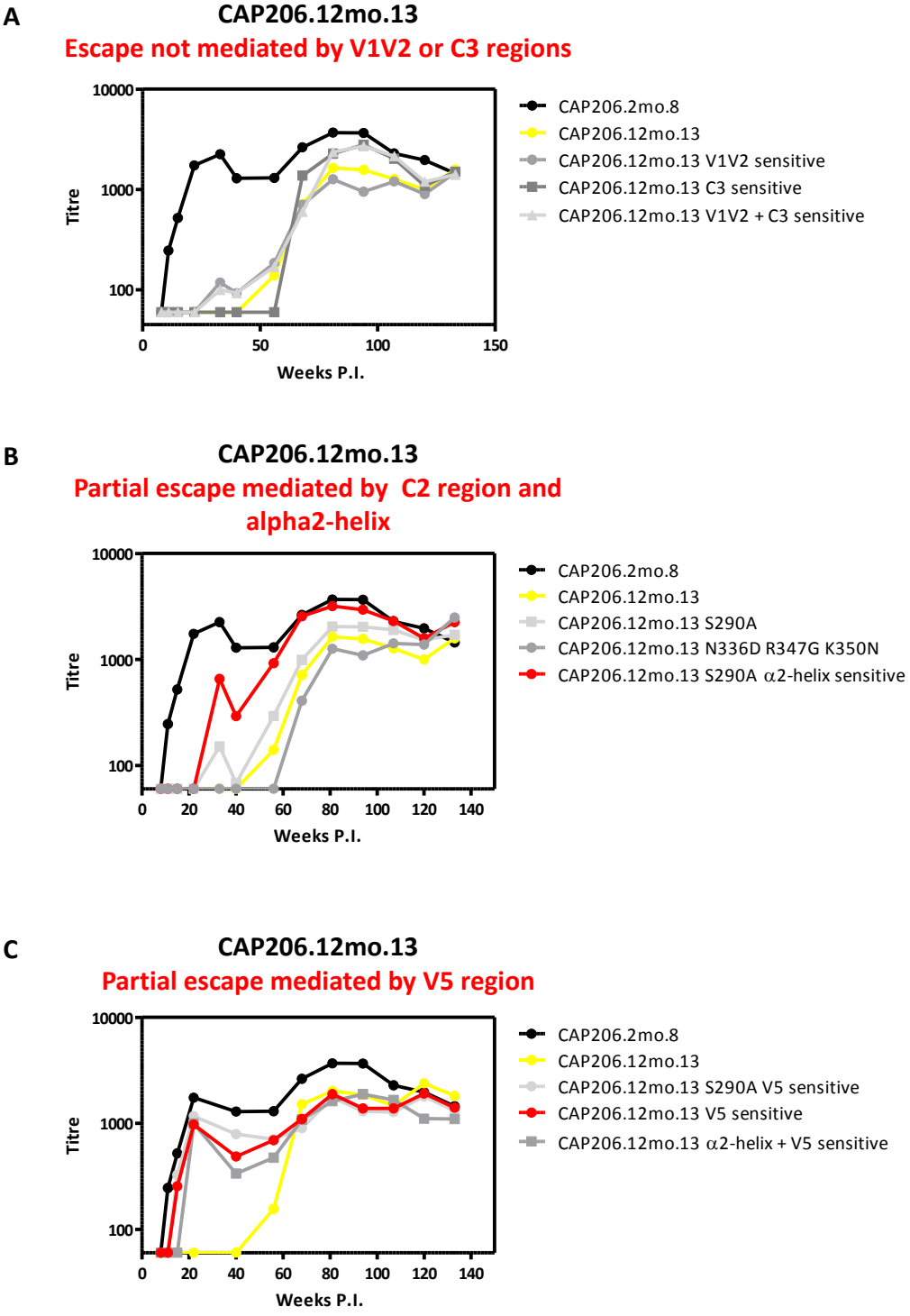

Figure 38. Pathways of neutralisation escape in CAP206.12mo.13. The acute and 12 month clones are shown in black and yellow curves respectively. **(A)** Escape in CAP206.12mo.13 was not mediated by mutations in the V1V2 (grey circles) and C3 (grey squares) regions alone or in conjunction with each other (grey triangles). **(B)** Back-mutation of three residues in the alpha2-helix (grey circles) did not have an effect on neutralisation sensitivity. The S290A mutation in the C2 region (grey) mediated partial escape from an early neutralisation response however reversion of position 290 and the alpha2-helix mutations concurrently (red) caused a significant shift in the neutralisation sensitivity especially after 33 weeks p.i. **(C)** The V5 loop back-mutant (red) restored significant sensitivity prior to 40 weeks p.i. Back-mutating position 290 (grey circles) or the alpha2-helix (grey squares) in the presence of the V5 region back-mutations had no further effect on neutralisation. y axis: ID_{50} titres. x axis: weeks p.i.

An alpha2-helix back-mutant, which introduced three mutations into the 12 month clone, was created, but this construct (CAP206.12mo.13 N336D R347G K350N) did not show increased neutralisation sensitivity when compared to the 12 month clone (Figure 38 B). When only position 290 in the C2 region was back-mutated, a brief spike in neutralisation sensitivity at 33 week p.i., which waned after 40 weeks p.i., was observed (Figure 38 B). The mutation at position 290 of the C2 region was structurally proximal to mutations at the N-terminus of the alpha2-helix, therefore the effect of these 4 mutations in concert was investigated. The resulting construct (CAP206.12mo.13 S290A alpha2-helix sensitive) showed a similar spike in neutralisation sensitivity at 33 weeks p.i., but in addition became as sensitive as the acute clone after 40 weeks p.i. (Figure 38 B). Notably, the initial spike in neutralisation sensitivity of the C2 region back-mutant (CAP206.12mo.13 S290A) was 3-fold lower than CAP206.12mo.13 S290A alpha2-helix sensitive. These data suggest that mutations in both the C2 region and alpha2-helix resulted in escape from an AnAb response that developed after 33 weeks p.i.

Although neutralisation escape from the later AnAb response was accounted for by mutations in the C2 region and alpha2-helix, neutralisation escape from AnAbs prior to 33 weeks p.i. had still not been defined. Therefore the potential role of mutations in the V5 loop, which was proximal to mutations at the C-terminus of the alpha2-helix, was investigated. The V5 loop back-mutant (CAP206.12mo.13 V5 sensitive) showed the greatest neutralisation sensitivity prior to 40 weeks p.i. (Figure 38 C). However no additional increase in sensitivity was observed when either position S290 (CAP206.12mo.13 S290A V5 sensitive) or the alpha2-helix (CAP206.12mo.13 alpha2-helix + V5 sensitive) were back-mutated with those in the V5 loop. A construct that contained the relevant back-mutations in the C2 region, alpha2-helix and V5 loop was also created, however it failed to produce infectious pseudoviruses and could not be tested for neutralisation sensitivity. These results support the hypothesis that an early response, prior to 40 weeks p.i., was escaped via mutations in the V5 loop.

In CAP206.12mo.13 therefore, the V1V2 and C3 regions alone did not contribute to neutralisation escape. As with CAP244, mutations were found at each of the termini of the alpha2-helix, with mutations in the V5 loop clustering with the mutations at the C-terminus of the alpha2-helix, while mutations in the C2 region clustered with those at the N-terminus of the alpha2-helix. An AnAb response that developed prior to 40 weeks p.i. was escaped by mutations in the V5 loop, whilst a

later AnAb response, that developed after 40 weeks p.i. and targeted the C3V4 region, was escaped by mutations in the C2 region and alpha2-helix.

4.4 Summary

This chapter investigated the escape pathways employed by 5 individuals who mounted a response to the C3V4 region within 2 years of HIV-1 infection. The results indicate that while neutralisation escape can be mediated by the C3V4 region alone, escape via other regions in addition to the C3V4 region occurs in the majority of cases. Regions that were shown to mediate escape from an anti-C3V4 response were the C2 region, V3 loop, C4 region and V5 loop. The alpha2-helix has previously been hypothesised to be an important mediator of neutralisation escape (Gnanakaran et al., 2007; Rong et al., 2007b), however in this study escape via mutations in the alpha2-helix alone was observed in just a single clone. This suggests that while the alpha2-helix can mediate neutralisation escape, this pathway of neutralisation escape does not confer a significant advantage. Furthermore, escape via multiple mechanisms among different clones isolated from the same individual was observed in 3 C3V4 responders, further illustrating the large array of diverse yet viable escape options at the disposal of HIV-1. In two individuals, where escape was investigated at 12 months p.i. as opposed to 6 months p.i., two clusters of mutations at opposite ends of the alpha2-helix were observed, suggesting the existence of two potential sub-epitopes within the C3V4 region.

Chapter 5: Discussion and Conclusions

Early AnAbs in subtype C infections have a limited number of specificities (Moore et al., 2009) with anti-C3V4 responses being very common (Moore et al., 2008; Moore et al., 2009; Rong et al., 2009). This study has confirmed, in an additional 10 subtype C infected individuals, that the C3V4 region is indeed a major target of the early AnAb response. In addition, identification of individuals infected with subtype C who do not develop an anti-C3V4 response, has enabled us to determine factors which contribute to the development of such a response. We have investigated the neutralisation escape pathways in 5 C3V4 responders and shown that while mutations in the alpha2-helix can be important for mediating neutralisation escape, the alpha2-helix rarely performs this function alone, and generally requires interaction with other regions. Lastly we have shown in three cases that neutralisation escape can occur by multiple pathways within a single individual.

Here we made use of C3V4 chimeras to detect anti-C3V4 responses. A caveat regarding the use of chimeras is the fact that the replacement of a portion of gp120 in one virus with that from another may cause conformational disruptions in the envelope due to variations in length, glycosylation and amino acid properties (Moore et al., 2008). These conformational disruptions could expose neutralising epitopes that are normally occluded in the trimeric structure, which may cause the detection of "false positive" anti-C3V4 responses. Most HIV-1 infected individuals develop anti-V3 and anti-CD4 binding site antibodies, which are normally non-neutralising as their epitopes are inaccessible. However, those specificities do have the capacity to neutralise when there is unusual exposure of epitopes due to conformational problems or in T cell adapted viruses which have been cultured in the absence of antibody pressure (Mascola and McNeil, 1995). Therefore heterologous plasmas containing these specificities can be used to test for exposure of these regions, which would indicate conformational disruption of the envelope (Binley et al., 2004; Conley et al., 1994; Corti et al., 2010; Davis et al., 2009; Gorny et al., 2006; Hioe et al., 2010; Moore et al., 2008). These experiments minimise the risk of unusual neutralisation sensitivity, and validate the use of individual chimera in detecting anti-C3V4 responses. All chimeras used in this study were resistant to neutralisation by several unrelated plasmas, suggesting that they were conformationally intact. Moreover, because immune pressure on a region leads to increased variation through the course of HIV-1 infection (Choisy et al., 2004; Gaschen et al., 2002; Moore et al., 2009; Tang et al., 2011), the use of chimeras to determine C3V4 responses was also validated by the presence of mutations in the C3V4 regions of later viruses isolated from 13 responders for whom longitudinal sequences were available.

Another caveat with the use of chimeras may be reduced sensitivity to C3V4 responses when compared with the autologous parental viruses. Indeed twelve of the fourteen C3V4 responder chimeras were less sensitive than the autologous parents. In 9 cases, the chimera only became sensitive at later time points compared to the autologous parent. There are a number of possible reasons for reduced neutralisation sensitivity of chimeras. If the epitope was not fully encompassed in the C3V4 region, neutralising antibodies targeting this region may not bind as efficiently to the chimera, resulting in a decrease in titres (Li et al., 2011b; Walker et al., 2009; Watkins et al., 1996). In addition, lower overall titres, caused by partial epitope recapitulation, could explain why the chimeras did not detect earlier (and therefore lower titre) responses. Alternatively the lack of sensitivity of some chimeras to earlier time points may suggest the presence of an initial AnAb response targeting a different region of the envelope (Moore et al., 2008; Moore et al., 2009). The neutralisation curves for three C3V4 chimeras had a biphasic shape, suggesting the development of multiple and possibly subtly different anti-C3V4 responses, similar to a recent paper on anti-V1V2 antibodies (Lynch et al., 2011). Alternatively the re-emergence of the initial anti-C3V4 response at a later time point may occur due to the resurgence of early viruses from viral reservoirs. Linked to this is the possibility that an initial anti-C3V4 antibody response has affinity matured with time (Corti et al., 2010; Huber et al., 2010; Lynch et al., 2011; Walker et al., 2009; Wrammert et al., 2011; Wu et al., 2010; Xiao et al., 2009).

The C3V4 chimeras for all the non-responders were completely resistant to neutralisation by plasma from the autologous parent. However, as described above, the potential for incomplete epitope recapitulation within chimeric constructs also makes it possible that some anti-C3V4 responses were not detected, leading to the classification of “false negatives”. In four non-responders for whom longitudinal sequences were available, mutations in the C3V4 region did arise by 6 months p.i., which may suggest that the C3V4 region is a target for AnAbs in these individuals. However the V4 loop is highly variable and mutations in this region may be due to a range of other reasons, such as pressure from cytotoxic T cell (CTL) immune responses (Johnson et al., 1993; Li et al., 2011a; Ross and Rodrigo, 2002).

Although the use of chimeras is common for these kinds of studies, an improvement to this approach, which future studies could utilise, would be to identify a neutralisation resistant backbone for each C3V4 chimera that is similar in length and glycosylation pattern to the autologous virus. A second modification to limit the number of “false negatives” would be to test all non-responders in

more than one backbone to increase the certainty that there is no anti-C3V4 response in those individuals.

Through the comparison of C3V4 responders and non-responders we have shown that a shorter V4 loop and fewer PNGs in the C3V4 region were associated with an anti-C3V4 response. The differences in the number of PNGs in the C3V4 region were not significant when normalised for the length of the V4 loop, and was therefore a direct consequence of the length of the V4 loop, consistent with previous studies (Gnanakaran et al., 2007). Longer variable loop lengths can occlude neutralisation epitopes within the envelope, and shorter variable loop lengths have been associated with increased neutralisation sensitivity (Gray et al., 2007; Pugach et al., 2004; Rong et al., 2007c; Saunders et al., 2005; Stamatatos et al., 1998). Similarly the role of glycans in occluding neutralisation epitopes has been previously described (Wei et al., 2003). N-linked glycans protrude 15 to 20 Å from the surface of gp120 and then branch out to form an "umbrella" of mannose moieties, making each at least 20 times the mass of the average amino acid side chain, and illustrating the manner in which glycans can shield neutralisation epitopes (Wei et al., 2003; Zhang et al., 2004). Therefore a less densely glycosylated region is more exposed and may offer less steric hindrance for antibody binding. A shorter V4 loop and fewer PNGs in the C3V4 region may therefore promote an anti-C3V4 response through increased exposure and accessibility of this region.

This study also showed that development of an anti-C3V4 response was associated with higher overall neutralisation titres within the first 2 years of infection. In subtype C infected individuals, the early AnAb response has been shown to be more potent than in subtype B infections (Li et al., 2006b). The increased exposure and therefore immunogenic nature of the C3V4 region in subtype C viruses may result in the elicitation of a potent anti-C3V4 response, which in turn may contribute to higher overall AnAb titres.

The mechanisms of neutralisation escape from early anti-C3V4 responses were investigated in 11 clones isolated at 6 or 12 months p.i. from 5 C3V4 responders. In 10 of the 11 clones studied here, escape mutations affected potential N-linked glycosylation sequons in multiple regions. The role of the evolving glycan shield in mediating neutralisation escape had been demonstrated in numerous longitudinal studies (Lynch et al., 2011; Mo et al., 1997; Moore et al., 2009; Papandreou et al., 1996; Rong et al., 2009; Wei et al., 2003; Wu et al., 1996). Following the addition of sugar moieties to the

free amide of an asparagine residue in the sequon NXT/S (where X is any amino acid except proline), oligomannose precursors are converted to oligomannose, hybrid or complex glycans (Gagneux and Varki, 1999; Kornfeld and Kornfeld, 1985). Glycans that are less accessible to processing enzymes are converted into oligomannose glycans, while the more accessible glycans are converted into larger complex glycans that may possess multiple kinds and sizes of antennae (Kornfeld and Kornfeld, 1985).

This differential processing of glycans may play a role in the various neutralisation escape pathways. For example, in two 6 month clones of CAP255, neutralisation escape occurred via the insertion of PNGs in either the V4 loop alone, or together in both the V3 and V4 loops. Figure 39 shows the V3 and V4 loop PNGs modelled onto the predicted gp120 structures for each clone. The difference in the number of PNGs required for neutralisation escape in each of these clones may be accounted for by the size of the PNGs, which is a direct consequence of their accessibility to processing enzymes. As shown in Figure 39, the close proximity of 2 PNGs may limit their access to processing enzymes causing CAP255.6mo.5 to possess 2 smaller PNGs, while CAP255.5mo.10 may possess a single, yet larger PNG. This larger PNG at the N-terminus of the V4 loop in CAP255.6mo.10 may be sufficient to mask the epitope or sterically hinder antibody binding. In contrast a PNG at the C-terminus of the V4 loop may be smaller due to the presence of a PNG at the base of the V3 loop and would therefore be unable to perform this function alone. In 4 other clones isolated from CAP136 and CAP244, similar changes that altered potential N-linked glycosylation sequons mediated neutralisation escape. Overall the evolving glycan shield had a significant effect on mediating neutralisation escape.

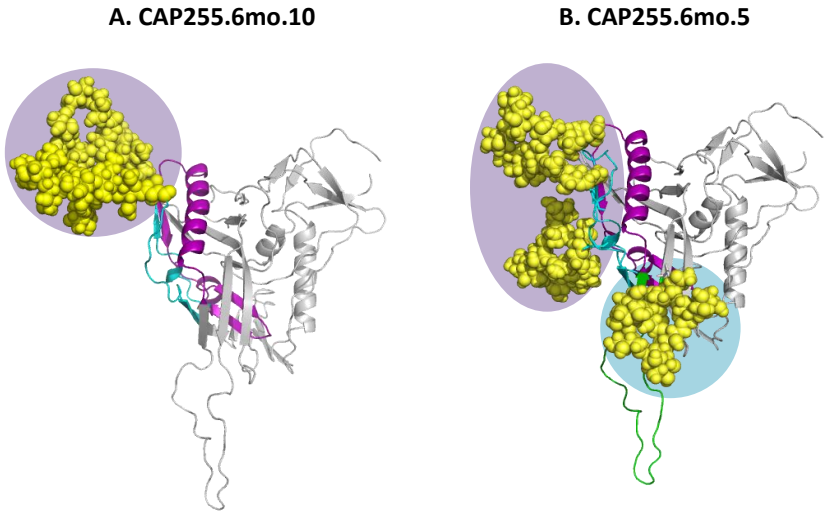

Figure 39. Spatial arrangement of potential N-linked glycans implicated in neutralisation escape in CAP255 6 month clones. Potential glycans involved in mediating escape in **(A)** CAP255.6mo.10 and **(B)** CAP255.6mo.5 are plotted as spheres on their gp120 homology models. The V3 (green) and V4 (cyan) loops, and the C3 (purple) region are highlighted. A purple sphere indicates the PNGs in the V4 loop, while the blue sphere indicates the 295 glycan at the base of the V3 loop.

Although this study has focussed on escape pathways in subtype C viruses, it is not clear whether AnAbs target similar epitopes in both HIV-1 subtype B and subtype C infections. Interestingly, potential N-linked glycans at position 295 at the base of the V3 loop and 415 in the V4 loop have been implicated in mediating neutralisation escape in two subtype B infected individuals (Tang et al., 2011). In two clones from CAP136 and in one clone from CAP255 mutations affecting PNGs in the same vicinity at the base of the V3 loop also mediated neutralisation escape. This suggests an area within the C3V4 region that may be a common neutralisation target in both subtype B and C viruses.

Mutations in the alpha2-helix of subtype C viruses have been associated with neutralisation resistance in linked donor-recipient transmission pairs (Rong et al., 2007c). In addition, switching between negatively and positively charged residues in the alpha2-helix has been implicated in mediating escape from AnAbs in early infection (Gnanakaran *et al,* 2007). The alpha2-helix was therefore proposed to directly mediate neutralisation escape via charge changes. In this study, numerous charge changes within the alpha2-helix and entire C3V4 region were involved in neutralisation escape in ten of the 11 clones, however these charge changes in the alpha2-helix mediated neutralisation escape in only 1 clone. In the remaining 10 clones, mutations that affected PNGs in regions proximal to the alpha2-helix were also required. Our results therefore clearly indicate that although neutralisation escape can be mediated by mutations solely in the alpha2-

helix, this is not a common pathway and that charge changes play an minor role, likely compensatory in nature, in mediating neutralisation escape.

In the majority of clones examined (8 of 11), mutations in regions outside of the C3V4 region (the C2, V3, C4 and V5 regions) were required for neutralisation escape. This finding supports previous suggestions that interaction of the alpha2-helix with other regions in gp120 may mediate neutralisation escape (Rong et al., 2007c). This finding is not surprising given that the C3V4 region is an integral part of the outer domain, with the alpha2-helix forming the core of the C3V4 region. The alpha2-helix is structurally proximal to the V5 loop at the C-terminus and to the C2, V3 and C4 regions at the N-terminus. Depending on the length and position of the highly flexible V4 loop, this structure may also lie in close proximity to the alpha2-helix and indeed molecular dynamic simulations of subtype C viruses have suggested an interaction between the two (Gnanakaran et al., 2007). These observations support a mechanism whereby mutations in other regions of the envelope may mediate neutralisation escape from an anti-C3V4 response.

In 2 individuals, CAP244 and CAP206, escape mutations that arose by 12 months p.i. were localised to 2 distinct clusters at opposite termini of the alpha2-helix (Figure 40). Long-range intra-protein communication is transmittable via side chain fluctuations (Dubay et al., 2011). It is not uncommon therefore for distant protein regions, up to 60 Å away, to affect each other via side chain plasticity. The average distance from the N-terminus to the C-terminus of the alpha2-helix is 30 Å. Distances between the C3V4 region and other regions that have been shown to mediate neutralisation escape (the C2, C4, V3 and V5 regions) fall within this radius. This further suggests the possibility that mutations in regions proximal to the C3V4 region may permit escape from an anti-C3V4 response.

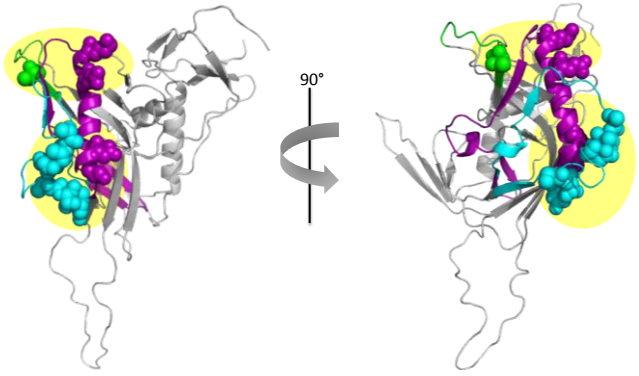

Figure 40. Two distinct clusters of escape mutations suggest multiple epitopes within the C3V4 region. Two views of gp120 show the location of mutations in both CAP244 and CAP206 12 month clones in the C3 region (purple), V4 loop (cyan) and V5 loop (green). Yellow circles indicate the presence of two clusters of mutations.

However an alternate explanation may be that the two clusters in CAP244 and CAP206 could suggest the presence of two distinct "sub-epitopes" within the C3V4 domain. The surface area of an epitope is between 600 $Å^2$ and 1100 $Å^2$ (Chakrabarti and Janin, 2002; Laver et al., 1990; Lo Conte et al., 1999; Rubinstein et al., 2008). Indeed the surface area of the VRC01 and PGT128 monoclonal antibody epitopes are 1089 $Å^2$ and 1081 $Å^2$ respectively. The surface area encompassing these two clusters is closer to 2000 $Å^2$ (excluding the surface area of any PNGs). Therefore it seems unlikely that these two clusters would form part of a single epitope. The presence of "sub-epitopes" within the C3V4 domain could further explain why this region is so commonly targeted in HIV-1 subtype C infections.

Finally, in 3 of the 5 individuals, clones isolated from each individual used different pathways to escape the anti-C3V4 response, suggesting multiple mechanisms of escape. Figure 41 shows the location of the escape mutations on the respective gp120 homology models for the 6 month clones of CAP228 and CAP136. Despite the fact that each clone escaped via a different pathway, the clustering of the mutations suggested that the same face of the outer domain and therefore a single epitope was targeted in each individual. Therefore the plasticity of the envelope may simply permit escape by multiple mechanisms from a single specificity. An alternative explanation stems from a recent finding by Lynch and colleagues who isolated 3 mAbs derived from 3 distinct B cells (Lynch et al., 2011). Although each mAb targeted and depended on the same residues in the V1 region, each of the 3 was unique. Therefore an AnAb response directed to a single region of the envelope may consist of multiple, subtly different antibodies. This in turn could suggest a reason that different pathways mediating neutralisation escape from a response targeting a single region can develop within a single individual. In addition, multiple antibodies targeting the C3V4 region could contribute to higher autologous titres in C3V4 responders when compared to non-responders.

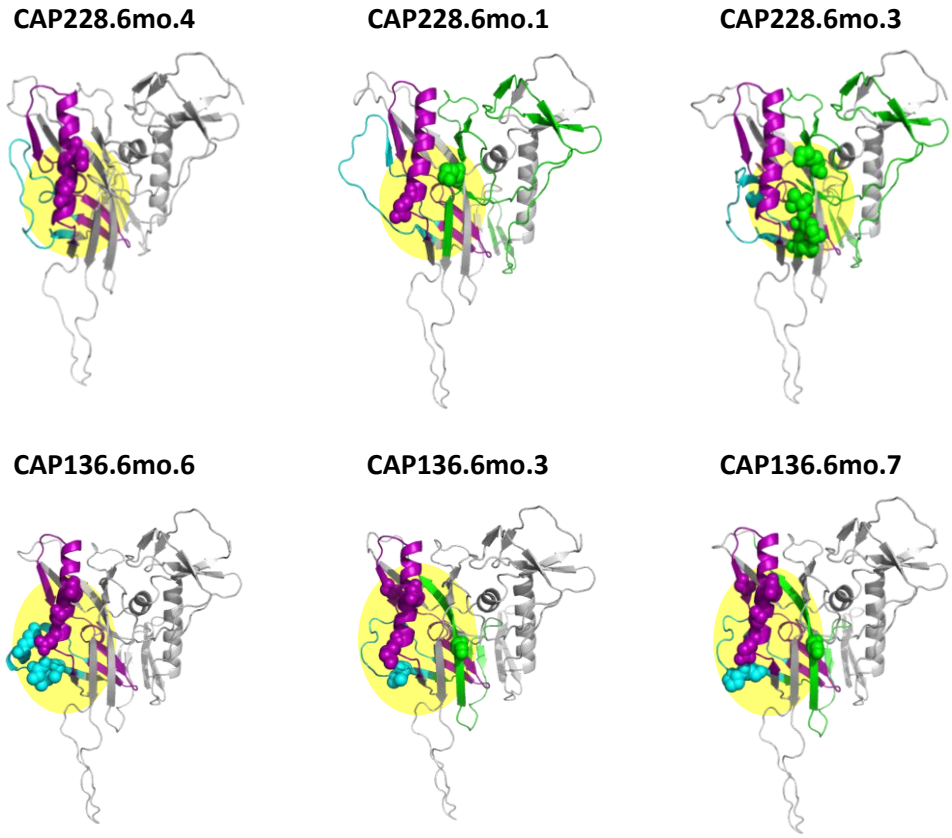

Figure 41. Neutralisation escape in CAP228 and CAP136. Mutations involved in escape from the early AnAb response in clones isolated at 6 months p.i. from CAP228 and CAP136 are shown as spheres on their respective gp120 homology models. The V4 loop (cyan), C2 (green in CAP288 clones), C4 (green in CAP136 clones) and C3 (purple) regions are highlighted. The yellow shading highlights the area where all the mutations in each individual are located.

Multiple, concurrent pathways to escape are not unexpected given the high degree of diversity of the HIV-1 envelope. However this result emphasises the immense array of options available for viral adaptation. The presence of many simultaneously occurring escape variants further suggests that these distinct paths to escape incur similar fitness costs. Multiple mechanisms of escape from anti-V1V2 responses in chronic subtype C infection have been identified in three individuals (Lynch et al., 2011; Nonyane et al., 2011; Rong et al., 2009), which suggests that this is a common trend in neutralisation escape in HIV-1 infections.

The development of an early AnAb response targeting the anti-C3V4 response does not necessarily predispose an individual to develop bnAbs as the number of individuals who develop bnAbs does not significantly differ between the C3V4 responder and non-responder groups ((Gray et al., 2011) and data not shown). In addition, the number of pathways that can be employed to escape an anti-C3V4 response suggests that the extreme diversity of this region in subtype C viruses may continue to increase as the pandemic progresses. However numerous bnAbs isolated from HIV-1 infected

individuals depend on the 332 glycan within the C3V4 region (Trkola et al., 1996; Walker et al., 2011), therefore this region may stimulate the development of protective antibodies. Therefore an immunogen including the C3V4 region would likely have to be modified, through the inclusion of glycans on a long V4 loop, to dampen the immunogenicity of the majority of the C3V4 region and to direct the humoral immune system towards the 332 glycan.

5.1 Conclusions

The C3V4 region has been confirmed as highly immunogenic in HIV-1 subtype C viruses. Within subtype C viruses, shorter V4 loops and fewer PNGs in the C3V4 region make this region more exposed, more accessible and therefore more likely to elicit an anti-C3V4 response. The immunogenicity of the C3V4 region potentially contributes to the high neutralisation titres observed in most subtype C infections. Although the alpha2-helix plays a pivotal role in the formation of the C3V4 epitope, it seldom mediates escape alone. Viruses that elicit an anti-C3V4 response can easily escape neutralisation through mutations in many other regions in the outer domain, due the integral nature of the C3V4 region within the outer domain. The size of the C3V4 region together with escape mutations found at opposite ends of the region, could suggest the presence of multiple sub-epitopes within the C3V4 domain; one at the C-terminus of the alpha2-helix, in close proximity the V5 loop and the other at the N-terminal end of the alpha2-helix. Even within a single individual, multiple mechanisms of escape, some involving regions other than the C3V4 region were observed. As there are between 5 and 8 potential N-linked glycosylation sequons in the C3V4 region, the potential for the evolving glycan shield in mediating escape from this region is significant and this has been confirmed experimentally here. Overall these findings have emphasised the adaptability and plasticity of this region in the context of viral evasion of host defences. Future studies will focus on identifying possible “sub-epitopes” within the C3V4 region, through the isolation of early monoclonal antibodies. In addition, the evolution of the glycan shield of transmitted viruses as a consequence of escape from the AnAb response has been implicated in the development of bnAb epitopes (Moore et al., 2011), therefore the role of glycosylation in mediating escape from anti-C3V4 responses will be further characterised.

Chapter 6: References

Abdool Karim, Q., Abdool Karim, S.S., Frohlich, J.A., Grobler, A.C., Baxter, C., Mansoor, L.E., Kharsany, A.B., Sibeko, S., Mlisana, K.P., Omar, Z., Gengiah, T.N., Maarschalk, S., Arulappan, N., Mlotshwa, M., Morris, L., Taylor, D., 2010. Effectiveness and safety of tenofovir gel, an antiretroviral microbicide, for the prevention of HIV infection in women. Science 329, 1168-1174.

Abrahams, M.R., Anderson, J.A., Giorgi, E.E., Seoighe, C., Mlisana, K., Ping, L.H., Athreya, G.S., Treurnicht, F.K., Keele, B.F., Wood, N., Salazar-Gonzalez, J.F., Bhattacharya, T., Chu, H., Hoffman, I., Galvin, S., Mapanje, C., Kazembe, P., Thebus, R., Fiscus, S., Hide, W., Cohen, M.S., Karim, S.A., Haynes, B.F., Shaw, G.M., Hahn, B.H., Korber, B.T., Swanstrom, R., Williamson, C., 2009. Quantitating the multiplicity of infection with human immunodeficiency virus type 1 subtype C reveals a non-poisson distribution of transmitted variants. J Virol 83, 3556-3567.

Allan, J.S., Coligan, J.E., Barin, F., McLane, M.F., Sodroski, J.G., Rosen, C.A., Haseltine, W.A., Lee, T.H., Essex, M., 1985. Major glycoprotein antigens that induce antibodies in AIDS patients are encoded by HTLV-III. Science 228, 1091-1094.

Allers, K., Hutter, G., Hofmann, J., Loddenkemper, C., Rieger, K., Thiel, E., Schneider, T., 2011. Evidence for the cure of HIV infection by CCR5Delta32/Delta32 stem cell transplantation. Blood 117, 2791-2799.

Arnold, K., Bordoli, L., Kopp, J., Schwede, T., 2006. The SWISS-MODEL workspace: a web-based environment for protein structure homology modelling. Bioinformatics 22, 195-201.

Arthos, J., Cicala, C., Martinelli, E., Macleod, K., Van Ryk, D., Wei, D., Xiao, Z., Veenstra, T.D., Conrad, T.P., Lempicki, R.A., McLaughlin, S., Pascuccio, M., Gopaul, R., McNally, J., Cruz, C.C., Censoplano, N., Chung, E., Reitano, K.N., Kottilil, S., Goode, D.J., Fauci, A.S., 2008. HIV-1 envelope protein binds to and signals through integrin alpha4beta7, the gut mucosal homing receptor for peripheral T cells. Nat Immunol 9, 301-309.

Auvert, B., Taljaard, D., Lagarde, E., Sobngwi-Tambekou, J., Sitta, R., Puren, A., 2005. Randomized, controlled intervention trial of male circumcision for reduction of HIV infection risk: the ANRS 1265 Trial. PLoS Med 2, e298.

Baba, T.W., Liska, V., Hofmann-Lehmann, R., Vlasak, J., Xu, W., Ayehunie, S., Cavacini, L.A., Posner, M.R., Katinger, H., Stiegler, G., Bernacky, B.J., Rizvi, T.A., Schmidt, R., Hill, L.R., Keeling, M.E., Lu, Y., Wright, J.E., Chou, T.C., Ruprecht, R.M., 2000. Human neutralizing monoclonal antibodies of the IgG1 subtype protect against mucosal simian-human immunodeficiency virus infection. Nat Med 6, 200-206.

Bachmann, M.F., Zinkernagel, R.M., 1997. Neutralizing Antiviral B cell Responses. Annu Rev Immunol 15, 36.

Bahmanyar, M., Fayaz, A., Nour-Salehi, S., Mohammadi, M., Koprowski, H., 1976. Successful protection of humans exposed to rabies infection. Postexposure treatment with the new human diploid cell rabies vaccine and antirabies serum. JAMA 236, 2751-2754.

Bar, K.J., Tsao, C., Iyer, S.S., Decker, J.M., Yang, Y., Bonsignori, M., Chen, X., Hwang, K.K., Montefiori, D.C., Liao, H.X., Harber, P., Fishcer, W., Li, H., Georgiev, I., McLellan, J.S., Pavlicek, J.W., Gao, F., Haynes, B.F., Hahn, B.H., Kwong, P.D., Shaw, G.M., 2012. Early low-titer neutralizing antibodies impede HIV-1 replication and select for virus escape. PLoS pathogens 8.

Beasley, R.P., Hwang, L.Y., Stevens, C.E., Lin, C.C., Hsieh, F.J., Wang, K.Y., Sun, T.S., Szmuness, W., 1983. Efficacy of hepatitis B immune globulin for prevention of perinatal transmission of the hepatitis B virus carrier state: final report of a randomized double-blind, placebo-controlled trial. Hepatology 3, 135-141.

Bennett, A.E., Liu, J., Van Ryk, D., Bliss, D., Arthos, J., Henderson, R.M., Subramaniam, S., 2007. Cryo electron tomographic analysis of an HIV neutralizing protein and its complex with native viral gp120. J Biol Chem.

Binley, J.M., Wrin, T., Korber, B., Zwick, M.B., Wang, M., Chappey, C., Stiegler, G., Kunert, R., Zolla-Pazner, S., Katinger, H., Petropoulos, C.J., Burton, D.R., 2004. Comprehensive cross-clade neutralization analysis of a panel of anti-human immunodeficiency virus type 1 monoclonal antibodies. J Virol 78, 13232-13252.

Briggs, J.A., Johnson, M.C., Simon, M.N., Fuller, S.D., Vogt, V.M., 2006. Cryo-electron microscopy reveals conserved and divergent features of gag packing in immature particles of Rous sarcoma virus and human immunodeficiency virus. J Mol Biol 355, 157-168.

Burrer, R., Haessig-Einius, S., Aubertin, A.M., Moog, C., 2005. Neutralizing as well as non-neutralizing polyclonal immunoglobulin (Ig)G from infected patients capture HIV-1 via antibodies directed against the principal immunodominant domain of gp41. Virology 333, 102-113.

Burton, D.R., 2002. Antibodies, viruses and vaccines. Nat Rev Immunol 2, 706-713.

Burton, D.R., Pyati, J., Koduri, R., Sharp, S.J., Thornton, G.B., Parren, P.W., Sawyer, L.S., Hendry, R.M., Dunlop, N., Nara, P.L., et al., 1994. Efficient neutralization of primary isolates of HIV-1 by a recombinant human monoclonal antibody. Science 266, 1024-1027.

Cao, J., Sullivan, N., Desjardin, E., Parolin, C., Robinson, J., Wyatt, R., Sodroski, J., 1997. Replication and neutralization of human immunodeficiency virus type 1 lacking the V1 and V2 variable loops of the gp120 envelope glycoprotein. J Virol 71, 9808-9812.

Carugo, O., Pongor, S., 2001. A normalized root-mean-square distance for comparing protein three-dimensional structures. Protein Sci 10, 1470-1473.

Chakrabarti, P., Janin, J., 2002. Dissecting protein-protein recognition sites. Proteins 47, 334-343.

Chan, D.C., Kim, P.S., 1998. HIV entry and its inhibition. Cell 93, 681-684.

Chen, B., Vogan, E.M., Gong, H., Skehel, J.J., Wiley, D.C., Harrison, S.C., 2005. Structure of an unliganded simian immunodeficiency virus gp120 core. Nature 433, 834-841.

Chen, X., Lu, M., Poon, B.K., Wang, Q., Ma, J., 2009. Structural improvement of unliganded simian immunodeficiency virus gp120 core by normal-mode-based X-ray crystallographic refinement. Acta Crystallogr D Biol Crystallogr 65, 339-347.

Chohan, B., Lang, D., Sagar, M., Korber, B., Lavreys, L., Richardson, B., Overbaugh, J., 2005. Selection for human immunodeficiency virus type 1 envelope glycosylation variants with shorter V1-V2 loop sequences occurs during transmission of certain genetic subtypes and may impact viral RNA levels. J Virol 79, 6528-6531.

Choi, B.K., Bobrowicz, P., Davidson, R.C., Hamilton, S.R., Kung, D.H., Li, H., Miele, R.G., Nett, J.H., Wildt, S., Gerngross, T.U., 2003. Use of combinatorial genetic libraries to humanize N-linked glycosylation in the yeast Pichia pastoris. Proc Natl Acad Sci U S A 100, 5022-5027.

Choisy, M., Woelk, C.H., Guegan, J.F., Robertson, D.L., 2004. Comparative study of adaptive molecular evolution in different human immunodeficiency virus groups and subtypes. J Virol 78, 1962-1970.

Conley, A.J., Gorny, M.K., Kessler, J.A., 2nd, Boots, L.J., Ossorio-Castro, M., Koenig, S., Lineberger, D.W., Emini, E.A., Williams, C., Zolla-Pazner, S., 1994. Neutralization of primary human immunodeficiency virus type 1 isolates by the broadly reactive anti-V3 monoclonal antibody, 447-52D. J Virol 68, 6994-7000.

Cooper, E.R., Charurat, M., Mofenson, L., Hanson, I.C., Pitt, J., Diaz, C., Hayani, K., Handelsman, E., Smeriglio, V., Hoff, R., Blattner, W., 2002. Combination antiretroviral strategies for the treatment of pregnant HIV-1-infected women and prevention of perinatal HIV-1 transmission. J Acquir Immune Defic Syndr 29, 484-494.

Corti, D., Langedijk, J.P., Hinz, A., Seaman, M.S., Vanzetta, F., Fernandez-Rodriguez, B.M., Silacci, C., Pinna, D., Jarrossay, D., Balla-Jhagjhoorsingh, S., Willems, B., Zekveld, M.J., Dreja, H., O'Sullivan, E., Pade, C., Orkin, C., Jeffs, S.A., Montefiori, D.C., Davis, D., Weissenhorn, W., McKnight, A., Heeney, J.L., Sallusto, F., Sattentau, Q.J., Weiss, R.A., Lanzavecchia, A., 2010. Analysis of memory B cell responses and isolation of novel monoclonal antibodies with neutralizing breadth from HIV-1-infected individuals. PLoS One 5, e8805.

Crispin, M.D., Ritchie, G.E., Critchley, A.J., Morgan, B.P., Wilson, I.A., Dwek, R.A., Sim, R.B., Rudd, P.M., 2004. Monoglucosylated glycans in the secreted human complement component C3: implications for protein biosynthesis and structure. FEBS Lett 566, 270-274.

D'Argenio, D.A., Wilson, C.B., 2010. A decade of vaccines: Integrating immunology and vaccinology for rational vaccine design. Immunity 33, 437-440.

Davis, K.L., Gray, E.S., Moore, P.L., Decker, J.M., Salomon, A., Montefiori, D.C., Graham, B.S., Keefer, M.C., Pinter, A., Morris, L., Hahn, B.H., Shaw, G.M., 2009. High titer HIV-1 V3-specific antibodies with broad reactivity but low neutralizing potency in acute infection and following vaccination. Virology 387, 414-426.

Decroly, E., Benjannet, S., Savaria, D., Seidah, N.G., 1997. Comparative functional role of PC7 and furin in the processing of the HIV envelope glycoprotein gp160. FEBS Lett 405, 68-72.

Delwart, E.L., Pan, H., Sheppard, H.W., Wolpert, D., Neumann, A.U., Korber, B., Mullins, J.I., 1997. Slower evolution of human immunodeficiency virus type 1 quasispecies during progression to AIDS. J Virol 71, 7498-7508.

Derdeyn, C.A., Decker, J.M., Bibollet-Ruche, F., Mokili, J.L., Muldoon, M., Denham, S.A., Heil, M.L., Kasolo, F., Musonda, R., Hahn, B.H., Shaw, G.M., Korber, B.T., Allen, S., Hunter, E., 2004. Envelope-constrained neutralization-sensitive HIV-1 after heterosexual transmission. Science 303, 2019-2022.

Dimitrov, A.S., Rawat, S.S., Jiang, S., Blumenthal, R., 2003. Role of the fusion peptide and membrane-proximal domain in HIV-1 envelope glycoprotein-mediated membrane fusion. Biochemistry 42, 14150-14158.

Dimitrov, D.S., 2004. Virus entry: molecular mechanisms and biomedical applications. Nat Rev Microbiol 2, 109-122.

Diskin, R., Marcovecchio, P.M., Bjorkman, P.J., 2010. Structure of a clade C HIV-1 gp120 bound to CD4 and CD4-induced antibody reveals anti-CD4 polyreactivity. Nat Struct Mol Biol 17, 608-613.

Dubay, K.H., Bothma, J.P., Geissler, P.L., 2011. Long-range intra-protein communication can be transmitted by correlated side-chain fluctuations alone. PLoS Comput Biol 7, e1002168.

Earl, P.L., Doms, R.W., Moss, B., 1990. Oligomeric structure of the human immunodeficiency virus type 1 envelope glycoprotein. Proc Natl Acad Sci U S A 87, 648-652.

Euler, Z., van Gils, M.J., Bunnik, E.M., Phung, P., Schweighardt, B., Wrin, T., Schuitemaker, H., 2010. Cross-reactive neutralizing humoral immunity does not protect from HIV type 1 disease progression. J Infect Dis 201, 1045-1053.

Feng, Y., Broder, C.C., Kennedy, P.E., Berger, E.A., 1996. HIV-1 entry cofactor: functional cDNA cloning of a seven-transmembrane, G protein-coupled receptor. Science 272, 872-877.

Finzi, A., Xiang, S.H., Pacheco, B., Wang, L., Haight, J., Kassa, A., Danek, B., Pancera, M., Kwong, P.D., Sodroski, J., 2010. Topological layers in the HIV-1 gp120 inner domain regulate gp41 interaction and CD4-triggered conformational transitions. Mol Cell 37, 656-667.

Freed, E.O., Martin, M.A., 1996. Domains of the human immunodeficiency virus type 1 matrix and gp41 cytoplasmic tail required for envelope incorporation into virions. J Virol 70, 341-351.

Frost, S.D., Wrin, T., Smith, D.M., Kosakovsky Pond, S.L., Liu, Y., Paxinos, E., Chappey, C., Galovich, J., Beauchaine, J., Petropoulos, C.J., Little, S.J., Richman, D.D., 2005. Neutralizing antibody responses drive the evolution of human immunodeficiency virus type 1 envelope during recent HIV infection. Proc Natl Acad Sci U S A 102, 18514-18519.

Furuta, R.A., Wild, C.T., Weng, Y., Weiss, C.D., 1998. Capture of an early fusion-active conformation of HIV-1 gp41. Nat Struct Biol 5, 276-279.

Gagneux, P., Varki, A., 1999. Evolutionary considerations in relating oligosaccharide diversity to biological function. Glycobiology 9, 747-755.

Gaschen, B., Korber, B., Foley, D.T., 1999. Global variation in the V3 region, in: C Kuiken, B.F., B Hahn,P MArx, F McCutchan, J Mellors, J Mullins, S Wolinsky B Korber (Ed.), Human Retroviruses and AIDS. Los Alamos: Los Alamos National Laboratories, pp. 594-602.

Gaschen, B., Taylor, J., Yusim, K., Foley, B., Gao, F., Lang, D., Novitsky, V., Haynes, B., Hahn, B.H., Bhattacharya, T., Korber, B., 2002. Diversity considerations in HIV-1 vaccine selection. Science 296, 2354-2360.

Gellis, S.S., McGuinnes, A.C., Peters, M., 1945. Study of prevention of mumps orchitis by gamma globulin. Am. J. Med. Sci. 210, 5.

Gentile, M., Adrian, T., Scheidler, A., Ewald, M., Dianzani, F., Pauli, G., Gelderblom, H.R., 1994. Determination of the size of HIV using adenovirus type 2 as an internal length marker. J Virol Methods 48, 43-52.

Gilbert, P.B., Berger, J.O., Stablein, D., Becker, S., Essex, M., Hammer, S.M., Kim, J.H., Degruttola, V.G., 2011. Statistical interpretation of the RV144 HIV vaccine efficacy trial in Thailand: a case study for statistical issues in efficacy trials. J Infect Dis 203, 969-975.

Gnanakaran, S., Lang, D., Daniels, M., Bhattacharya, T., Derdeyn, C.A., Korber, B., 2007. Clade-specific differences between human immunodeficiency virus type 1 clades B and C: diversity and correlations in C3-V4 regions of gp120. J Virol 81, 4886-4891.

Gorny, M.K., Williams, C., Volsky, B., Revesz, K., Wang, X.H., Burda, S., Kimura, T., Konings, F.A., Nadas, A., Anyangwe, C.A., Nyambi, P., Krachmarov, C., Pinter, A., Zolla-Pazner, S., 2006. Cross-clade neutralizing activity of human anti-V3 monoclonal antibodies derived from the cells of individuals infected with non-B clades of human immunodeficiency virus type 1. J Virol 80, 6865-6872.

Gram, G.J., Hemming, A., Bolmstedt, A., Jansson, B., Olofsson, S., Akerblom, L., Nielsen, J.O., Hansen, J.E., 1994. Identification of an N-linked glycan in the V1-loop of HIV-1 gp120 influencing neutralization by anti-V3 antibodies and soluble CD4. Arch Virol 139, 253-261.

Gray, E.S., Madiga, M.C., Hermanus, T., Moore, P.L., Wibmer, C.K., Tumba, N.L., Werner, L., Mlisana, K., Sibeko, S., Williamson, C., Abdool Karim, S.S., Morris, L., 2011. The neutralization breadth of HIV-1 develops incrementally over four years and is associated with CD4+ T cell decline and high viral load during acute infection. J Virol 85, 4828-4840.

Gray, E.S., Moore, P.L., Choge, I.A., Decker, J.M., Bibollet-Ruche, F., Li, H., Leseka, N., Treurnicht, F., Mlisana, K., Shaw, G.M., Karim, S.S., Williamson, C., Morris, L., 2007. Neutralizing antibody responses in acute human immunodeficiency virus type 1 subtype C infection. J Virol 81, 6187-6196.

Gray, R.H., Kiwanuka, N., Quinn, T.C., Sewankambo, N.K., Serwadda, D., Mangen, F.W., Lutalo, T., Nalugoda, F., Kelly, R., Meehan, M., Chen, M.Z., Li, C., Wawer, M.J., 2000. Male circumcision and HIV acquisition and transmission: cohort studies in Rakai, Uganda. Rakai Project Team. AIDS 14, 2371-2381.

Groothuis, J.R., Simoes, E.A., Levin, M.J., Hall, C.B., Long, C.E., Rodriguez, W.J., Arrobio, J., Meissner, H.C., Fulton, D.R., Welliver, R.C., et al., 1993. Prophylactic administration of respiratory syncytial virus immune globulin to high-risk infants and young children. The Respiratory Syncytial Virus Immune Globulin Study Group. N Engl J Med 329, 1524-1530.

Guex, N., Peitsch, M.C., 1997. SWISS-MODEL and the Swiss-PdbViewer: an environment for comparative protein modeling. Electrophoresis 18, 2714-2723.

Gurunathan, S., 2011. Moving Forward from RV144: An Industrial Perspective, AIDS Vaccine 2011, Bangkok, Thailand.

Hallenberger, S., Moulard, M., Sordel, M., Klenk, H.D., Garten, W., 1997. The role of eukaryotic subtilisin-like endoproteases for the activation of human immunodeficiency virus glycoproteins in natural host cells. J Virol 71, 1036-1045.

Hammon, W.M., Coriell, L.L., Wehrle, P.F., Stokes, J., Jr., 1953. Evaluation of Red Cross gamma globulin as a prophylactic agent for poliomyelitis. IV. Final report of results based on clinical diagnoses. J Am Med Assoc 151, 1272-1285.

Hanahan, D., 1983. Studies on transformation of Escherichia coli with plasmids. J Mol Biol 166, 557-580.

Haynes, B.F., 2011. Case control study of the RV144 trial for immune correlates: the analysis and way forward, AIDS Vaccine 2011, Bangkok, Thailand.

Helseth, E., Olshevsky, U., Furman, C., Sodroski, J., 1991. Human immunodeficiency virus type 1 gp120 envelope glycoprotein regions important for association with the gp41 transmembrane glycoprotein. J Virol 65, 2119-2123.

Hessell, A.J., Hangartner, L., Hunter, M., Havenith, C.E., Beurskens, F.J., Bakker, J.M., Lanigan, C.M., Landucci, G., Forthal, D.N., Parren, P.W., Marx, P.A., Burton, D.R., 2007. Fc receptor but not complement binding is important in antibody protection against HIV. Nature 449, 101-104.

Hessell, A.J., Poignard, P., Hunter, M., Hangartner, L., Tehrani, D.M., Bleeker, W.K., Parren, P.W., Marx, P.A., Burton, D.R., 2009. Effective, low-titer antibody protection against low-dose repeated mucosal SHIV challenge in macaques. Nat Med 15, 951-954.

Hioe, C.E., Wrin, T., Seaman, M.S., Yu, X., Wood, B., Self, S., Williams, C., Gorny, M.K., Zolla-Pazner, S., 2010. Anti-V3 monoclonal antibodies display broad neutralizing activities against multiple HIV-1 subtypes. PLoS One 5, e10254.

Hocqueloux, L., Prazuck, T., Avettand-Fenoel, V., Lafeuillade, A., Cardon, B., Viard, J.P., Rouzioux, C., 2010. Long-term immunovirologic control following antiretroviral therapy interruption in patients treated at the time of primary HIV-1 infection. AIDS 24, 1598-1601.

Hofmann-Lehmann, R., Vlasak, J., Rasmussen, R.A., Smith, B.A., Baba, T.W., Liska, V., Ferrantelli, F., Montefiori, D.C., McClure, H.M., Anderson, D.C., Bernacky, B.J., Rizvi, T.A., Schmidt, R., Hill, L.R., Keeling, M.E., Katinger, H., Stiegler, G., Cavacini, L.A., Posner, M.R., Chou, T.C., Andersen, J., Ruprecht, R.M., 2001. Postnatal passive immunization of neonatal macaques with a triple combination of human monoclonal antibodies against oral simian-human immunodeficiency virus challenge. J Virol 75, 7470-7480.

Huang, C.C., Lam, S.N., Acharya, P., Tang, M., Xiang, S.H., Hussan, S.S., Stanfield, R.L., Robinson, J., Sodroski, J., Wilson, I.A., Wyatt, R., Bewley, C.A., Kwong, P.D., 2007. Structures of the CCR5 N terminus and of a tyrosine-sulfated antibody with HIV-1 gp120 and CD4. Science 317, 1930-1934.

Huang, C.C., Tang, M., Zhang, M.Y., Majeed, S., Montabana, E., Stanfield, R.L., Dimitrov, D.S., Korber, B., Sodroski, J., Wilson, I.A., Wyatt, R., Kwong, P.D., 2005. Structure of a V3-containing HIV-1 gp120 core. Science 310, 1025-1028.

Huber, M., Le, K.M., Doores, K.J., Fulton, Z., Stanfield, R.L., Wilson, I.A., Burton, D.R., 2010. Very few substitutions in a germ line antibody are required to initiate significant domain exchange. J Virol 84, 10700-10707.

Hutter, G., Nowak, D., Mossner, M., Ganepola, S., Mussig, A., Allers, K., Schneider, T., Hofmann, J., Kucherer, C., Blau, O., Blau, I.W., Hofmann, W.K., Thiel, E., 2009. Long-term control of HIV by CCR5 Delta32/Delta32 stem-cell transplantation. N Engl J Med 360, 692-698.

Janeway, C.A., 1945. Use of Concentrated Human Serum gamma-Globulin in the Prevention and Attenuation of Measles. Bull N Y Acad Med 21, 202-222.

Johnson, R.P., Trocha, A., Buchanan, T.M., Walker, B.D., 1993. Recognition of a highly conserved region of human immunodeficiency virus type 1 gp120 by an HLA-Cw4-restricted cytotoxic T-lymphocyte clone. J Virol 67, 438-445.

Keele, B.F., Giorgi, E.E., Salazar-Gonzalez, J.F., Decker, J.M., Pham, K.T., Salazar, M.G., Sun, C., Grayson, T., Wang, S., Li, H., Wei, X., Jiang, C., Kirchherr, J.L., Gao, F., Anderson, J.A., Ping, L.H., Swanstrom, R., Tomaras, G.D., Blattner, W.A., Goepfert, P.A., Kilby, J.M., Saag, M.S., Delwart, E.L., Busch, M.P., Cohen, M.S., Montefiori, D.C., Haynes, B.F., Gaschen, B., Athreya, G.S., Lee, H.Y., Wood, N., Seoighe, C., Perelson, A.S., Bhattacharya, T., Korber, B.T., Hahn, B.H., Shaw, G.M., 2008. Identification and characterization of transmitted and early founder virus envelopes in primary HIV-1 infection. Proc Natl Acad Sci U S A 105, 7552-7557.

Klatzmann, D., Montagnier, L., 1986. Approaches to AIDS therapy. Nature 319, 10-11.

Korber, B.T., MacInnes, K., Smith, R.F., Myers, G., 1994. Mutational trends in V3 loop protein sequences observed in different genetic lineages of human immunodeficiency virus type 1. J Virol 68, 6730-6744.

Kornfeld, R., Kornfeld, S., 1985. Assembly of asparagine-linked oligosaccharides. Annu Rev Biochem 54, 631-664.

Korns, R.F., 1952. Prophylaxis of German measles with immune serum globulin. J Infect Dis 90, 183-189.

Krachmarov, C., Pinter, A., Honnen, W.J., Gorny, M.K., Nyambi, P.N., Zolla-Pazner, S., Kayman, S.C., 2005. Antibodies that are cross-reactive for human immunodeficiency virus type 1 clade a and

clade B V3 domains are common in patient sera from Cameroon, but their neutralization activity is usually restricted by epitope masking. J Virol 79, 780-790.

Krachmarov, C.P., Honnen, W.J., Kayman, S.C., Gorny, M.K., Zolla-Pazner, S., Pinter, A., 2006. Factors determining the breadth and potency of neutralization by V3-specific human monoclonal antibodies derived from subjects infected with clade A or clade B strains of human immunodeficiency virus type 1. J Virol 80, 7127-7135.

Kwong, P.D., Doyle, M.L., Casper, D.J., Cicala, C., Leavitt, S.A., Majeed, S., Steenbeke, T.D., Venturi, M., Chaiken, I., Fung, M., Katinger, H., Parren, P.W., Robinson, J., Van Ryk, D., Wang, L., Burton, D.R., Freire, E., Wyatt, R., Sodroski, J., Hendrickson, W.A., Arthos, J., 2002. HIV-1 evades antibody-mediated neutralization through conformational masking of receptor-binding sites. Nature 420, 678-682.

Kwong, P.D., Wyatt, R., Robinson, J., Sweet, R.W., Sodroski, J., Hendrickson, W.A., 1998. Structure of an HIV gp120 envelope glycoprotein in complex with the CD4 receptor and a neutralizing human antibody. Nature 393, 648-659.

LaBranche, C.C., Galasso, G., Moore, J.P., Bolognesi, D.P., Hirsch, M.S., Hammer, S.M., 2001. HIV fusion and its inhibition. Antiviral Res 50, 95-115.

Lasky, L.A., Groopman, J.E., Fennie, C.W., Benz, P.M., Capon, D.J., Dowbenko, D.J., Nakamura, G.R., Nunes, W.M., Renz, M.E., Berman, P.W., 1986. Neutralization of the AIDS retrovirus by antibodies to a recombinant envelope glycoprotein. Science 233, 209-212.

Laver, W.G., Air, G.M., Webster, R.G., Smith-Gill, S.J., 1990. Epitopes on protein antigens: misconceptions and realities. Cell 61, 553-556.

Lavreys, L., Rakwar, J.P., Thompson, M.L., Jackson, D.J., Mandaliya, K., Chohan, B.H., Bwayo, J.J., Ndinya-Achola, J.O., Kreiss, J.K., 1999. Effect of circumcision on incidence of human immunodeficiency virus type 1 and other sexually transmitted diseases: a prospective cohort study of trucking company employees in Kenya. J Infect Dis 180, 330-336.

Lemey, P., Pybus, O.G., Wang, B., Saksena, N.K., Salemi, M., Vandamme, A.M., 2003. Tracing the origin and history of the HIV-2 epidemic. Proc Natl Acad Sci U S A 100, 6588-6592.

Leonard, C.K., Spellman, M.W., Riddle, L., Harris, R.J., Thomas, J.N., Gregory, T.J., 1990. Assignment of intrachain disulfide bonds and characterization of potential glycosylation sites of the type 1 recombinant human immunodeficiency virus envelope glycoprotein (gp120) expressed in Chinese hamster ovary cells. J Biol Chem 265, 10373-10382.

Levy, J.A., 1993. Pathogenesis of human immunodeficiency virus infection. Microbiol Rev 57, 183-289.

Li, B., Decker, J.M., Johnson, R.W., Bibollet-Ruche, F., Wei, X., Mulenga, J., Allen, S., Hunter, E., Hahn, B.H., Shaw, G.M., Blackwell, J.L., Derdeyn, C.A., 2006a. Evidence for potent autologous neutralizing antibody titers and compact envelopes in early infection with subtype C human immunodeficiency virus type 1. J Virol 80, 5211-5218.

Li, J., Lord, C.I., Haseltine, W., Letvin, N.L., Sodroski, J., 1992. Infection of cynomolgus monkeys with a chimeric HIV-1/SIVmac virus that expresses the HIV-1 envelope glycoproteins. J Acquir Immune Defic Syndr 5, 639-646.

Li, M., Salazar-Gonzalez, J.F., Derdeyn, C.A., Morris, L., Williamson, C., Robinson, J.E., Decker, J.M., Li, Y., Salazar, M.G., Polonis, V.R., Mlisana, K., Karim, S.A., Hong, K., Greene, K.M., Bilska, M., Zhou, J., Allen, S., Chomba, E., Mulenga, J., Vwalika, C., Gao, F., Zhang, M., Korber, B.T., Hunter, E., Hahn, B.H., Montefiori, D.C., 2006b. Genetic and neutralization properties of subtype C human immunodeficiency virus type 1 molecular env clones from acute and early heterosexually acquired infections in Southern Africa. J Virol 80, 11776-11790.

Li, T., Steede, N.K., Hossain, M., Nguyen, H., Freytag, L.C., Robinson, J., Landry, S.J., 2011a. Skewing the helper T cell responses to HIV gp120 with mutations and adjuvants, Keystone Symposium on Protection from HIV: Targeted Intervention Stategies, Whistler, British Columbia, Canada.

Li, Y., O'Dell, S., Walker, L.M., Wu, X., Guenaga, J., Feng, Y., Schmidt, S.D., McKee, K., Louder, M.K., Ledgerwood, J.E., Graham, B.S., Haynes, B.F., Burton, D.R., Wyatt, R.T., Mascola, J.R., 2011b.

Mechanism of neutralization by the broadly neutralizing HIV-1 monoclonal antibody VRC01. J Virol 85, 8954-8967.

Liao, H.X., Chen, X., Munshaw, S., Zhang, R., Marshall, D.J., Vandergrift, N., Whitesides, J.F., Lu, X., Yu, J.S., Hwang, K.K., Gao, F., Markowitz, M., Heath, S.L., Bar, K.J., Goepfert, P.A., Montefiori, D.C., Shaw, G.C., Alam, S.M., Margolis, D.M., Denny, T.N., Boyd, S.D., Marshal, E., Egholm, M., Simen, B.B., Hanczaruk, B., Fire, A.Z., Voss, G., Kelsoe, G., Tomaras, G.D., Moody, M.A., Kepler, T.B., Haynes, B.F., 2011. Initial antibodies binding to HIV-1 gp41 in acutely infected subjects are polyreactive and highly mutated. J Exp Med 208, 2237-2249.

Lo Conte, L., Chothia, C., Janin, J., 1999. The atomic structure of protein-protein recognition sites. J Mol Biol 285, 2177-2198.

Lu, M., Blacklow, S.C., Kim, P.S., 1995. A trimeric structural domain of the HIV-1 transmembrane glycoprotein. Nat Struct Biol 2, 1075-1082.

Luciw, P.A., Pratt-Lowe, E., Shaw, K.E., Levy, J.A., Cheng-Mayer, C., 1995. Persistent infection of rhesus macaques with T-cell-line-tropic and macrophage-tropic clones of simian/human immunodeficiency viruses (SHIV). Proc Natl Acad Sci U S A 92, 7490-7494.

Lynch, R.M., Rong, R., Boliar, S., Sethi, A., Li, B., Mulenga, J., Allen, S., Robinson, J.E., Gnanakaran, S., Derdeyn, C.A., 2011. The B cell response is redundant and highly focused on V1V2 during early subtype C infection in a Zambian seroconverter. J Virol 85, 905-915.

Mascola, J.R., Lewis, M.G., Stiegler, G., Harris, D., VanCott, T.C., Hayes, D., Louder, M.K., Brown, C.R., Sapan, C.V., Frankel, S.S., Lu, Y., Robb, M.L., Katinger, H., Birx, D.L., 1999. Protection of Macaques against pathogenic simian/human immunodeficiency virus 89.6PD by passive transfer of neutralizing antibodies. J Virol 73, 4009-4018.

Mascola, J.R., Montefiori, D.C., 2010. The role of antibodies in HIV vaccines. Annu Rev Immunol 28, 413-444.

Mascola, J.R., Stiegler, G., VanCott, T.C., Katinger, H., Carpenter, C.B., Hanson, C.E., Beary, H., Hayes, D., Frankel, S.S., Birx, D.L., Lewis, M.G., 2000. Protection of macaques against vaginal transmission of a pathogenic HIV-1/SIV chimeric virus by passive infusion of neutralizing antibodies. Nat Med 6, 207-210.

Matthews, T., Salgo, M., Greenberg, M., Chung, J., DeMasi, R., Bolognesi, D., 2004. Enfuvirtide: the first therapy to inhibit the entry of HIV-1 into host CD4 lymphocytes. Nat Rev Drug Discov 3, 215-225.

May, M.T., Sterne, J.A., Costagliola, D., Sabin, C.A., Phillips, A.N., Justice, A.C., Dabis, F., Gill, J., Lundgren, J., Hogg, R.S., de Wolf, F., Fatkenheuer, G., Staszewski, S., d'Arminio Monforte, A., Egger, M., 2006. HIV treatment response and prognosis in Europe and North America in the first decade of highly active antiretroviral therapy: a collaborative analysis. Lancet 368, 451-458.

McElrath, M.J., Haynes, B.F., 2010. Induction of immunity to human immunodeficiency virus type-1 by vaccination. Immunity 33, 542-554.

McLellan, J.S., Pancera, M., Carrico, C., Gorman, J., Julien, J.P., Khayat, R., Louder, R., Pejchal, R., Sastry, M., Dai, K., O'Dell, S., Patel, N., Shahzad-ul-Hussan, S., Yang, Y., Zhang, B., Zhou, T., Zhu, J., Boyington, J.C., Chuang, G.Y., Diwanji, D., Georgiev, I., Kwon, Y.D., Lee, D., Louder, M.K., Moquin, S., Schmidt, S.D., Yang, Z.Y., Bonsignori, M., Crump, J.A., Kapiga, S.H., Sam, N.E., Haynes, B.F., Burton, D.R., Koff, W.C., Walker, L.M., Phogat, S., Wyatt, R., Orwenyo, J., Wang, L.X., Arthos, J., Bewley, C.A., Mascola, J.R., Nabel, G.J., Schief, W.R., Ward, A.B., Wilson, I.A., Kwong, P.D., 2011. Structure of HIV-1 gp120 V1/V2 domain with broadly neutralizing antibody PG9. Nature 480, 336-343.

Melikyan, G.B., Markosyan, R.M., Hemmati, H., Delmedico, M.K., Lambert, D.M., Cohen, F.S., 2000. Evidence that the transition of HIV-1 gp41 into a six-helix bundle, not the bundle configuration, induces membrane fusion. J Cell Biol 151, 413-423.

Mo, H., Stamatatos, L., Ip, J.E., Barbas, C.F., Parren, P.W., Burton, D.R., Moore, J.P., Ho, D.D., 1997. Human immunodeficiency virus type 1 mutants that escape neutralization by human monoclonal antibody IgG1b12. off. J Virol 71, 6869-6874.

Moebius, U., Clayton, L.K., Abraham, S., Harrison, S.C., Reinherz, E.L., 1992. The human immunodeficiency virus gp120 binding site on CD4: delineation by quantitative equilibrium and kinetic binding studies of mutants in conjunction with a high-resolution CD4 atomic structure. J Exp Med 176, 507-517.

Montefiori, D., 2004. Evaluating neutralizing antibodies againts HIV, SIV and SHIV in luciferase reporter gene assays., in: J. E. Coligan, A.M.K., D. H. Margulies, E. M. Shevach, W. Strober, and R. Coico (Ed.), Current Protocols in Immunology. John Wiley & Sons., New York, NY., pp. 12.11.11-12.11.15.

Montefiori, D.C., 2009. Measuring HIV neutralization in a luciferase reporter gene assay. Methods Mol Biol 485, 395-405.

Montefiori, D.C., Cornell, R.J., Zhou, J.Y., Zhou, J.T., Hirsch, V.M., Johnson, P.R., 1994. Complement control proteins, CD46, CD55, and CD59, as common surface constituents of human and simian immunodeficiency viruses and possible targets for vaccine protection. Virology 205, 82-92.

Moore, J.P., Willey, R.L., Lewis, G.K., Robinson, J., Sodroski, J., 1994. Immunological evidence for interactions between the first, second, and fifth conserved domains of the gp120 surface glycoprotein of human immunodeficiency virus type 1. J Virol 68, 6836-6847.

Moore, P.L., Gray, E., Choge, I., Ranchobe, N., Mlisana, K., Karim, S.A., Williamson, C., Morris, L., 2007. The C3-V4 region is a major target of autologous neutralizing antibodies in HIV-1 subtype C infection. J Virol in press.

Moore, P.L., Crooks, E.T., Porter, L., Zhu, P., Cayanan, C.S., Grise, H., Corcoran, P., Zwick, M.B., Franti, M., Morris, L., Roux, K.H., Burton, D.R., Binley, J.M., 2006. Nature of nonfunctional envelope proteins on the surface of human immunodeficiency virus type 1. J Virol 80, 2515-2528.

Moore, P.L., Gray, E.S., Choge, I.A., Ranchobe, N., Mlisana, K., Abdool Karim, S.S., Williamson, C., Morris, L., 2008. The c3-v4 region is a major target of autologous neutralizing antibodies in human immunodeficiency virus type 1 subtype C infection. J Virol 82, 1860-1869.

Moore, P.L., Gray, E.S., Hermanus, T., Sheward, D., Tumba, N., Wibmer, C.K., Bhiman, J.N., Sibeko, S., Abdool Karim, S., Williamson, C., Morris, L., 2011. Evolution of HIV-1 Transmitted/Founder Viruses Results in the Formation of Epitopes for Later Broadly Cross-Neutralizing Antibodies, AIDS Vaccine 2011, Bangkok, Thailand.

Moore, P.L., Ranchobe, N., Lambson, B.E., Gray, E.S., Cave, E., Abrahams, M.R., Bandawe, G., Mlisana, K., Abdool Karim, S.S., Williamson, C., Morris, L., 2009. Limited neutralizing antibody specificities drive neutralization escape in early HIV-1 subtype C infection. PLoS pathogens 5, e1000598.

Munoz-Barroso, I., Salzwedel, K., Hunter, E., Blumenthal, R., 1999. Role of the membrane-proximal domain in the initial stages of human immunodeficiency virus type 1 envelope glycoprotein-mediated membrane fusion. J Virol 73, 6089-6092.

Muster, T., Steindl, F., Purtscher, M., Trkola, A., Klima, A., Himmler, G., Ruker, F., Katinger, H., 1993. A conserved neutralizing epitope on gp41 of human immunodeficiency virus type 1. J Virol 67, 6642-6647.

Nakowitsch, S., Quendler, H., Fekete, H., Kunert, R., Katinger, H., Stiegler, G., 2005. HIV-1 mutants escaping neutralization by the human antibodies 2F5, 2G12, and 4E10: in vitro experiments versus clinical studies. Aids 19, 1957-1966.

Nermut, M.V., Grief, C., Hashmi, S., Hockley, D.J., 1993. Further evidence of icosahedral symmetry in human and simian immunodeficiency virus. AIDS Res Hum Retroviruses 9, 929-938.

Nonyane, M., Sheward, D., Ranchobe, N., Gray, E.S., Abdool Karim, S., Williamson, C., Morris, L., Moore, P.L., Study, T.C., 2011. Charactersing Autologous Neutralizing Antibody Specificities and Escape in a HIV-1 Subtype C Infected Individual with Broadly Cross-Neutralizing Activity, 5th SA AIDS Conference, Durban, South Africa.

Olshevsky, U., Helseth, E., Furman, C., Li, J., Haseltine, W., Sodroski, J., 1990. Identification of individual human immunodeficiency virus type 1 gp120 amino acids important for CD4 receptor binding. J Virol 64, 5701-5707.

Pancera, M., Majeed, S., Ban, Y.E., Chen, L., Huang, C.C., Kong, L., Kwon, Y.D., Stuckey, J., Zhou, T., Robinson, J.E., Schief, W.R., Sodroski, J., Wyatt, R., Kwong, P.D., 2010. Structure of HIV-1 gp120 with gp41-interactive region reveals layered envelope architecture and basis of conformational mobility. Proc Natl Acad Sci U S A 107, 1166-1171.

Pantophlet, R., Burton, D.R., 2006. GP120: target for neutralizing HIV-1 antibodies. Annu Rev Immunol 24, 739-769.

Papandreou, M.J., Idziorek, T., Miquelis, R., Fenouillet, E., 1996. Glycosylation and stability of mature HIV envelope glycoprotein conformation under various conditions. FEBS Lett 379, 171-176.

Parren, P.W., Burton, D.R., 2001. The antiviral activity of antibodies in vitro and in vivo. Adv Immunol 77, 195-262.

Parren, P.W., Burton, D.R., Sattentau, Q.J., 1997. HIV-1 antibody--debris or virion? Nat Med 3, 366-367.

Parren, P.W., Marx, P.A., Hessell, A.J., Luckay, A., Harouse, J., Cheng-Mayer, C., Moore, J.P., Burton, D.R., 2001. Antibody protects macaques against vaginal challenge with a pathogenic R5 simian/human immunodeficiency virus at serum levels giving complete neutralization in vitro. J Virol 75, 8340-8347.

Pejchal, R., Doores, K.J., Walker, L.M., Khayat, R., Huang, P.S., Wang, S.K., Stanfield, R.L., Julien, J.P., Ramos, A., Crispin, M., Depetris, R., Katpally, U., Marozsan, A., Cupo, A., Maloveste, S., Liu, Y., McBride, R., Ito, Y., Sanders, R.W., Ogohara, C., Paulson, J.C., Feizi, T., Scanlan, C.N., Wong, C.H., Moore, J.P., Olson, W.C., Ward, A.B., Poignard, P., Schief, W.R., Burton, D.R., Wilson, I.A., 2011. A potent and broad neutralizing antibody recognizes and penetrates the HIV glycan shield. Science 334, 1097-1103.

Piantadosi, A., Panteleeff, D., Blish, C.A., Baeten, J.M., Jaoko, W., McClelland, R.S., Overbaugh, J., 2009. Breadth of neutralizing antibody response to human immunodeficiency virus type 1 is affected by factors early in infection but does not influence disease progression. J Virol 83, 10269-10274.

Piller, S.C., Dubay, J.W., Derdeyn, C.A., Hunter, E., 2000. Mutational analysis of conserved domains within the cytoplasmic tail of gp41 from human immunodeficiency virus type 1: effects on glycoprotein incorporation and infectivity. J Virol 74, 11717-11723.

Pinter, A., Honnen, W.J., He, Y., Gorny, M.K., Zolla-Pazner, S., Kayman, S.C., 2004. The V1/V2 domain of gp120 is a global regulator of the sensitivity of primary human immunodeficiency virus type 1 isolates to neutralization by antibodies commonly induced upon infection. J Virol 78, 5205-5215.

Plantier, J.C., Leoz, M., Dickerson, J.E., De Oliveira, F., Cordonnier, F., Lemee, V., Damond, F., Robertson, D.L., Simon, F., 2009. A new human immunodeficiency virus derived from gorillas. Nat Med 15, 871-872.

Platt, E.J., Wehrly, K., Kuhmann, S.E., Chesebro, B., Kabat, D., 1998. Effects of CCR5 and CD4 cell surface concentrations on infections by macrophagetropic isolates of human immunodeficiency virus type 1. J Virol 72, 2855-2864.

Plotkin, S.A., Plotkin, S.L., 2011. The development of vaccines: how the past led to the future. Nat Rev Microbiol 9, 889-893.

Poignard, P., Saphire, E.O., Parren, P.W., Burton, D.R., 2001. gp120: Biologic aspects of structural features. Annu Rev Immunol 19, 253-274.

Pollard, S.R., Rosa, M.D., Rosa, J.J., Wiley, D.C., 1992. Truncated variants of gp120 bind CD4 with high affinity and suggest a minimum CD4 binding region. EMBO J 11, 585-591.

Pugach, P., Kuhmann, S.E., Taylor, J., Marozsan, A.J., Snyder, A., Ketas, T., Wolinsky, S.M., Korber, B.T., Moore, J.P., 2004. The prolonged culture of human immunodeficiency virus type 1 in primary lymphocytes increases its sensitivity to neutralization by soluble CD4. Virology 321, 8-22.

Rerks-Ngarm, S., Pitisuttithum, P., Nitayaphan, S., Kaewkungwal, J., Chiu, J., Paris, R., Premsri, N., Namwat, C., de Souza, M., Adams, E., Benenson, M., Gurunathan, S., Tartaglia, J., McNeil, J.G., Francis, D.P., Stablein, D., Birx, D.L., Chunsuttiwat, S., Khamboonruang, C., Thongcharoen, P., Robb, M.L., Michael, N.L., Kunasol, P., Kim, J.H., 2009. Vaccination with ALVAC and AIDSVAX to prevent HIV-1 infection in Thailand. N Engl J Med 361, 2209-2220.

Reynolds, S.J., Shepherd, M.E., Risbud, A.R., Gangakhedkar, R.R., Brookmeyer, R.S., Divekar, A.D., Mehendale, S.M., Bollinger, R.C., 2004. Male circumcision and risk of HIV-1 and other sexually transmitted infections in India. Lancet 363, 1039-1040.

Richman, D.D., Wrin, T., Little, S.J., Petropoulos, C.J., 2003. Rapid evolution of the neutralizing antibody response to HIV type 1 infection. Proc Natl Acad Sci U S A 100, 4144-4149.

Rizzuto, C.D., Wyatt, R., Hernandez-Ramos, N., Sun, Y., Kwong, P.D., Hendrickson, W.A., Sodroski, J., 1998. A conserved HIV gp120 glycoprotein structure involved in chemokine receptor binding. Science 280, 1949-1953.

Robertson, D.L., Anderson, J.P., Bradac, J.A., Carr, J.K., Foley, B., Funkhouser, R.K., Gao, F., Hahn, B.H., Kalish, M.L., Kuiken, C., Learn, G.H., Leitner, T., McCutchan, F., Osmanov, S., Peeters, M., Pieniazek, D., Salminen, M., Sharp, P.M., Wolinsky, S., Korber, B., 2000. HIV-1 nomenclature proposal. Science 288, 55-56.

Rong, R., Bibollet-Ruche, F., Mulenga, J., Allen, S., Blackwell, J.L., Derdeyn, C.A., 2007a. Role of V1V2 and Other Human Immunodeficiency Virus Type 1 Envelope Domains in Resistance to Autologous Neutralization during Clade C Infection. J Virol 81, 1350-1359.

Rong, R., Gnanakaran, S., Decker, J.M., Bibollet-Ruche, F., Taylor, J., Sfakianos, J.N., Mokili, J.L., Muldoon, M., Mulenga, J., Allen, S., Hahn, B.H., Shaw, G.M., Blackwell, J.L., Korber, B.T., Hunter, E., Derdeyn, C.A., 2007b. Unique mutational patterns in the envelope {alpha}2 amphipathic helix and acquisition of length in gp120 hyper-variable domains are associated with resistance to autologous neutralization of subtype C human immunodeficiency virus type 1. J Virol 81, 5658-5668.

Rong, R., Gnanakaran, S., Decker, J.M., Bibollet-Ruche, F., Taylor, J., Sfakianos, J.N., Mokili, J.L., Muldoon, M., Mulenga, J., Allen, S., Hahn, B.H., Shaw, G.M., Blackwell, J.L., Korber, B.T., Hunter, E., Derdeyn, C.A., 2007c. Unique Mutational Patterns in the Envelope {alpha}2 Amphipathic Helix and Acquisition of Length in gp120 Hypervariable Domains Are Associated with Resistance to Autologous Neutralization of Subtype C Human Immunodeficiency Virus Type 1. J Virol 81, 5658-5668.

Rong, R., Li, B., Lynch, R.M., Haaland, R.E., Murphy, M.K., Mulenga, J., Allen, S.A., Pinter, A., Shaw, G.M., Hunter, E., Robinson, J.E., Gnanakaran, S., Derdeyn, C.A., 2009. Escape from autologous neutralizing antibodies in acute/early subtype C HIV-1 infection requires multiple pathways. PLoS pathogens 5, e1000594.

Ross, A.H., 1962. Modification of chicken pox in family contacts by administration of gamma globulin. N Engl J Med 267, 369-376.

Ross, A.L., Brave, A., Scarlatti, G., Manrique, A., Buonaguro, L., 2010. Progress towards development of an HIV vaccine: report of the AIDS Vaccine 2009 Conference. Lancet Infect Dis 10, 305-316.

Ross, H.A., Rodrigo, A.G., 2002. Immune-mediated positive selection drives human immunodeficiency virus type 1 molecular variation and predicts disease duration. J Virol 76, 11715-11720.

Rousso, I., Mixon, M.B., Chen, B.K., Kim, P.S., 2000. Palmitoylation of the HIV-1 envelope glycoprotein is critical for viral infectivity. Proc Natl Acad Sci U S A 97, 13523-13525.

Rubinstein, N.D., Mayrose, I., Halperin, D., Yekutieli, D., Gershoni, J.M., Pupko, T., 2008. Computational characterization of B-cell epitopes. Mol Immunol 45, 3477-3489.

Rusert, P., Krarup, A., Magnus, C., Brandenberg, O.F., Weber, J., Ehlert, A.K., Regoes, R.R., Gunthard, H.F., Trkola, A., 2011. Interaction of the gp120 V1V2 loop with a neighboring gp120 unit shields the HIV envelope trimer against cross-neutralizing antibodies. J Exp Med 208, 1419-1433.

Sagar, M., Wu, X., Lee, S., Overbaugh, J., 2006. Human immunodeficiency virus type 1 V1-V2 envelope loop sequences expand and add glycosylation sites over the course of infection, and these modifications affect antibody neutralization sensitivity. J Virol 80, 9586-9598.

Sakuragi, S., Shibata, R., Mukai, R., Komatsu, T., Fukasawa, M., Sakai, H., Sakuragi, J., Kawamura, M., Ibuki, K., Hayami, M., et al., 1992. Infection of macaque monkeys with a chimeric human and simian immunodeficiency virus. J Gen Virol 73 (Pt 11), 2983-2987.

Salazar-Gonzalez, J.F., Bailes, E., Pham, K.T., Salazar, M.G., Guffey, M.B., Keele, B.F., Derdeyn, C.A., Farmer, P., Hunter, E., Allen, S., Manigart, O., Mulenga, J., Anderson, J.A., Swanstrom, R., Haynes, B.F., Athreya, G.S., Korber, B.T., Sharp, P.M., Shaw, G.M., Hahn, B.H., 2008. Deciphering human immunodeficiency virus type 1 transmission and early envelope diversification by single-genome amplification and sequencing. J Virol 82, 3952-3970.

Salzwedel, K., West, J.T., Hunter, E., 1999. A conserved tryptophan-rich motif in the membrane-proximal region of the human immunodeficiency virus type 1 gp41 ectodomain is important for Env-mediated fusion and virus infectivity. J Virol 73, 2469-2480.

Sanders, R.W., Venturi, M., Schiffner, L., Kalyanaraman, R., Katinger, H., Lloyd, K.O., Kwong, P.D., Moore, J.P., 2002. The mannose-dependent epitope for neutralizing antibody 2G12 on human immunodeficiency virus type 1 glycoprotein gp120. J Virol 76, 7293-7305.

Sather, D.N., Armann, J., Ching, L.K., Mavrantoni, A., Sellhorn, G., Caldwell, Z., Yu, X., Wood, B., Self, S., Kalams, S., Stamatatos, L., 2009. Factors associated with the development of cross-reactive neutralizing antibodies during human immunodeficiency virus type 1 infection. J Virol 83, 757-769.

Sattentau, Q.J., Moore, J.P., 1991. Conformational changes induced in the human immunodeficiency virus envelope glycoprotein by soluble CD4 binding. J Exp Med 174, 407-415.

Sattentau, Q.J., Moore, J.P., 1995. Human immunodeficiency virus type 1 neutralization is determined by epitope exposure on the gp120 oligomer. J Exp Med 182, 185-196.

Saunders, C.J., McCaffrey, R.A., Zharkikh, I., Kraft, Z., Malenbaum, S.E., Burke, B., Cheng-Mayer, C., Stamatatos, L., 2005. The V1, V2, and V3 regions of the human immunodeficiency virus type 1 envelope differentially affect the viral phenotype in an isolate-dependent manner. J Virol 79, 9069-9080.

Scanlan, C.N., Pantophlet, R., Wormald, M.R., Ollmann Saphire, E., Stanfield, R., Wilson, I.A., Katinger, H., Dwek, R.A., Rudd, P.M., Burton, D.R., 2002. The broadly neutralizing anti-human immunodeficiency virus type 1 antibody 2G12 recognizes a cluster of alpha1-->2 mannose residues on the outer face of gp120. J Virol 76, 7306-7321.

Schonning, K., Jansson, B., Olofsson, S., Nielsen, J.O., Hansen, J.S., 1996. Resistance to V3-directed neutralization caused by an N-linked oligosaccharide depends on the quaternary structure of the HIV-1 envelope oligomer. Virology 218, 134-140.

Schwede, T., Kopp, J., Guex, N., Peitsch, M.C., 2003. SWISS-MODEL: An automated protein homology-modeling server. Nucleic Acids Res 31, 3381-3385.

Shibata, R., Kawamura, M., Sakai, H., Hayami, M., Ishimoto, A., Adachi, A., 1991. Generation of a chimeric human and simian immunodeficiency virus infectious to monkey peripheral blood mononuclear cells. J Virol 65, 3514-3520.

Simon, F., Mauclere, P., Roques, P., Loussert-Ajaka, I., Muller-Trutwin, M.C., Saragosti, S., Georges-Courbot, M.C., Barre-Sinoussi, F., Brun-Vezinet, F., 1998. Identification of a new human immunodeficiency virus type 1 distinct from group M and group O. Nat Med 4, 1032-1037.

Snydman, D.R., Werner, B.G., Heinze-Lacey, B., Berardi, V.P., Tilney, N.L., Kirkman, R.L., Milford, E.L., Cho, S.I., Bush, H.L., Jr., Levey, A.S., et al., 1987. Use of cytomegalovirus immune globulin to prevent cytomegalovirus disease in renal-transplant recipients. N Engl J Med 317, 1049-1054.

Sougrat, R., Bartesaghi, A., Lifson, J.D., Bennett, A.E., Bess, J.W., Zabransky, D.J., Subramaniam, S., 2007. Electron tomography of the contact between T cells and SIV/HIV-1: implications for viral entry. PLoS pathogens 3, e63.

Stamatatos, L., Cheng-Mayer, C., 1998. An envelope modification that renders a primary, neutralization-resistant clade B human immunodeficiency virus type 1 isolate highly susceptible to neutralization by sera from other clades. J Virol 72, 7840-7845.

Stamatatos, L., Wiskerchen, M., Cheng-Mayer, C., 1998. Effect of major deletions in the V1 and V2 loops of a macrophage-tropic HIV type 1 isolate on viral envelope structure, cell entry, and replication. AIDS Res Hum Retroviruses 14, 1129-1139.

Stiegler, G., Kunert, R., Purtscher, M., Wolbank, S., Voglauer, R., Steindl, F., Katinger, H., 2001. A potent cross-clade neutralizing human monoclonal antibody against a novel epitope on gp41 of human immunodeficiency virus type 1. AIDS Res Hum Retroviruses 17, 1757-1765.

Subramaniam, S., 2006. The SIV surface spike imaged by electron tomography: one leg or three? PLoS pathogens 2, e91.

Tan, K., Liu, J., Wang, J., Shen, S., Lu, M., 1997. Atomic structure of a thermostable subdomain of HIV-1 gp41. Proc Natl Acad Sci U S A 94, 12303-12308.

Tang, H., Robinson, J., Gnanakaran, S., Todd, C., Li, M., Rosenberg, E.S., Walker, B., Korber, B., Montefiori, D.C., 2007. Single amino acid changes on the silent face of gp120 associated with autologous neutralization-escape in HIV-1 infection, AIDS Vacine 07, AIDS Vacine 07. Seattle, USA.

Tang, H., Robinson, J.E., Gnanakaran, S., Li, M., Rosenberg, E.S., Perez, L.G., Haynes, B.F., Liao, H.X., Labranche, C.C., Korber, B.T., Montefiori, D.C., 2011. epitopes immediately below the base of the V3 loop of gp120 as targets for the initial autologous neutralizing antibody response in two HIV-1 subtype B-infected individuals. J Virol 85, 9286-9299.

Tomaras, G.D., Yates, N.L., Liu, P., Qin, L., Fouda, G.G., Chavez, L.L., Decamp, A.C., Parks, R.J., Ashley, V.C., Lucas, J.T., Cohen, M., Eron, J., Hicks, C.B., Liao, H.X., Self, S.G., Landucci, G., Forthal, D.N., Weinhold, K.J., Keele, B.F., Hahn, B.H., Greenberg, M.L., Morris, L., Karim, S.S., Blattner, W.A., Montefiori, D.C., Shaw, G.M., Perelson, A.S., Haynes, B.F., 2008. Initial B-cell responses to transmitted human immunodeficiency virus type 1: virion-binding immunoglobulin M (IgM) and IgG antibodies followed by plasma anti-gp41 antibodies with ineffective control of initial viremia. J Virol 82, 12449-12463.

Trkola, A., Kuster, H., Rusert, P., Joos, B., Fischer, M., Leemann, C., Manrique, A., Huber, M., Rehr, M., Oxenius, A., Weber, R., Stiegler, G., Vcelar, B., Katinger, H., Aceto, L., Gunthard, H.F., 2005. Delay of HIV-1 rebound after cessation of antiretroviral therapy through passive transfer of human neutralizing antibodies. Nat Med 11, 615-622.

Trkola, A., Purtscher, M., Muster, T., Ballaun, C., Buchacher, A., Sullivan, N., Srinivasan, K., Sodroski, J., Moore, J.P., Katinger, H., 1996. Human monoclonal antibody 2G12 defines a distinctive neutralization epitope on the gp120 glycoprotein of human immunodeficiency virus type 1. J Virol 70, 1100-1108.

Trono, D., Van Lint, C., Rouzioux, C., Verdin, E., Barre-Sinoussi, F., Chun, T.W., Chomont, N., 2010. HIV persistence and the prospect of long-term drug-free remissions for HIV-infected individuals. Science 329, 174-180.

van Loggerenberg, F., Mlisana, K., Williamson, C., Auld, S.C., Morris, L., Gray, C.M., Abdool Karim, Q., Grobler, A., Barnabas, N., Iriogbe, I., Abdool Karim, S.S., 2008. Establishing a cohort at high risk of HIV infection in South Africa: challenges and experiences of the CAPRISA 002 acute infection study. PLoS ONE 3, e1954.

Veazey, R.S., Shattock, R.J., Pope, M., Kirijan, J.C., Jones, J., Hu, Q., Ketas, T., Marx, P.A., Klasse, P.J., Burton, D.R., Moore, J.P., 2003. Prevention of virus transmission to macaque monkeys by a vaginally applied monoclonal antibody to HIV-1 gp120. Nat Med 9, 343-346.

Voynow, J.A., Kaiser, R.S., Scanlin, T.F., Glick, M.C., 1991. Purification and characterization of GDP-L-fucose-N-acetyl beta-D-glucosaminide alpha 1----6fucosyltransferase from cultured human skin fibroblasts. Requirement of a specific biantennary oligosaccharide as substrate. J Biol Chem 266, 21572-21577.

Walker, L.M., Huber, M., Doores, K.J., Falkowska, E., Pejchal, R., Julien, J.P., Wang, S.K., Ramos, A., Chan-Hui, P.Y., Moyle, M., Mitcham, J.L., Hammond, P.W., Olsen, O.A., Phung, P., Fling, S., Wong, C.H., Phogat, S., Wrin, T., Simek, M.D., Koff, W.C., Wilson, I.A., Burton, D.R., Poignard, P., 2011. Broad neutralization coverage of HIV by multiple highly potent antibodies. Nature 477, 466-470.

Walker, L.M., Phogat, S.K., Chan-Hui, P.Y., Wagner, D., Phung, P., Goss, J.L., Wrin, T., Simek, M.D., Fling, S., Mitcham, J.L., Lehrman, J.K., Priddy, F.H., Olsen, O.A., Frey, S.M., Hammond, P.W., Kaminsky, S., Zamb, T., Moyle, M., Koff, W.C., Poignard, P., Burton, D.R., 2009. Broad and potent neutralizing antibodies from an African donor reveal a new HIV-1 vaccine target. Science 326, 285-289.

Walker, L.M., Simek, M.D., Priddy, F., Gach, J.S., Wagner, D., Zwick, M.B., Phogat, S.K., Poignard, P., Burton, D.R., 2010. A limited number of antibody specificities mediate broad and potent serum neutralization in selected HIV-1 infected individuals. PLoS pathogens 6.

Watkins, B.A., Buge, S., Aldrich, K., Davis, A.E., Robinson, J., Reitz, M.S., Jr., Robert-Guroff, M., 1996. Resistance of human immunodeficiency virus type 1 to neutralization by natural antisera occurs through single amino acid substitutions that cause changes in antibody binding at multiple sites. J Virol 70, 8431-8437.

Wei, X., Decker, J.M., Liu, H., Zhang, Z., Arani, R.B., Kilby, J.M., Saag, M.S., Wu, X., Shaw, G.M., Kappes, J.C., 2002. Emergence of resistant human immunodeficiency virus type 1 in patients receiving fusion inhibitor (T-20) monotherapy. Antimicrob Agents Chemother 46, 1896-1905.

Wei, X., Decker, J.M., Wang, S., Hui, H., Kappes, J.C., Wu, X., Salazar-Gonzalez, J.F., Salazar, M.G., Kilby, J.M., Saag, M.S., Komarova, N.L., Nowak, M.A., Hahn, B.H., Kwong, P.D., Shaw, G.M., 2003. Antibody neutralization and escape by HIV-1. Nature 422, 307-312.

Wrammert, J., Koutsonanos, D., Li, G.M., Edupuganti, S., Sui, J., Morrissey, M., McCausland, M., Skountzou, I., Hornig, M., Lipkin, W.I., Mehta, A., Razavi, B., Del Rio, C., Zheng, N.Y., Lee, J.H., Huang, M., Ali, Z., Kaur, K., Andrews, S., Amara, R.R., Wang, Y., Das, S.R., O'Donnell, C.D., Yewdell, J.W., Subbarao, K., Marasco, W.A., Mulligan, M.J., Compans, R., Ahmed, R., Wilson, P.C., 2011. Broadly cross-reactive antibodies dominate the human B cell response against 2009 pandemic H1N1 influenza virus infection. J Exp Med 208, 181-193.

Wu, L., Gerard, N.P., Wyatt, R., Choe, H., Parolin, C., Ruffing, N., Borsetti, A., Cardoso, A.A., Desjardin, E., Newman, W., Gerard, C., Sodroski, J., 1996. CD4-induced interaction of primary HIV-1 gp120 glycoproteins with the chemokine receptor CCR-5. Nature 384, 179-183.

Wu, X., Yang, Z.Y., Li, Y., Hogerkorp, C.M., Schief, W.R., Seaman, M.S., Zhou, T., Schmidt, S.D., Wu, L., Xu, L., Longo, N.S., McKee, K., O'Dell, S., Louder, M.K., Wycuff, D.L., Feng, Y., Nason, M., Doria-Rose, N., Connors, M., Kwong, P.D., Roederer, M., Wyatt, R.T., Nabel, G.J., Mascola, J.R., 2010. Rational design of envelope identifies broadly neutralizing human monoclonal antibodies to HIV-1. Science 329, 856-861.

Wyatt, R., Kwong, P.D., Desjardins, E., Sweet, R.W., Robinson, J., Hendrickson, W.A., Sodroski, J.G., 1998. The antigenic structure of the HIV gp120 envelope glycoprotein. Nature 393, 705-711.

Wyatt, R., Sodroski, J., 1998. The HIV-1 envelope glycoproteins: fusogens, antigens, and immunogens. Science 280, 1884-1888.

Xiao, X., Chen, W., Feng, Y., Zhu, Z., Prabakaran, P., Wang, Y., Zhang, M.Y., Longo, N.S., Dimitrov, D.S., 2009. Germline-like predecessors of broadly neutralizing antibodies lack measurable binding to HIV-1 envelope glycoproteins: implications for evasion of immune responses and design of vaccine immunogens. Biochem Biophys Res Commun 390, 404-409.

Yang, X., Mahony, E., Holm, G.H., Kassa, A., Sodroski, J., 2003. Role of the gp120 inner domain beta-sandwich in the interaction between the human immunodeficiency virus envelope glycoprotein subunits. Virology 313, 117-125.

Zanetti, G., Briggs, J.A., Grunewald, K., Sattentau, Q.J., Fuller, S.D., 2006. Cryo-electron tomographic structure of an immunodeficiency virus envelope complex in situ. PLoS pathogens 2, e83.

Zhang, M., Gaschen, B., Blay, W., Foley, B., Haigwood, N., Kuiken, C., Korber, B., 2004. Tracking global patterns of N-linked glycosylation site variation in highly variable viral glycoproteins: HIV, SIV, and HCV envelopes and influenza hemagglutinin. Glycobiology 14, 1229-1246.

Zhu, P., Liu, J., Bess, J., Jr., Chertova, E., Lifson, J.D., Grise, H., Ofek, G.A., Taylor, K.A., Roux, K.H., 2006. Distribution and three-dimensional structure of AIDS virus envelope spikes. Nature 441, 847-852.

Zwick, M.B., Jensen, R., Church, S., Wang, M., Stiegler, G., Kunert, R., Katinger, H., Burton, D.R., 2005. Anti-human immunodeficiency virus type 1 (HIV-1) antibodies 2F5 and 4E10 require surprisingly few crucial residues in the membrane-proximal external region of glycoprotein gp41 to neutralize HIV-1. J Virol 79, 1252-1261.

Zwick, M.B., Labrijn, A.F., Wang, M., Spenlehauer, C., Saphire, E.O., Binley, J.M., Moore, J.P., Stiegler, G., Katinger, H., Burton, D.R., Parren, P.W., 2001. Broadly neutralizing antibodies targeted to the

membrane-proximal external region of human immunodeficiency virus type 1 glycoprotein gp41. J Virol 75, 10892-10905.

Appendix 1: Primer Sequences

Primer Name	Primer Sequence 5'-3'
General PCR Primers	
OFM19	GCACTCAAGGCAAGCTTTATTGAGGCTTA
VIF1	GGGTTTATTACAGGGACAGCAGAG
EnvAStop	CACCGGCTTAGGCATCTCCTATAGCAGGAAGAA
EnvM	TAGCCCTTCCAGTCCCCCCTTTTCTTTTA
T7	TAATACGACTCACTATAGGG
V3 fo	ACATAAGACAAGCACATTGTAACATTA
V3 re	TAATGTTACAATGTGCTTGTCTTATGT
V4 alone fo	GGAGAATTTTTCTATTGCAATAC
V4 alone re	GTATTGCAATAGAAAAATTCTCC
C4 fo	CAGAATAAAACAAATTATAAACATGTGGCA
C4 re	TGCCACATGTTTATAATTTGTTTTATTCTG
V1-fwd	GTGTAAAGTTGACCCCACTCTG
V1-rev	CAGAGTGGGGTCAACTTTACAC
V2-fwd	CAGGCCTGTGTTATGGTTGAGG
V2-rev	CCTCAACCATAACACAGGCCTG
Sequencing Primers	
A589re	CAGAGTGGGGTTAACTTTACAC
E175	TTTAGCATGTGATGCACAAAATAG
EnvB	AGAAAGAGCAGAAGACAGTGGCAATGA
A589	GTGTAAAGTTAACCCCACTCTG
A590	AATCGCGAAACCAGCCGGCGCACAAT
Br	AATTTCTAGGTCCCCTCCTGA
E85	GTCCCTCATATCTGCTCCTCCAGGTCTG
EnvArev	TGCTGCTCCCAAGAACCCAA
Df	AGCACATTGTAACATTAGT
gp41Fo	GCCAGTGGTATCAACTCAAC
Envup	TTCAGACCTGGAGGAGGAGATATGAGGG
Nr	GGTGAGTATCCCTGCCTAACTCTA
E220	TATCAAAATGGCTGTGGTATATAA
E240	ATAATGATAGTAGGAGGCTTGATAGGC
MPERseq	CACAAGCACAATATACAGGTTACTTGAAGACTCGCAAAACCAGCAGG
EnvM	TAGCCCTTCCAGTCCCCCCTTTTCTTTTA
CT1Fo	GGTGGGAAGCTCTTAAGTATCTGGGAAGTC
CT1Re	GACTTCCCAGATACTTAAGAGCTTCCCACC

Heterologous Chimera Primers	
84-69-84 C3 fo	ATAAGACAAGCACATTGTAACATTAGCAAACAG
84-69-84 C3 re	CTGTTTGCTAATGTTACAATGTGCTTGTCTTAT
84-69-84 V4 fo	TGCAAAATAAAACAAATTATAAACATGTGGCAG
84-69-84 V4 re	CTGCCACATGTTTATAATTTGTTTTATTTTGCA
88-200-88.C3 6mo end fo	GGAGAATTTTTCTATTGC
88-200-88.C3 6mo end re	GCAATAGAAAAATTCTCC
88-200-88.alpha2 6mo end fo	TTCCCTAATAAAACAAAAATA
88-200-88.alpha2 6mo end re	TATTTTTGTTTTATTAGGGAA
88-269-88 C3 fo	ATAAGACAAGCATATTGTAACATT
88-269-88 C3 re	AATGTTACAATATGCTTGTCTTAT
88-269-88 V4 fo	CCATGCAGAATAAAACAGATTATC
88-269-88 V4 re	GATAATCTGTTTTATTCTGCATGG
88.69/174-88 C3 fo	ATAAGACAAGCACATTGTAACATT
88-69/174-88 C3 re	AATGTTACAATGTGCTTGTCTTAT
88-69/174-88 V4 fo	CCATGCAGAATAAAACAAATTATA
88-69/174-88 V4 re	TATAATTTGTTTTATTCTGCATGG
88.136V3 fo	ATAAGACAAGCACATTGTAACATTAGTAAGGATCTCTGGAATGAAACCTTA
88.136V3 re	TAAGGTTTCATTCCAGAGATCCTTACTAATGTTACAATGTGCTTGTCTTAT
136.88C4 fo	AATAGCACAAACATCACACTCCCATGCAGAATAAAACAAATTATAAACATGTGG
136.88C4 re	CCACATGTTTATAATTTGTTTTATTCTGCATGGGAGTGTGATGTTTGTGCTATT
88.200V3 fo	ATAAGACAAGCACATTGTAACATTAGTAAAACGCAATGGGGCGAAATTTTA
88.200V3 re	TAAAATTTCGCCCCATTGCGTTTTACTAATGTTACAATGTGCTTGTCTTAT
200.88C4 fo	GAAAACGAAACCATCACACTCCCATGCAGAATAAAACAAATTATAAACATGTGG
200.88C4 re	CCACATGTTTATAATTTGTTTTATTCTGCATGGGAGTGTGATGGTTTCGTTTTC
88.221V3 fo	ATAAGACAAGCACATTGTAACATTAATGGAACTAAATGGAATGAAACTTTA
88.221V3 re	TAAAGTTTCATTCCATTTAGTTCCATTAATGTTACAATGTGCTTGTCTTAT
221.88C4 fo	GCAAACATAACCCTCACACTCCCATGCAGAATAAAACAAATTATAAACATGTGG
221.88C4 re	CCACATGTTTATAATTTGTTTTATTCTGCATGGGAGTGTGAGGGTTATGTTTGC
Virus-specific Chimera Primers	
228 C2 6-2moAC fo	GCCAAAACAATAATAGTACACCTTAATGAGTCTATAGAAATTGTGTGTACAAGGCCCAAC
228 C2 6-2moAC re	CCTTATACTTTTTCTTGTATTATTGTTGGGCCTTGTACACACAATTTCTATAGACTCATTAAGG
CAP206V3-fo	GAAGCCCATTGTAACCTTAGTAAAGATGCA
CAP206V3-re	TGCATCTTTACTAAGGTTACAATGGGCTTC

CAP206V4-fo	ACAATCATACTCCCATGTAGAATAAAACAA
CAP206V4-re	TTGTTTTATTCTACATGGGAGTATGATTGT
206 6/12mo V5s fo	CTGTTATTGACGCGTGACAAAGACCCAGGGCAGGAGAACAGCAGCACA GAGACATTCAGACCT
206 6/12mo V5s re	AGGTCTGAATGTCTCTGTGCTGCTGTTCTCCTGCCCTGGGTCTTTGTCACG CGTCAATAACAG
244.3.16.3 V4 fo	CAATTTATAAGGATGTGGCAGAAGGTA
244.3.16.3 V4 re	TACCTTCTGCCACATCCTTATAAATTG
244.3.16 alpha2s back fo	GCTTTAATTGTAGAGGAGAATTTTTCTATTGC
244.3.16.alpha2s back re	GCAATAGAAAAATTCTCCTCTACAATTAAAGC
244.3.16.3 V4 fo	CAATTTATAAGGATGTGGCAGAAGGTA
244.3.16.3 V4 re	TACCTTCTGCCACATCCTTATAAATTG
244.3.16 alpha2s back fo	GCTTTAATTGTAGAGGAGAATTTTTCTATTGC
244.3.16.alpha2s back re	GCAATAGAAAAATTCTCCTCTACAATTAAAGC
255 C2 6mo chim fo	CAAAACAATAATAGTACATCTCAATGAATCTGTAGAGATTAATTGTACAA GACCC
255 C2 6mo chim re	GGGTCTTGTACAATTAATCTC ACAGATTCATTGAGATGTACTATTATTGTTTTG
200 alpha2/C3 6mo fo	ATAAGACAAGCACATTGTAAC
200 alpha2/C3 6mo re	GTTACAATGTGCTTGTCTTAT
200 alpha2 end 6mo fo	CACTTCCCTAATAGAACA
200 alpha2 end 6mo re	TGTTCTATTAGGGAAGTG
200 V4 6mo fo	CCATGCAGAATAAAACAAATT
200 V4 6mo re	AATTTGTTTTATTCTGCATGG
136 C3 6mo fo	ATAAGAAAAGCACATTGTAAT
136 C3 6mo re	ATTACAATGTGCTTTTCTTAT
255 alpha2 6/12mo end fo	GAACACTTCCCTAATAAGACA
255 alpha2 6/12mo end re	TGTCTTATTAGGGAAGTGTTC
255 V4 6/12mo fo	TGCAGAATAAAACAAATTATA
255 V4 6/12mo re	TATAATTTGTTTTATTCTGCA
255 C2 changes 6/12mo fo	ATAGTACATCTCAATGAATCTGTAG
255 C2 changes 6/12mo re	CTACAGATTCATTGAGATGTACTAT
Virus-specific Mutagenesis Primers	
206.12mo-2mo alpha2 MUT fo	CCTTAGTAAAGATGCATGGAACACAACTCTAGAACAGATAAAAGG
206.12mo-2mo alpha2 MUT re	CCTTTTATCTGTTCTAGAGTTGTGTTCCATGCATCTTTACTAAGG
206 6/12moC2 MUT fo	CAATAATAGTACACCTTAATAAAGCTATAGAAATTGTGTGTAC
206 6/12moC2 MUT re	GTACACACAATTTCTATAGCTTTATTAAGGTGTACTATTATTG
206.12mo.C2 MUT fo	GTACACCTTAATAAATCTATAGAAATTGTGTGTACAAGACCTGGC
206.12mo.C2 MUT re	GCCAGGTCTTGTACACACAATTTCTATAGATTTATTAAGGTGTAC
206.12mo.C2 MUT fo	GTACACCTTAATAAATCTATAGAAATTGTGTGTACAAGACCTGGC
206.12mo.C2 MUT re	GCCAGGTCTTGTACACACAATTTCTATAGATTTATTAAGGTGTAC
244 12mo-2mo alpha2 chim fo	GGAGATATAAGACAAGCATATTGTAACATTGATAAAGGGGCCTGGAATA AAACTTTACAACAGG

244 12mo-2mo alpha2 chim re	CCTGTTGTAAAGTTTTATTCCAGGCCCCTTTATCAATGTTACAATATGCTTGTCTTATATCTCC
244 12mo MUT T465I fo	GGCAAATGACACAAACAACATAGAGACATTCAGACCTGGAGG
244 12mo MUT T465I re	CCTCCAGGTCTGAATGTCTCTATGTTGTTTGTGTCATTTGCC
255.3.4/5C3res-sens-fo	GCACATTGTAACATTAGCAAAGATAAATGGGACAAAACTTTACACAGGGTAAGTG
255.3.4/5C3res-sens-re	CACTTACCCTGTGTAAAGTTTTGTCCCATTTATCTTTGCTAATGTTACAATGTGC
255.6mo.T297I MUTfo	CATCTCAATAAATCTGTAGAGATTAATTGTATAAGACCCAATAATAATACAAGG
255.6mo.T297I MUTre	CCTTGTATTATTATTGGGTCTTATACAATTAATCTCTACAGATTTATTGAGATG
255.6mo.N448K MUTfo	GCAGGAAACATAACATGTAAATCAAAGATCACAGGGC
255.6mo.N448K MUTre	GCCCTGTGATCTTTGATTTACATGTTATGTTTCCTGC
255.6mo.K446E MUTfo	GCAGGAAACATAACATGTGAATCAAATATCACAGGGC
255.6mo.K446E MUTre	GCCCTGTGATATTTGATTCACATGTTATGTTTCCTGC
136 6mo MUT S448N fo	GGAAACATAACATGTAACTCAAATATCACAGGGCTACTATTAAC
136 6mo MUT S448N re	GTTAATAGTAGCCCTGTGATATTTGAGTTACATGTTATGTTTCC
136alpha2back mut 6mo fo	GTAAGGAGCTCTGGAATGAAACCTTACAAAGGGTAAC
136alpha2back mut 6mo re	GTTACCCTTTGTAAGGTTTCATTCCAGAGCTCCTTAC
200.12mo.MUT.N339S/T341A fo	GTAAAGAGGAATGGAGCAGAGCTTTAGAAAGGGTAAAGG
200.12mo.MUT.N339S/T341A re	CCTTTACCCTTTCTAAAGCTCTGCTCCATTCCTCTTTAC
228.3.3a/4aC3res-sens-fo	AGTAAAAAAGATTGGAACAAAACCTTAGAAGGGGTAAAGAAGAAATTAGGAGAA
228.3.3a/4aC3res-sens-re	TTCTCCTAATTTCTTCTTTACCCCTTCTAAGGTTTTGTTCCAATCTTTTTTACT
228.3.1C3res-sens-fo	CACTGTAACATTAGTAAAAAAGATTGGAACAAAACCTTAGAAGGGG
228.3.1C3res-sens-re	CCCCTTCTAAGGTTTTGTTCCAATCTTTTTTACTAATGTTACAGTG

Appendix 2: Ethics Clearance

UNIVERSITY OF THE WITWATERSRAND, JOHANNESBURG
Division of the Deputy Registrar (Research)

HUMAN RESEARCH ETHICS COMMITTEE (MEDICAL)
R14/49 Ms Jinal N Bhiman

CLEARANCE CERTIFICATE	**M10273**
PROJECT	Autologous Neutralizing Antibody Specificities Characterizing the C3V4 Region and Defining the Mechanisms of Escape
INVESTIGATORS	Ms Jinal N Bhiman.
DEPARTMENT	Patholoyg/AIDS Virology Unit
DATE CONSIDERED	
DECISION OF THE COMMITTEE*	Approved unconditionally

Unless otherwise specified this ethical clearance is valid for 5 years and may be renewed upon application.

DATE 15/03/2010 **CHAIRPERSON** .....
(Professor PE Cleaton-Jones)

*Guidelines for written 'informed consent' attached where applicable
cc: Supervisor : Dr P Moore

DECLARATION OF INVESTIGATOR(S)

To be completed in duplicate and **ONE COPY** returned to the Secretary at Room 10004, 10th Floor, Senate House, University.
I/We fully understand the conditions under which I am/we are authorized to carry out the abovementioned research and I/we guarantee to ensure compliance with these conditions. Should any departure to be contemplated from the research procedure as approved I/we undertake to resubmit the protocol to the Committee. **I agree to a completion of a yearly progress report.**

PLEASE QUOTE THE PROTOCOL NUMBER IN ALL ENQUIRIES

Appendix 3: Plagiarism Declaration

Postgraduate Office, Faculty of Health Sciences
Wits Medical School, 7 York Road, PARKTOWN, 2193, Johannesburg • Tel: (011) 717 2745 • Fax: (011) 717 2119 • e-mail: healthpg@health.wits.ac.za

PLAGIARISM DECLARATION TO BE SIGNED BY ALL HIGHER DEGREE STUDENTS

SENATE PLAGIARISM POLICY: APPENDIX ONE

I JINAL N. BHIMAN (Student number: 0408743N) am a student registered for the degree of MSc (MED) in the academic year 2012.

I hereby declare the following:

- I am aware that plagiarism (the use of someone else's work without their permission and/or without acknowledging the original source) is wrong.
- I confirm that the work submitted for assessment for the above degree is my own unaided work except where I have explicitly indicated otherwise.
- I have followed the required conventions in referencing the thoughts and ideas of others.
- I understand that the University of the Witwatersrand may take disciplinary action against me if there is a belief that this in not my own unaided work or that I have failed to acknowledge the source of the ideas or words in my writing.

Signature: JVBhiman Date: 28 FEBRUARY 2012

Appendix 4: Examiner 1 Comments

UNIVERSITY OF THE WITWATERSRAND FACULTY OF HEALTH SCIENCE

EXAMINATION OF DISSERTATION (M.Sc.)

TITLE
Autologous neutralising antibody specificities in HIV-1 subtype C: Characterising the C3V4 region and defining the mechanisms of escape

CANDIDATE
J Bhiman

Dissertation Overview

A major focus of HIV vaccine research involves defining regions on the viral envelope surface glycoprotein (Env) that are conserved and vulnerable to neutralising antibodies (Nabs). Several molecular features of Env (sequence heterogeneity, hyperglycosylation, conformational flexibility) underlie the inability of infected individuals to raise broad and potent anti-Env Nabs against this target during the acute phase of infection. While most individuals develop robust, early antibody responses against the virus, these typically have very limited specificities, and ongoing low level, error-prone viral replication eventually allows a population of viruses resistant to this "autologous" response to emerge. Nevertheless, a significant number of HIV-positive individuals go on to develop broadly neutralising Nabs after prolonged infection with the virus, and so understanding the nature of viral escape from autologous Nabs, and how broader responses evolve with time are fundamentally important objectives of HIV vaccine research.

In this study, through a series of elegant molecular approaches, J Bhiman characterised early autologous neutralising antibody (AnAb) responses to the C3V4 regions of a panel of HIV-1 Subtype C Envs. Several Env-encoding fragments were amplified from HIV-positive sera, and used to construct Env-pseudotyped viruses; these were used in neutralisation assays to define anti-C3V4 responses. Longitudinal isolation and sequencing of viral envelopes from the same patients provided insights into the potential mechanism of viral escape from the early AnAb. By introducing certain mutations into the Env genes of C3V4-chimeric pseudovirions, the author was able to describe how mutations in C3V4 and surrounding regions potentially contribute to escape from the early autologous neutralising antibodies.

General Comments

The thesis is written in a style that is appropriate for a M.Sc. dissertation, and the candidate has shown a good understanding of the basic molecular concepts relevant to her work. Her work has involved mastering a broad variety of fundamental molecular and bioinformatic research tools (PCR, cloning, cell culturing, site-directed mutagenesis, homology modelling), and the outputs generated by applying these has generally been of a very high quality. The experiments described are laborious

and technically challenging, and the candidate's successful execution of these is a commendable accomplishment. There are very few grammatical/typographical errors, illustrations/diagrams/gel images are clear, concise and understandable and the candidate is to be commended for submitting a generally very well constructed manuscript. Overall, therefore, my comments are minor in nature, and I feel the candidate has fulfilled the requirements for being awarded the degree of M.Sc. There are several points/suggestions I have raised which should be addressed to the satisfaction of the candidate's supervisor/HOD before the submission is approved, however. Congratulations on an excellent piece of work.

Specific Comments - Styles/Grammar/Typographical Errors

1. Page vi, Results, line 2: Since this is the first time the term is introduced, the full term for PNG should be included (ie potential N-linked glycan)

2. Page 3, Figure 1 legend: change "Schematic of..." to "Schematic representation of..."

3. Page 7, 2nd paragraph, line 6: change "brief" to "short-lived" or insert "state" between "intermediate" and ""prior".

4. Page 16, 1st paragraph final line: change "...(2011);...) to "...(2011),...)

5. Page 27, section 2.6, line 11: "14 00" should surely be "14 000"

6. Page 28, top paragraph, final line: the final concentration of ampicillin in the plates should be 100 µg/ml (as opposed to 100 mg/ml stated); same error in section 2.10, line 2.

7. The conventional approach to describing centrifugal force of centrifugation involves stating a value followed by "× g", unlike that used by the author, for example, in section 2.11, paragraph 2 line 4 ("2000 G"). This error occurs serially, and should be corrected in each case.

8. Page 31, section 2.12.3, paragraph 2, line 6: change "...in 100 ul of cDNA" to "...in 100 ul of plasma/blood"

9. Page 34/35: By convention a "Results" title should appear at the beginning of Section 3 (as for Materials and Methods (Chapter 2) and Discussion and Conclusions (Chapter 4) etc...

10. Page 37, Figure 13 legend: change "Schematic" to "Diagram"

11. Page 55, 1st Paragraph, line 4: change "S410Y" to "S401Y".

12. Page 61, top paragraph, line 4: insert "to" between "proximal" and "the".

13. Page 73, top paragraph, line 9: Change "Alternately" to "Alternatively"

14. Page 78, paragraph 2, line 8: "...stems from a recent finding by Lynch *et al* (2011),..." is an incorrect citation format. An alternative suggestion is: "..."...stems from a recent finding by Lynch and colleagues who isolated 3 MAbs derived from 3 distinct B cells (Lynch *et al.* 2011)".

Specific Comments – Content/Technical

1. Page 14, 2nd paragraph, line 17: what does the author mean by "slightly raised profile"?

2. Page 29, section 2.11, paragraph 2: the author states "Fifty microlitres of this mixture was (sic) added to each well and plates were centrifuged at 2000 G for 30 minutes". This is followed by "Supernatants were removed by centrifuging at 150 G for 1 minute". I suspect that a step is missing in between these 2 (possibly plate inversion), and I also wonder whether "150 G" is the correct speed.

3. Page 30, section 2.12, line 9: Change "...with PCR introduced errors at an introduced rate of 8×10^{-5}..." to "...with PCR errors introduced at a rate of 8×10^{-5}...". Also, qualify the error rate (8×10^{-5}) correctly – is this per base? per amplicon? per cycle?

4. Page 32, top paragraph: the author states that "If less than 30% of the total number of reactions were positive, these were considered to be derived from single templates...". It would be informative to know how many independent PCRs were performed from the same diluted sample.

5. Page 38, Section 3.2: unless I have misunderstood the rationale behind the approach to assessing the conformational integrity of the C3V4 chimeras, surely "non-neutralising" as it appears in the final line of this section should be "neutralizing"?

6. Page 39, 2nd paragraph: the author describes the transient nature of the anti-C3V4 response in certain individuals (CAP136, CAP228, CAP244, CAP255) over time ("an initial peak, a dip and then a second peak"). Are these changes in titre values statistically significant, and if so, how does one explain this trend in the context of ongoing viral evolution?

7. Section 4 (Starting page 47): The author uses SGA to identify "potential escape mutations". To what extent can one be confident that the identified sequences are representative of the population of viral species prevailing at that time? Another way of putting this is if the identified mutations are indeed contributing significantly to escape from the AnAb, then one would expect these to be present in a representative proportion of circulating viruses. Does the author have any evidence to suggest that this is the case?

8. Page 48, paragraph 2: It would be informative to see a more detailed description on the concept of entropy plotting, and whether the author understands, in biophysical terms, what information an entropy plot conveys that enables her "to identify areas likely to contain escape mutations". For example, what is the basis for the claim that "Regions with the highest entropy were potentially under the most immune pressure"?

Appendix 5: Examiner 2 Comments

I. Examiner's summary:

HIV-1/AIDS is a global problem with health, economic, and social ramifications. Regions such as sub-Saharan Africa have been disproportionately affected and an effective vaccine is desperately needed. A greater understanding of what regions of the HIV-1 envelope are targeted by neutralizing antibodies, during early subtype C HIV-1 infection will provide important clues about how to design effective vaccine immunogens. These studies are particularly important, as subtype C HIV predominates in South Africa and also accounts for more than half of all worldwide infections.

Ms. Bhiman has investigated whether early neutralizing antibodies target the HIV-1 envelope gp120 C3V4 region in recently subtype C HIV-1 infected subjects from the CAPRISA cohort. Previous studies by Dr. Moore and others have implicated this region, and in particular the α2 helix located in C3, in resistance to antibody neutralization. Ms. Bhiman determined that 14 out of 22 individuals had plasma neutralizing antibodies that targeted this region, using a strategy of measuring neutralization of chimeric envelopes containing this region by plasma collected at 3 years post-infection. She then characterized features of the envelope antigens in the C3V4 responders and nonresponders, and defined potential neutralization epitopes and mechanisms of viral escape in a subset of the responders.

The C3V4 responders tended to have higher autologous neutralizing antibody titers the nonresponders. The C3V4 responders were also infected with viruses whose envelopes were less glycosylated in this region, suggesting that greater exposure could have increased its immunogenicity. The neutralizing antibody response and viral escape mechanisms of 5 the C3V4 responders were studied in greater detail by creating a panel of mutants and chimeras specific for each subject and testing their sensitivity to neutralization by early plasma samples. The α2 helix was involved in neutralization escape, but often determinants outside of the α2 helix were also necessary. Thus Ms. Bhiman provides strong evidence that the C3V4 region is immunogenic and constitutes a major target for neutralizing antibodies in early subtype C HIV-1 infection. The existence of multiple escape pathways illustrates the flexibility of this region. The findings provide novel insight into the early neutralizing antibody response in natural infection. Overall, this is a very well-conceived and nicely written dissertation that represents a great deal of detailed experimentation and thoughtful interpretation of results.

II. Minor points for consideration:

Background

The background is very thorough and the figures are nicely done. In particular, Table 1 and Fig. 8 illustrate strong points. Fig. 9 is also a very nice schematic of the temporal nature neutralizing antibody responses in early infection. The candidate demonstrates a strong command of the background literature, which is extensive.

In Section 1.4 on Neutralizing Antibodies, until more in depth studies have been done, such as next generation sequencing on early samples, it remains possible that early antibodies (neutralizing or non-neutralizing) do exert pressure on the virus. There may be low levels of neutralizing antibodies, undetectable in assays such as the TZM-bl, but nevertheless present in vivo shaping the viral population at early time points. The timing of in vitro detection of neutralizing antibodies (12-20 weeks post-infection) could lag behind their activity in vivo.

Section 1.6 Study Objectives, the C3V4 region is a major target for neutralizing antibodies, but to state that it is 'the major target' is a bit strong. After all, 8 subjects in this study did not show evidence of targeting this region, and V1V2 is also a common target. However the C3V4 region is likely also involved in neutralization of other subtypes as well (subtype B in Tang et al. and subtype A in unpublished data from M. Murphy/C. Derdeyn).

The study of this region as a neutralization target in subtype C HIV-1 is a strongly supported and clearly justified, and its importance may reach across subtypes.

While the objectives are very clearly described, the candidate could state his/her hypotheses more directly. As an example, "Neutralization escape in C3V4 responders is mediated by mutations in the α2 helix" might be one way to state a hypothesis that was tested here.

Materials and Methods

The Materials and Methods section is complete and well written. The level of detail and description is impressive. In some places mg/μl should be μg/ml (i.e. DEAE-dextran) or mg/ml should be μg/ml (i.e. ampicillin). The experiments are well-conceived, carefully designed and thought out. Ms. Bhiman has a clear and through understanding of the experimental approach.

Results

The results are logically and clearly presented. A summary is provided for the mechanisms of escape in each subject, which is very helpful.

Chapter 3: The implication that greater exposure of the C3V4 region in responders vs. non-responders enhanced its immunogenicity and led to elicitation of a dominant neutralizing antibody response is an important finding with direct relevance to vaccine design. How could this be incorporated into the design of immunogens? The higher titer in C3V4 responders is also an interesting finding – does the candidate think that multiple antibodies target epitopes in this region and that this may be a contributing factor?

Chapter 4: This section represents a great deal of work and complicated results, yet it is clearly presented and summarized well. The definition of distinct pathways in different co-circulating escape variants is an important point with relevance to vaccine design. Neutralizing antibody targets that are so susceptible to viral escape may not be the best choice for vaccines.

Discussion

The discussion is well-written, cites relevant studies, and provides a summary of the results. Ms. Bhiman also presents some mechanistic models for the various escape pathways.

The detailed work showing that mutations within the α2 helix do not commonly mediate neutralization escape without contribution from neighboring glycans shed new light on results presented in a previous study by Rong et al. (2007c), and support an important but somewhat indirect involvement of this region in neutralization escape. Does Ms. Bhiman have any ideas on how to connect the high sequence variability particularly on the exposed face of the α2 helix with neutralization escape mediated by proximal PNGs?

An statement on the implications of this work for vaccine immunogens would strengthen the discussion. Would the C3V4 region be something to include or exclude from a vaccine immunogen? How could this information be exploited? Is anything known about the development of neutralizing antibody breadth in the C3V4 responders vs. the non-responders?

Appendix 6: List of corrections

Examiner 1 – Style/Grammar/Typographical Errors

1. Page vi, Results, line 2: sentence was altered as suggested.
2. Page 3, Figure 1 legend: sentence was altered as suggested.
3. Page 7, 2nd paragraph, line 6: "brief" has been replaced with "short-lived."
4. Page 16, 1st paragraph, line 6: sentence was altered as suggested.
5. Page 27, section 2.6. line 11: sentence was altered as suggested.
6. Page 28, 1st paragraph, line 5: both sentences were altered as suggested.
7. The conventional approach to describing centrifugal force of centrifugation, "x g", has replaced all previously used "G."
8. Page 31, section 2.12.3. paragraph 2, line 6, sentence was changed to: "For example, a viral load of 20 000 copies/ml would yield approximately 2000 cDNA copies in a 100 µl cDNA reaction, which would then be diluted to result in a 1 copy/µl concentration."
9. Page 36: A "Results" title page has been included.
10. Page 39, Figure 13 legend: sentence was altered as suggested.
11. Page 57, 1st paragraph, line 4: sentence was altered as suggested.
12. Page 63, 1st paragraph, line 4: sentence was altered as suggested.
13. Page 75, 1st paragraph, line 9: sentence was altered as suggested.
14. Page 80, 2nd paragraph, line 8: sentence was altered as suggested.

Examiner 1 – Content/Technical

1. Page 14, 2nd paragraph, line 17, sentence changed to: "As shown in Table 1, the alpha2-helix of subtype C viruses appears to be more solvent-exposed when compared to the alpha2-helix of subtype B viruses."

2. Page 29, section 2.11, paragraph 2, sentence was changed to: “Fifty microlitres of this mixture were added to each well and plates were centrifuged at 2 000 x g for 30 minutes. Plates were inverted and supernatants were removed by centrifuging at 150 x g for 1 minute.” 150 x g is the speed used in this laboratory for sequence clean-ups.

3. Page 30, section 2.12, line 9, sentence was changed to: “The use of single genome amplification (SGA) prevents intragenic recombination and reduces *in vitro* artefacts, with PCR errors introduced at a rate of less than 8 x 10^{-5} nucleotides per 3 kb envelope for the entire procedure due to the use of high fidelity enzymes (Salazar-Gonzalez et al., 2008).”

4. Page 32, 1st paragraph, line 5, sentence was changed to: “If less than 30 % of the total number of reactions were positive these were considered to be derived from single templates and selected for further use. Independent PCRs were performed at least twice for each cDNA.”

5. Page 40, section 3.2, line 10, sentence was changed to: “These results indicate that the conformational integrity of all 22 C3V4 chimeras was maintained, with no evidence of exposure of normally occluded epitopes.”

6. The examiner enquired about the biphasic shape of some C3V4 responder chimeras and asks what this implies in the context of viral evolution. In response to this a paragraph was included on page 75, 1st paragraph, line 11 of the “Discussion” chapter: “The neutralisation curves for three C3V4 chimeras had a biphasic shape, suggesting the development of multiple and possibly subtly different anti-C3V4 responses, similar to a recent paper on anti-V1V2 antibodies (Lynch et al., 2011). Alternatively the re-emergence of the initial anti-C3V4 response at a later time point may occur due to the resurgence of early viruses from viral reservoirs. Linked to this is the possibility that an initial anti-C3V4 antibody response has affinity matured with time (Corti et al., 2010; Huber et al., 2010; Lynch et al., 2011; Walker et al., 2009; Wrammert et al., 2011; Wu et al., 2010; Xiao et al., 2009).”

7. The examiner makes a good point here. We agree that a larger number of sequences from each time point would define whether potential escape mutations were present in the majority of the population. However single genome amplification is costly and a maximum of 10 sequences from 6 months post-infection (p.i.) and 20 sequences from 12 months p.i. was feasible for this project. Nevertheless, proof that these predicted escape mutations do contribute significantly to escape from autologous neutralising antibodies (AnAbs) is shown and discussed for each of the 5 individuals investigated. By back-mutating these residues in

the context of a neutralisation resistant later clone, neutralisation sensitivity, comparable to early clone was achieved. In addition the identification of multiple pathways of neutralisation escape suggests that a single given escape mutation might not necessarily be highly represented among circulating viruses.

8. The association of high entropy residues with immune escape in HIV-1 has been well-described elsewhere (Delwart et al., 1997; Frost et al., 2005; Moore et al., 2009; Richman et al., 2003; Rong et al., 2009; Wei et al., 2003). However we agree with the examiner that the creation of entropy plots and their subsequent use was not described in enough detail, and therefore we have included section 2.15 on page 32 of the "Materials and Methods" chapter as follows:

   "Entropy plots were generated using the Entropy-One tool from the Los Alamos National Laboratory HIV Sequence Database (http://www.hiv.lanl.gov/content/sequence/ENTROPY/entropy_one.html) to determine which regions of gp120 were highly variable among longitudinal clones. Shannon entropy is a quantitative measure of uncertainty in a data set. This tool uses a Monte Carol randomisation strategy to identify variability between aligned sequences. Each position in the sequence alignment undergoes multiple test or comparisons after which a Bonferroni correction is applied to set the threshold."

Examiner 2 – minor points for consideration

1. Page 17, section 1.4, paragraph 3, line 1, sentence altered as follows: "However, the autologous neutralising antibody (AnAb) response, which is directed to a person's own virus, is thought to develop much later at 12-20 weeks p.i. giving the virus ample time to establish infection (Delwart et al., 1997; Gray et al., 2007; Li et al., 2006a). The possibility of low levels of neutralising antibodies, undetectable with current assays, but nevertheless able to shape the viral population at early time points, has not yet been excluded (Bar et al., 2012)." The Bar et al journal article was only recently published on the 31st May 2012.

2. Page 19, section 1.6, line 1: sentence altered as suggested.

3. The examiner requested that a hypothesis be stated as part of the objectives. We therefore included the following statement on page 19, section 1.6, line 9 of the "Introduction" chapter: "We hypothesised that a more exposed C3V4 region may lead to an early

autologous anti-C3V4 response and that mutations in the alpha2-helix mediate neutralisation escape from these anti-C3V4 responses."

4. Page 25, 1st paragraph, line 4: sentence altered as suggested.

5. Page 28, 1st paragraph, line 5: sentence altered as suggested.

6. The examiner suggested that multiple antibodies targeting the C3V4 region could contribute to the higher autologous titres observed in C3V4 responders as opposed to non-responders. For this reason the following sentence has been included on page 81, 2nd paragraph, line 2 of the Discussion" chapter: "In addition, multiple antibodies targeting the C3V4 region could contribute to higher autologous titres in C3V4 responders when compared to non-responders." In addition, see point 8 for a discussion of the relevance of these findings to immunogen design.

7. The examiner enquired about a link between the high sequence variability of the alpha2-helix and mediation of neutralisation escape by proximal potential N-linked glycans (PNGs). In response to this, the following sentence was included on pages 78, 2nd paragraph, line 9 of the "Discussion" chapter: "Our results therefore clearly indicate that although neutralisation escape can be mediated by mutations solely in the alpha2-helix, this is not a common pathway and that charge changes play an minor role, likely compensatory in nature, in mediating neutralisation escape."

8. The examiner requested a statement relating the implications of this work on vaccine immunogen design. We have therefore included the following paragraph on page 81 of the "Discussion" chapter: "The development of an early AnAb response targeting the anti-C3V4 response does not necessarily predispose an individual to develop bnAbs as the number of individuals who develop bnAbs does not significantly differ between the C3V4 responder and non-responder groups ((Gray et al., 2011) and data not shown). In addition, the number of pathways that can be employed to escape an anti-C3V4 response suggests that the extreme diversity of this region in subtype C viruses may continue to increase as the pandemic progresses. However numerous bnAbs isolated from HIV-1 infected individuals depend on the 332 glycan within the C3V4 region (Trkola et al., 1996; Walker et al., 2011), therefore this region may stimulate the development of protective antibodies. Therefore an immunogen including the C3V4 region would likely have to be modified, through the inclusion of glycans on a long V4 loop, to dampen the immunogenicity of the majority of the C3V4 region and to direct the humoral immune system towards the 332 glycan."

Appendix 7: HOD/HOS Approval Letter

1 Modderfontein Road, Sandringham, 2131
Tel: +27 11 386 6362 Fax: +27 11 386 6333
Email: pennym@nicd.ac.za

8 June 2012

Postgraduate Office
Faculty of Health Sciences
University of the Witwatersrand
Johannesburg

Award of Degree MSc (MED): Ms Jinal Bhiman

Thesis Title: Autologous Neutralising Antibody Specificities in HIV-1 subtype C: Characterising the C3V4 Region and Defining the Mechanisms of Escape

We have reviewed the examiners report and the corrected thesis of Ms Bhiman and we are satisfied that all the corrections and suggestions made by the examiners have been satisfactory and adequately addressed.

We now support the award of the degree of MSc (Med) to Ms Jinal Bhiman at the next graduation ceremony.

Yours Sincerely

Dr Penny Moore
Supervisor

Prof Barry Schoub
Head of Department